NASA-CR-197165

NASw-4435

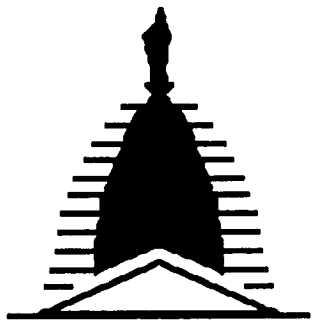

UNIVERSITY of
NOTRE DAME

NASA/USRA UNIVERSITY ADVANCED DESIGN PROGRAM 1993-1994

PROJECT CENTER MENTOR:
NASA-AMES DRYDEN FLIGHT RESEARCH FACILITY

FINAL DESIGN PROPOSAL

The Balsa Bullet

A HIGH SPEED, LOW-COST GENERAL AVIATION AIRCRAFT FOR "AEROWORLD"

April 1994

Department of Aerospace and Mechanical Engineering
University of Notre Dame
Notre Dame, IN 46556

Long Shot Aeronautics presents:

The Balsa Bullet

Final Design Proposal

Submitted on March 24, 1994 by

Kevin Eastland

Sean Greenwood

Dan Kelly

Chuck Leonard

John Rooff

Jeff Scherock

AE441: Aerospace Design
University of Notre Dame

Table of Nomenclature

A_π	Component Reference Area
AR	Aspect Ratio
b	Wing Span
c	Wing Chord
c_f	Flap Chord
C_{Di}	Aircraft Induced Drag Coefficient
C_{Do}	Aircraft Parasite Drag Coefficient
C_l	Section Lift Coefficient
C_L	Wing Lift Coefficient
$C_{L\alpha t}$	Horizontal Tail Lift Curve Slope
$C_{L\alpha v}$	Vertical Tail Lift Curve Slope
$C_{L\alpha w}$	Wing Lift Curve Slope
$C_{L\delta e}$	Horizontal Tail Lift Change due to Elevator Deflection
$C_{l\beta}$	Rolling Moment Coefficient due to Sideslip
$C_{l\delta r}$	Rolling Moment Coefficient due to Rudder Deflection
C_m	Pitching Moment Coefficient
C_{mac}	Pitching Moment Coefficient about the Aerodynamic Center
$C_{m\alpha}$	Pitching Moment Coefficient due to Angle of Attack
$C_{m\alpha f}$	Pitching Moment Coefficient Slope due to the Fuselage
$C_{m\delta e}$	Pitching Moment Coefficient due to Elevator Deflection
C_{mo}	Pitching Moment Coefficient at Zero Angle of Attack
$C_{n\beta}$	Yawing Moment Coefficient due to Sideslip
$C_{n\delta r}$	Yawing Moment Coefficient due to Rudder Deflection
C_P	Power Coefficient
CP1000	Cost per 1000 feet
CPF	Cost per Flight
CPFM	Cost per Flight Minute
C_T	Thrust Coefficient
$\frac{d\varepsilon}{d\alpha}$	Change in Downwash with Angle of Attack
d_{prop}	Propeller Diameter
e	Aircraft Oswald Efficiency Factor
g	Acceleration due to Gravity
H. Velocity	Horizontal Velocity
i_a	Armature Current
i_{ground}	Angle of Fuselage with Respect to Ground
i_t	Tail Incidence Angle
J	Propeller Advance Ratio
L	Aircraft Lift Force
L/D	Aircraft Lift to Drag Ratio
l_t	Horizontal Tail Moment Arm
l_v	Vertical Tail Moment Arm
n	Load Factor

P_{av}	Available Power
P_{req}	Required Power
R	Turn Radius
R/C	Rate of Climb
S	Wing Surface Area
S_e	Elevator Surface Area
S_t	Horizontal Tail Surface Area
S_r	Rudder Surface Area
S_v	Vertical Tail Surface Area
t/c	Wing Thickness to Chord Ratio
V	Velocity
V_{actual}	Armature Voltage
V_{cruise}	Cruise Velocity
V_H	Horizontal Tail Volume Ratio
V_{stall}	Stall Velocity
V_{TO}	Takeoff Velocity
V_V	Vertical Tail Volume Ratio
W	Weight
X_{ac}	Aerodynamic Center Position
X_{cg}	Center of Gravity Position
X_{NP}	Neutral Point Position
α	Angle of Attack
α_{L0}	Angle of Attack at Zero Lift
α_{stall}	Angle of Attack at Stall
β	Sideslip Angle
δ_e	Elevator Deflection Angle
δ_f	Flap Deflection Angle
δ_r	Rudder Deflection Angle
Γ	Dihedral Angle
γ	Glide Angle
μ	Coefficient of Friction
ϕ	Bank Angle
ρ	Density
τ	Flap Effectiveness Parameter
θ	Pitch Angle
θ_c	Climb Angle

TABLE OF CONTENTS

Appendices

1.0 EXECUTIVE SUMMARY

Long Shot Aeronautics has designed the first general aviation aircraft to service Aeroworld. In accordance with the mission definition provided by AE 441, INC. management, *Long Shot Aeronautics* parent company, *The Balsa Bullet* , shown in Figure 1-1, is a high speed low cost six passenger general aviation aircraft. It will cruise at a speed of 55 ft/s with a maximum speed of 75 ft/s for distances in excess of 27000 feet. This range and speed combination provide *The Balsa Bullet* with the capability to service any two existing airports in Aeroworld in an efficient and timely manner.

Overall, three major design drivers have been identified by the design team. The first is to provide a low cost airplane to the Aeroworld market. Maintaining the low cost objective will not simply meet the mission objective as defined by AE 441, INC. management but will also make the *Bullet* an economically viable option for a wide number of consumers. *The Balsa Bullet* has a total manufacturing cost of $1000 with a price to the consumer of only $2562. The second major driver is high speed performance. Once again this driver exists not only to meet the mission objective given *Long Shot Aeronautics* but it provides a desirable feature to the consumer, pride in owning the fastest aircraft in Aeroworld. The third design driver identified is the capability to service any runway in Aeroworld necessitating the ability to takeoff within 28 ft, the length of the shortest runways in Aeroworld. These design drivers provide three great reasons for the general public to purchase a *Bullet*.

The propulsion system consists of a Zinger 12-8 propeller mounted on a powerful Astro-15 motor located in the nose of the aircraft for symmetric thrust as well as weight balance. The motor is powered by thirteen 1000

Figure 1 - 1: Three View Sketch of *The Balsa Bullet*

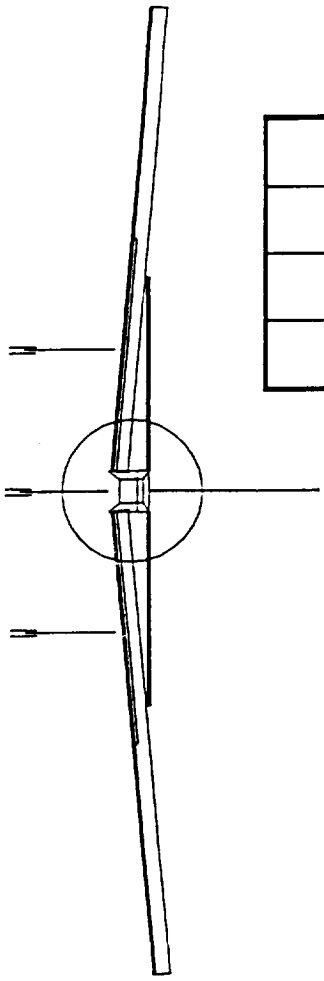

$S_W = 6.33\ ft^2$	$S_V = .50\ ft^2$
$c_W = .96$ ft	$c_V = .41$ ft
$S_h = 1.50\ ft^2$	length = 3.54 ft
$b_h = 2.74$ ft	Zinger 12 - 8 propeller

Scale: 1 inch = 1.74 feet

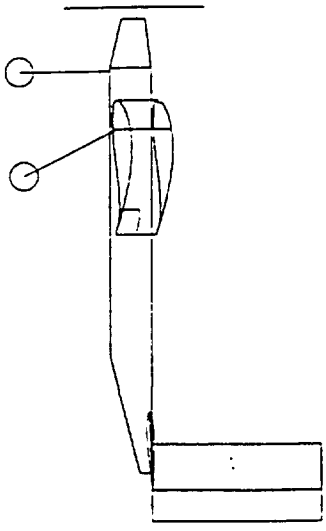

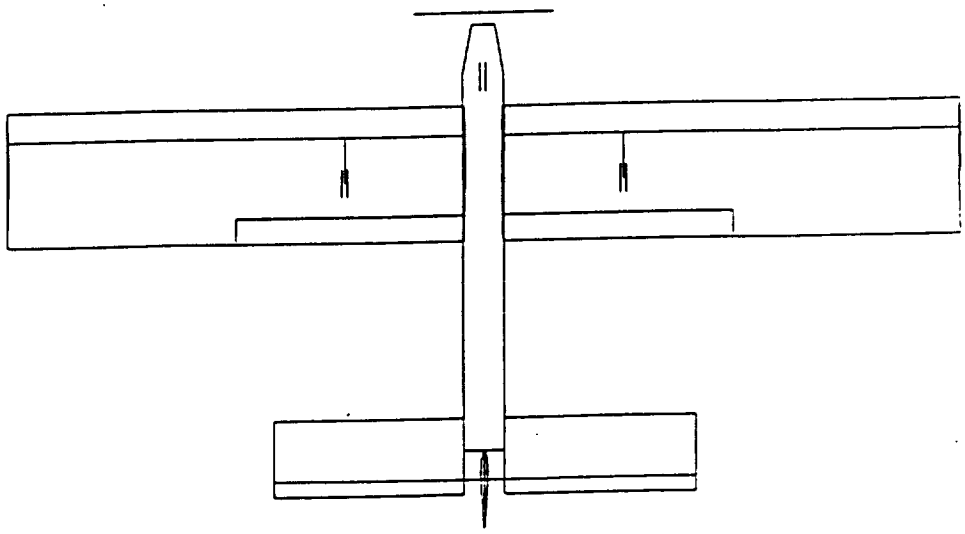

Figure 1-2: Internal Configuration

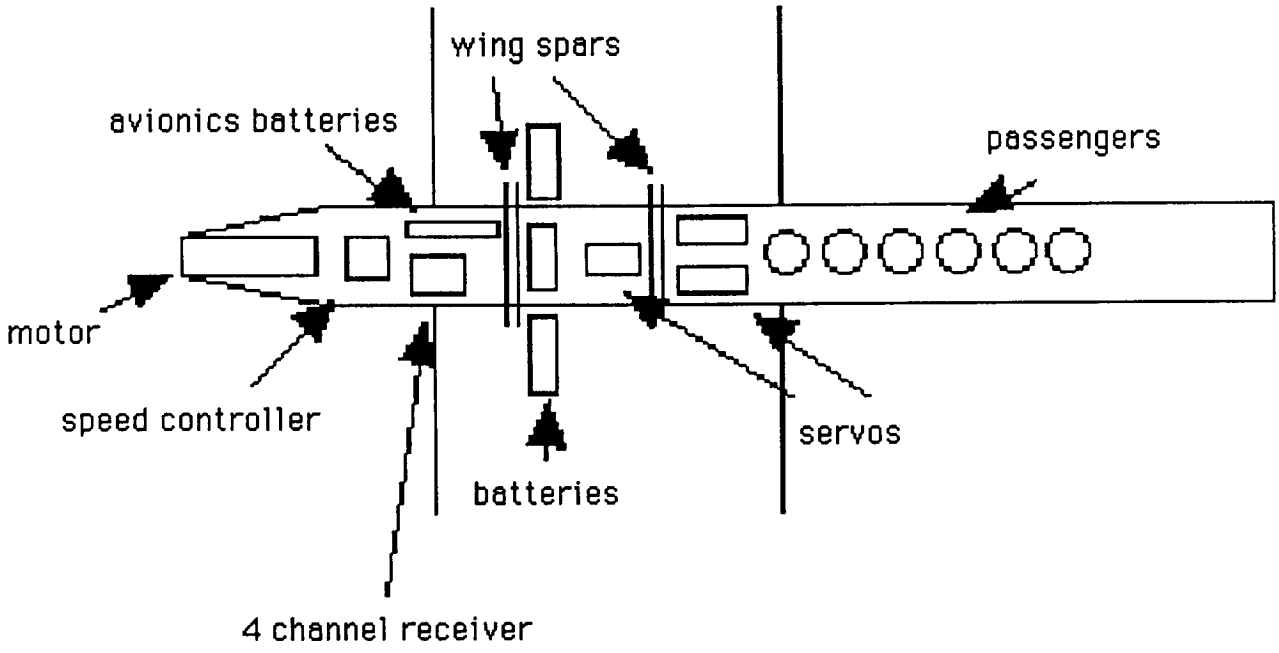

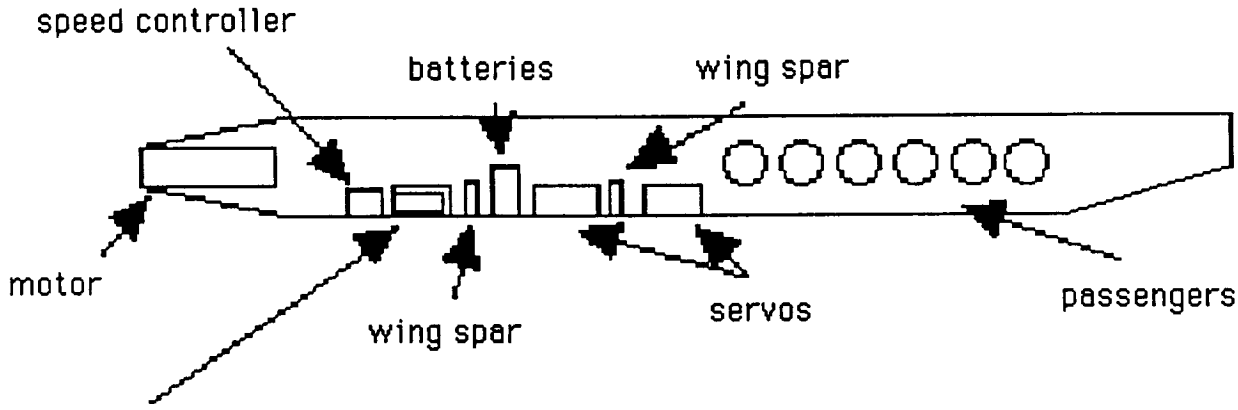

4 channel receiver and avionics batteries

milli-Amp hour Panasonic batteries located in the wing carry-through structure. The propulsion system is powerful enough to provide a cruise speed of 55 ft/s and a takeoff distance of 21 feet which will allow *The Balsa Bullet* to serve any airport in Aeroworld. The maximum takeoff weight is 4.60 pounds.

The aircraft configuration is a low rectangular wing monoplane with five degree wing dihedral. A design constraint of executing a level 60 ft radius turn at a speed less than 30 ft/s was placed on the aircraft. In relation to the cruise and maximum speed, this turn speed is low. As a result, a tradeoff exists between the large wing desired for low speed flight and the small wing desired for high speed flight. Selection of the wing size and characteristics had the most significant influence on the final design. In order to achieve the highest lift with the smallest wing possible, the FX-63-137 airfoil was chosen. The employs plain flaps extending twenty percent of the 11.52 inch chord and half the 6.33 foot span.

A rectangular fuselage provides each passenger with a spacious 18 in^3 seating and generous room for 9 in^3 of baggage. The rectangular fuselage was chosen over a more aerodynamic circular cross section because it requires less time to build thereby yielding a lower manufacturing cost consistent with the designs major objectives. The fuselage has an access hatch on the top for propulsion removal or installation in under twenty minutes.

The landing gear of *The Balsa Bullet* is exceptionally long as a result of the three inch grass outdoor takeoff requirement. The tricycle configuration was chosen to provide increased ground stability while providing fuselage grass clearance. The nosewheel landing gear is 8.0 inches long and the main gear are 7.8 inches long to provide propeller clearance. The main gear is slightly shorter to provide an aircraft take-off angle of attack of 2.25 degrees for

increased lift prior to rotation without further complicating wing attachment with an incidence angle.

The center of gravity of the Bullet at maximum takeoff weight is located at 27% of the mean aerodynamic chord. The neutral point of the aircraft is located at 49.2% of the mean aerodynamic chord, producing a static margin of 22.3% of the mean aerodynamic chord.

The control systems of the Bullet consist of a rudder which is fifty percent of the 0.5 square foot vertical tail and an elevator which is twenty percent of the 1.5 square foot horizontal stabilizer. Roll control is provided by rudder deflection and wing dihedral. A steerable nosewheel is also provided for improved ground handling. Unlike previous Aeroworld designs, *The Balsa Bullet* employs airfoil sections in the horizontal and vertical tails. The use of NACA 0009 airfoils reduces the drag while increasing aircraft performance and resistance to twist.

The critical technologies identified by the design team include flap effectiveness, mating the wing with the fuselage, and team manufacturing experience. Flaps are a concern due to uncertainty in their effectiveness on past designs. On some past aircraft, flaps appeared to be ineffective at best and sometimes a detriment while on other aircraft they seemed to be beneficial. It is difficult to ascertain whether airplanes employing flaps that proved detrimental or ineffective resulted from poor manufacturing of the wing and flap or if earlier designs failed to consider the drag increase associated with flaps and were unable to overcome it with their propulsion system. The wing and fuselage mating are a concern in two areas: attachment to the fuselage floor due to high stress concentrations, and at the edge of the fuselage where a tight seal must be made at the opening in the monokote where the wing carry-through enters the fuselage.

A critical technology which cannot be overlooked is the lack of experience of the design team in manufacturing. The lack of experience may have a negative impact on the final product and hurt the prototype's performance as a result of poor manufacturing rather than poor engineering.

The Balsa Bullet is not without it's weaknesses. Its predicted range will not allow it to fly directly from any airport in Aeroworld to any other airport including a one minute loiter and diversion to the nearest alternate airport. Though the *Bullet* was not designed to travel long distances non-stop, a competing aircraft of similar cost possessing a long range capability would be more attractive to a consumer. Also, the design is not aesthetically pleasing as a result of the square fuselage, wing, and empennage. These drawbacks may discourage some clientele from purchasing *The Balsa Bullet* .

Although *The Balsa Bullet* has these drawbacks, its economic appeal and high speed capability far outweighs them. *The Balsa Bullet's* affordability to a relatively large number of consumers will make it a success in Aeroworld, particularly as the first entry into the general aviation market.

Figure 1 - 2: Summary of *The Balsa Bullet* Specifications

Aerodynamics		**Empennage**	
Wing Area	6.33 sq ft	Horizontal Tail Area	2.958 sq ft
Aspect Ratio	7.2	Horizontal Tail Airfoil	NACA 0009
Span	6.75sq ft	Horizontal Tail Incidence Angle	-2.25 deg
Mean Chord	0.937 ft	Elevator Area	0.75 sq ft
Taper Ratio	1	Max Elevator Deflection	30 deg
Sweep	0 deg	Vertical Tail Area	0.5 sq ft
Dihedral	5 deg	Vertical Tail Airfoil	NACA 0009
Wing Airfoil Section	FX63-137	Rudder Area	0.25 sq ft
Wing Incidence Angle	0 deg	Max Rudder Deflection	30 deg
Flap Area	0.633 sq ft		
Max Flap Deflection	20 deg		
C_{Do}	0.0288		

Performance		**Propulsion**	
Take-Off Distance	21.3 ft	Engine	Astro 15
Velocity (min)	20.45 ft/s	Batteries	13 1.2V 1000maH
Velocity (max)	84.6 ft/s	Propeller	Zinger 12-8
Endurance (max)	13.92 min	Thrust (cruise)	0.528 lb
Range (max)	28692.2 ft	Thrust (max)	3.12 lb
		Propeller RPM (cruise)	4793.8

Structure		**Economics**	
Max Weight	4.6 lb	Direct Operationg Cost	$4.18
Fuselage Length	40 in	Cost per 1000 feet	$0.26
Fuselage Width	3.5 in	Total Aircraft Cost	$2562.11
Fuselage Height	3.5 in		

2.0 DESIGN REQUIREMENTS AND OBJECTIVES

AE 441, INC. management has decided to market the first general aviation aircraft to service Aeroworld. Currently, Aeroworld is serviced only by commercial transports thus leaving an entire market untapped. It has been determined that the first general aviation aircraft introduced to Aeroworld will be a low-cost, high speed, six passenger, electrically powered flight vehicle that will provide benign handling qualities without sacrificing performance. Lastly, the aircraft must be able to be mass produced.

2.1 Target Market

A map of Aeroworld, the *Bullet's* intended market, appears in Figure 2-1. As one can see, the majority of runways are 40 ft long but both City C and City O have runways which are only 28 ft long. *Long Shot Aeronautics* wishes to serve all cities in Aeroworld as both a convenience to our customer as well as maximizing availability in the market. Thus a 28 ft takeoff distance objective is imposed on the design by the design team.

Since a commercial transport fleet exists and it is not the nature of general aviation aircraft to fly great distances non-stop, the *Bullet* is targeted for a range of 16000 ft including diversion to the nearest alternate airport and a one minute loiter. By not trying to compete against the lower cost of commercial transports over great distances, the *Bullet* will require lower capacity batteries. Lower capacity batteries are cheaper to purchase than high capacity batteries and are lighter as well which provides a weight savings that translates into an additional cost savings.

Figure 2 - 1: Aeroworld

Aeroworld Airport Information

Below is a map of Aeroworld as well as a table of the latitude and longitude of each of the cities. Each latitude and longitude increment represents 500 ft.

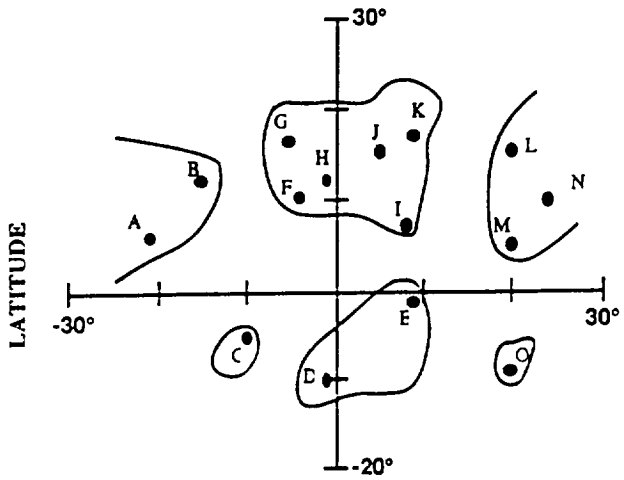

City	Longitude	Latitude	Runway Length Factor
A	-21	6	1
B	-15	12	0.8
C	-10	-5	0.7
D	-1	-10	1
E	9	-1	1
F	-4	10	1
G	-5	17	1
H	-1	12	1
I	8	7	1
J	5	15	1
K	9	17	1
L	20	15	1
M	20	5	1
N	24	10	1
O	20	-9	0.7

Figure 2-2 shows the numbers of flights for a given range between the airports of Aeroworld. With a design range of 16000 ft, *The Balsa Bullet* will serve approximately 56% of all possible flights. This percentage increases to 84% without loiter and diversion. It is important to note that all cities in Aeroworld are able to be served with a single stop.

For the market targeted by *Long Shot Aeronautics*, three primary design drivers have been identified: high speed to make the aircraft performance attractive to the consumer; low cost so a large number of consumers can purchase the *Bullet* ; and able to takeoff within 28 ft to enable the airplane to service every city in Aeroworld.

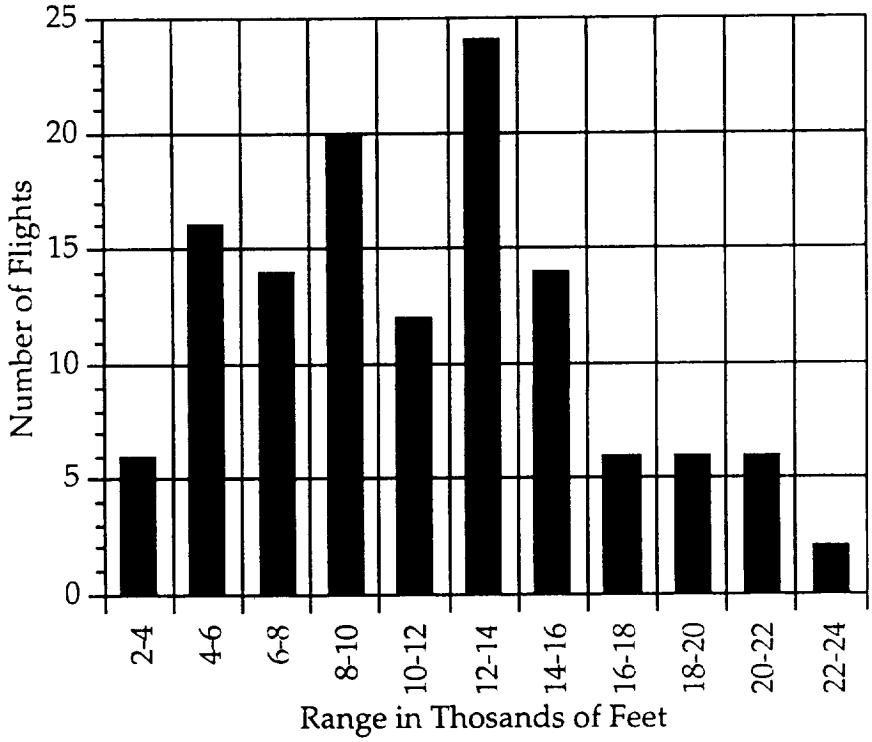

Figure 2 - 2: Number of Flights for a Given Range

2.2 Requirements

The following are the performance and manufacturing requirements and objectives for the proposed aircraft to operate successfully in Aeroworld as determined by AE441, INC. upper management and meet the constraints imposed by the indoor and outdoor flight test environments.

2.2.1 Performance

- Execute a level 60 ft radius turn at a speed less than 30 ft/s
- Fly a closed figure eight course less than 40 yds x 100 yds without exceeding an altitude of 25 ft
- Clear a 50 ft obstacle within 200 ft on open course with 3 inch grass rough field characteristics
- Maximum take-off distance of 40 ft indoors, 60 ft outdoors
- Range capability to service any two existing airports with stops for refueling

2.2.2 Manufacturing

- 6 passenger capability
- 4 in3 baggage per passenger
- Battery placement in wing carry-through structure
- Minimum propeller clearance of 3 inches
- Propulsion system installation in under 20 minutes
- $290.00 maximum limit on raw materials
- Maximum of 4 servos for a 4 channel transmitter
- 2 week maximum construction time
- Avionics crash survivability
- Must meet all pertinent FAA and FCC regulations

2.3 Objectives

The following are the performance and manufacturing objectives of *Long Shot Aeronautics* for the production of *The Balsa Bullet*. These are the characteristics deemed necessary and attainable to produce a high quality aircraft to the consumer.

2.3.1 Performance

- Minimum range of 16000 ft including loiter and diversion
- Maximum velocity: at least 75 ft/s
- Cruise velocity: at least 55 ft/s
- Maximum takeoff distance indoors of 25 ft

2.3.2 Manufacturing

- Maximum manufacturing time of 90 hrs
- Weight estimate: 4.60 lb max
- Manufacturing cost: $1600.00 max
- Minimum load factor of +2.0/-1.0
- Crash survivability of 12.0 lb
- 8 in^3 per passenger seating

2.4 Exceptions From Original DR&O

There are no exceptions to the DR&O submitted 25 January 1994.

3.0 CONCEPT SELECTION

3.1 Preliminary Concept Proposals

In order to produce a design to meet the requirements set forth by AE 441, INC. management, each of the six design team members submitted individual preliminary concept proposals. Electric engines are considered state-of-the-art in Aeroworld and appear in each concept. Only single engine concepts were considered in order to avoid the significant cost of purchasing a second engine in keeping with the design team's low cost objective of not exceeding $1600.00 in purchasing and manufacturing costs. From these six proposals the design team has the option to select one of the designs or attributes from each of the six designs to produce the final product. An overview of each proposal will be presented followed by the final design selection and rationale. Traits common to all the concepts will first be explained, however it should be noted that the assertions made are qualitative in nature due to the time constraints imposed in the design. Quantitative analysis was reserved for the final design selected.

In each preliminary design concept a rectangular fuselage was proposed. This results from the desire to produce a reliable low cost aircraft. A circular fuselage, while more aesthetic and aerodynamic, would be much more difficult to manufacture. The difficulty lies in making a circular cut across the grain of soft woods chosen for their low weight without splintering the piece being tooled. Additionally, there would be an increased tooling cost for circular cuts as opposed to straight cuts used in rectangular fuselage manufacture. Bending the wood used in longerons is also time consuming and requires precision to achieve a consistent desired circular fuselage shape. This difficulty in manufacturing the aircraft would lead to higher prices as a

result of the increased manufacturing time in turn damaging the design team's low cost objective. Additionally, *Long Shot Aeronautics* is compelled to build as simple a design as possible due to a lack of manufacturing experience.

Every preliminary design also suggested the use of tricycle landing gear with a steerable nose wheel. Tricycle landing gear are attractive for three major reasons. First, the possibility of ground looping which exists for a tail dragger configuration is not present with the tricycle gear. Secondly, a tailwheel would not raise the tail end of the fuselage out of the three inch grass increasing the takeoff roll. Third, a tricycle landing gear configuration also maintains a forward center of gravity position thus allowing for a smaller horizontal tail for control as a result of the increased moment arm.

A final attribute common to all six proposals entailed use of a rectangular wing. Taper would require different size ribs along the span whereas a rectangular wing uses ribs of a single size. All of the ribs can be cut at one time from a template for the rectangular wing thus lowering manufacturing time and overall cost. The *Bullet* does not operate at flight speeds which make sweeping the wing beneficial. Sweep would add a second angle in addition to the dihedral that must be accounted for in attaching the wing to the fuselage. This second angle is detrimental as the design would be complicated and probably require additional material to successfully attach the wing to the fuselage thereby increasing the cost.

3.1.1 Concept A

Concept A (see Figure 3-1a) is a high wing monoplane design with rectangular fuselage and a V-tail. The design employs tricycle landing gear and a rectangular wing with flaps. The high wing was chosen to provide roll

stability and simplify the manufacturing process by eliminating wing dihedral and allowing the wing to be attached to the upper surface of the fuselage by a simple bracket. By having a removable wing, the interior of the plane becomes more accessible while allowing the wing to be manufactured as a part separate from the fuselage construction. A major disadvantage of this design results from the requirement for battery placement within the wing carry-through structure. In doing so, a platform would need to be constructed to support the batteries. In addition to increased material costs, the center of gravity would be raised farther above the ground thereby increasing the possibility of tipping over on the necessarily long landing gear.

The V-tail was chosen as a way to reduce interference effects from the wing on the tail surface. Wing interference is important due to the short fuselage associated with a general aviation aircraft. The V-tail is complicated from a controls perspective as the system must allow for both synchronous as well as differential actuation of the control surface. Attaching a V-tail to a rectangular cross section would require an increase in structure over a simple cruciform tail due to the angle of attachment and loading experienced by the tail. Difficulty in construction, coordination of the control surface actuation, and a possible increase in weight and cost associated with the V-tail made this option unattractive.

Flaps are proposed as a way to provide the necessary lift for takeoff from all Aeroworld runways. The major advantage that results is a smaller wing. A smaller wing is more efficient at higher speeds than a lower wing. The disadvantage of flaps is a wing that is more difficult to construct than a wing without control surfaces. There is also a production cost increase associated with the purchase of a servo to control the flaps, additional weight from structure necessary to support the flaps, and increased time to

manufacture a wing with flaps over a wing without control surfaces. This cost can be offset in the long run through a decrease in operating costs associated with a more efficient cruise at a higher lift-to-drag ratio. The weight increase for additional structure for the flaps is offset through the decreased size of the wing when flaps are used.

3.1.2 Concept B

Concept B (Figure 3-1b) is a high rectangular wing monoplane with tricycle landing gear, cruciform tail, ailerons, and side by side passenger seating. The high wing was chosen for the same reasons as those listed in Concept A and carries with it the same disadvantages.

Side by side passenger seating was chosen to ease passenger access to seating and baggage areas. In doing so the fuselage has a greater frontal area than single file seating and a much greater profile drag. Additionally, the shorter fuselage associated with side by side seating will increase the horizontal tail area for control purposes as well as increase wing interference on the tail.

Ailerons were suggested as a way to improve the control of the aircraft in turns. The roll control provided by ailerons also minimizes the skidding and slipping sensations experienced by the passengers and pilot associated with maneuvering. The drawback of using ailerons instead of flaps is increased wing area leading to less efficient high speed characteristics, particularly in cruise, which will increase operating costs. Ailerons also incur a weight penalty because unlike flaps, there is not a decrease in wing size to offset the additional structure needed.

3.1.3 Concept C

Concept C (Figure 3-1c) is a low wing monoplane with tricycle landing gear, cruciform tail, tapered rear fuselage, and a canopy. The low rectangular wing employs dihedral to provide roll stability with ailerons for roll control. The low wing was chosen for improved aesthetic qualities as well as allowing battery placement lower to the ground. As proposed, the low dihedral wing will be more difficult to attach to the fuselage than the high wing designs for several reasons. The low wing is permanently mounted at an angle to the fuselage floor. This angle requires materials strong enough to sustain the concentrated loads at the point of attachment. The mating of the wing and fuselage at the root is difficult because a hole in the fuselage monokote must be made for the wing carry-through structure. This interface must be effectively sealed in order to not jeopardize aerodynamic integrity. These aspects of the design illustrate that unlike the high wing which can be built separate from the fuselage, the low wing must be built in close association with the fuselage.

The aft body is tapered for improved aerodynamics. Aft body tapering, although not extremely difficult, is more difficult than running a continuous straight beam down the length of the fuselage due to the need for an interface from which the tapering can begin. An increase in the number of joints increases the weight due to use of more glue. Taper may also decrease structural integrity barring increased structure due to the angled interfaces as well as complicate load path determination.

The use of a canopy on Concept C is a feature not found on previous Aeroworld designs. Previous designs internalized the pilots and passengers without really providing a way for the pilots to see forward of the aircraft without engine obstruction. The canopy could also be used as the interior

Figure 3 - 1: Concepts A, B, and C

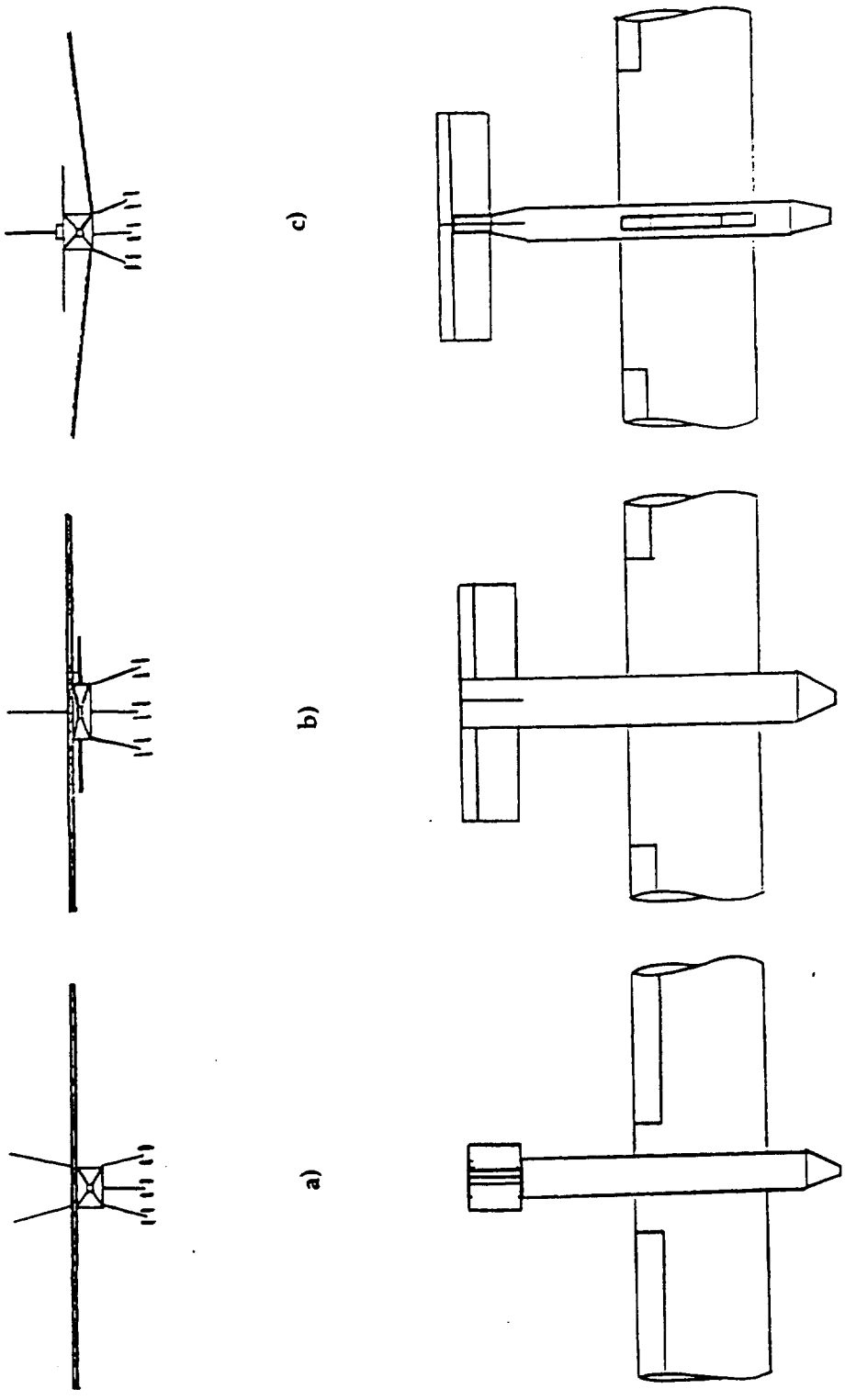

Figure 3-1: Concepts A, B, and C

access panel to meet the propulsion system removal requirement and provide interior access. An obvious drawback is the increased drag associated with a canopy over internalization of the pilot and passengers within the fuselage.

3.1.4 Concepts D, E, and F

These concepts, appearing in Figure 3-2, incorporate attributes previously mentioned in Concepts A, B, or C. As such they will have the same advantages and disadvantages previously noted.

Concept D is a high wing monoplane with cruciform tail, flaps, and canopy. Concept E is a low wing monoplane with side by side passenger seating, a canted forward fuselage to allow the pilots to see over the engine, fore and aft taper, and a cruciform tail. Concept F is a high wing monoplane employing a V-tail and midspan ailerons.

A summary of the major aircraft characteristics with their associated strengths and weaknesses appears in Table 3-1.

Feature	Strengths	Weaknesses
High wing	•inherent roll stability •easier to manufacture	•requires additional floor for batteries in carry-through •raises aircraft c.g.
Low wing	•meets battery placement requirement •lowers c.g.	•requires dihedral to provide roll stability •more difficult to build
Flaps	•decrease wing size •improve cruise and takeoff performance	•lose ailerons •poor performance on similar wing in earlier aircraft
Ailerons	•increase roll control and overall handling qualities	•lose flaps and associated benefits
Canopy	•provides forward view	•increases drag significantly
V-tail	•reduces wing interference on tail	•increased weight and difficult to build
Square fuselage	•easy to build therefore cheaper	•not as aerodynamic as a circular fuselage

Table 3-1: Strengths and Weaknesses for Various Concept Attributes

Figure 3 - 2: Concepts D, E, and F

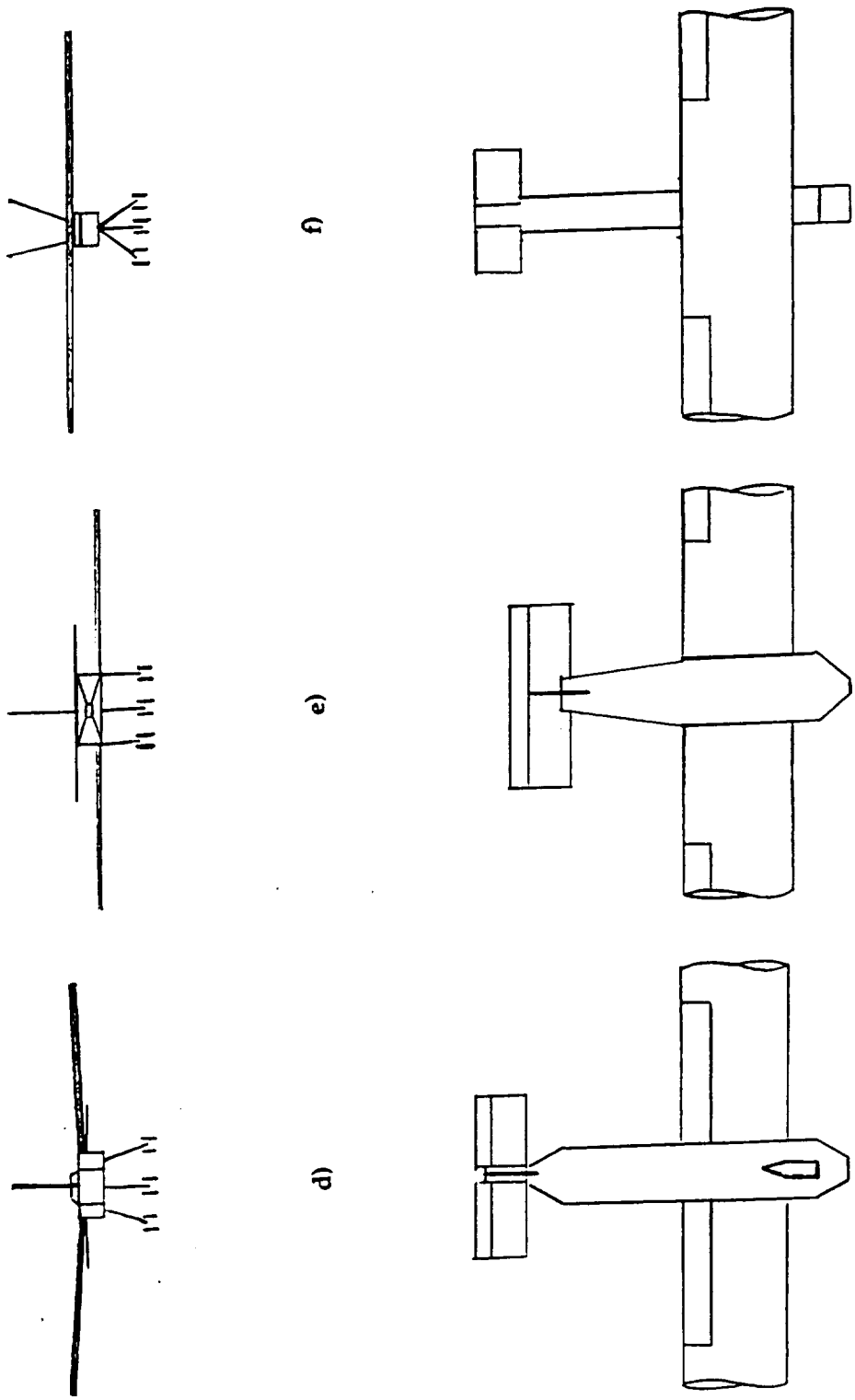

Figure 3-2: Concepts D, E, and F

3.2 Final Design Selection

The final design (Figure 3-3) chosen maintained the traits common to all six design proposals: tricycle landing gear, rectangular shaped fuselage, and a rectangular wing for the advantages stated earlier. A cruciform tail was chosen due to the manufacturing difficulties associated with a V-tail and because a large fleet of aircraft using the cruciform design are available for reference. Due to the battery placement requirement and the necessary use of unusually long landing gear for the outdoor flight test requirement, a low wing aircraft was chosen. This decision increased the final design's stability through a lower center of gravity and removed the need for additional structure other than a floor to support the batteries thereby reducing cost.

As the design analysis began, the configuration included ailerons instead of flaps. However, initial aerodynamic and performance analyses indicated the need for a smaller wing during cruise to achieve the necessary speed objectives and avoid large negative angles of attack to maintain a level cruise altitude. Without flaps, the large wing required to meet the stated takeoff distance of 25 ft would require a significant negative angle of attack to prevent the aircraft from climbing at the cruise speed assuming the increased drag associated with the wing and fuselage at this attitude could even enable the *Bullet* to reach its cruise velocity. The decrease in cruise efficiency would also impact negatively on the operating cost of the airplane. Flaps will also help meet the short field takeoff objective of the group. Given these factors the decision was made to switch to flaps from ailerons.

A canopy was not chosen due to the inherent drag penalty and negative effect on aircraft high speed performance, a major design driver. In light of the number of successful flights made in Aeroworld in aircraft without canopies, this decision seems to have little, if any sacrifice.

A feature which does not appear on the preliminary proposals but does appear on the final design is the use of an airfoil section for both the horizontal and vertical tail. By using an airfoil, the design experiences less drag than the flat plate sections appearing in the proposals. This drag decrease provides the *Bullet* with an increase in performance. Additionally, an airfoil is less subject to twist than a flat plate, thereby assuring a consistent response from the aircraft in flight.

Figure 3 - 3: *The Balsa Bullet*

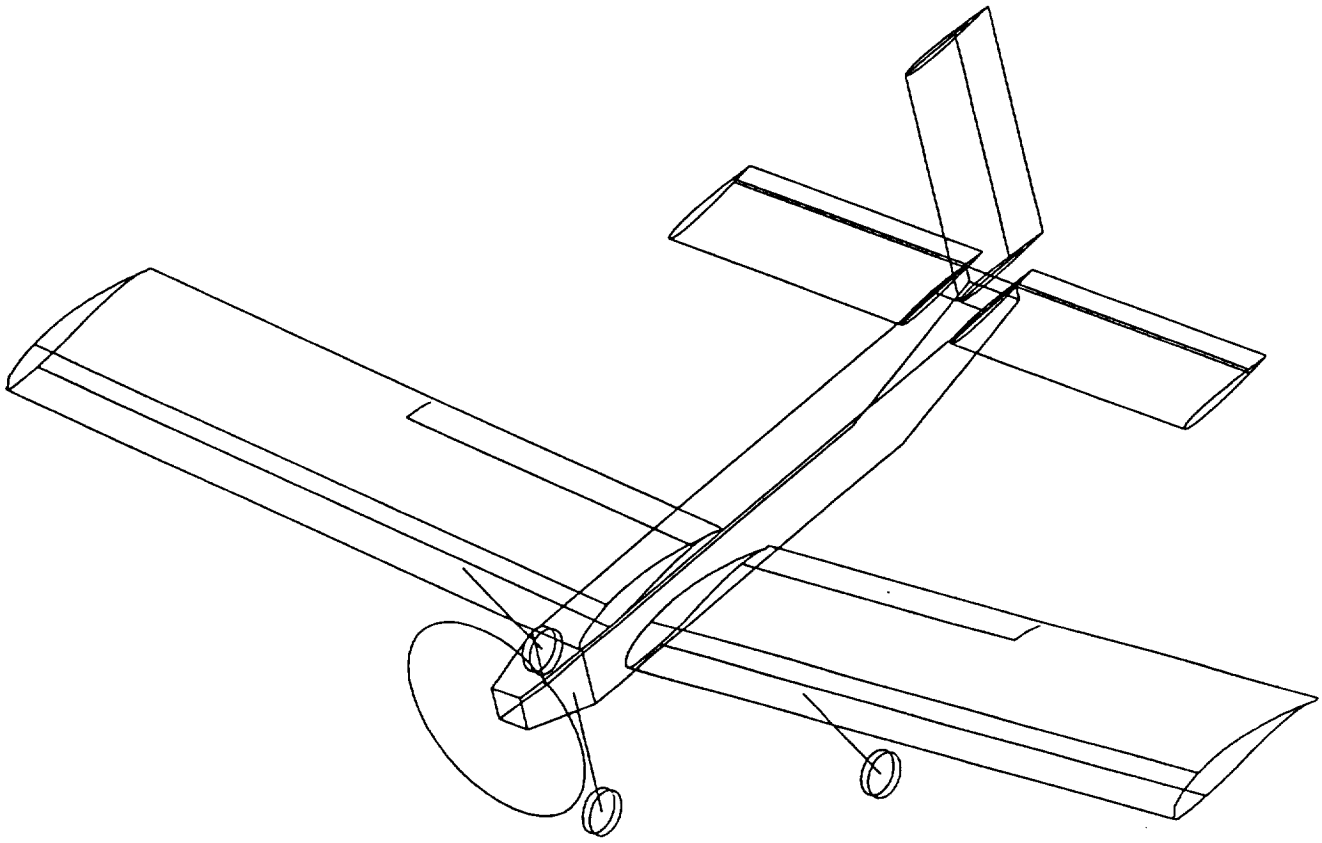

4.0 AERODYNAMICS

The aerodynamic design of *The Bullet* , especially the wing design, was the most difficult task in the design process. The high-speed(55 feet/second) versus short takeoff distance (25 feet) conflict was the primary driving factor in the design. Although this conflict was the primary design driver, cost and ease of manufacturing also played a significant role in the aerodynamic design. These drivers led to the major dilemma of whether or not to use flaps. The decision to implement flaps was made rather late in the design process to increase efficiency and decrease wing area.

It should also be noted that Reynolds number effects are a critical aerodynamic issue since *The Bullet* flies in a relatively low Reynolds number regime (Re = 350,000 for a cruise speed of 55 ft/s and chord length of .94 ft).

4.1 Airfoil Selection

The selection of an airfoil section for *The Bullet* was driven primarily by two main factors:

Design cruise speed goal of 55 feet/second
Takeoff distance of 25 feet

First, good aerodynamic performance is paramount not only for high speeds, but also for lower costs. The airfoil must exhibit low drag characteristics. Also, high lift characteristics are essential to attain takeoff requirements. Second, the geometry of the airfoil is crucial to the design of *The Bullet*. The airfoil must be at least an 1.25 inches thick to allow the batteries to be placed in the wing. Although this added thickness is a weight penalty, the structural resistance to longitudinal wing twist is reduced. Finally, because ease of manufacture is an important concern as well, airfoil geometry again becomes relevant.

In the low Reynolds number regime in which *The Bullet* will be operating, there are several airfoil sections which merit consideration. Using data from Reference 13, Table 4-1 lists several of these airfoil options.

Airfoil	Max Cl	% Thickness	% Camber	Cd @ 0 deg Re = 300,000
Aquila	1.3 @ 12 deg	9.38	4.05	.03
Clark Y	1.2 @ 10 deg	11.72	3.55	.011
WB 140-35	1.15 @ 10 deg	13.92	3.7	.01
FX-63 137	1.6 @ 12 deg	13.7	5.94	.01

TABLE 4-1: AIRFOIL DATA

In order to select an airfoil that meets the mission requirements some type of trade-off must occur between the strengths and weaknesses of particular airfoils. In order to meet the short takeoff distance without employing flaps, a high C_l is needed. Keeping in mind the requirement that the airfoil be at least 1.25 inches thick to place the batteries in the wing carry-through structure, thickness becomes important. The WB 140-35 was eliminated from consideration due to its low C_l, even though it was the thickest of the airfoils. The Aquila has a significantly less thickness ratio than the other airfoils, which means the chord would have to be 20% larger to fit the batteries in the wing carry-through structure. For the rectangular planform of *The Bullet*, the net result would be a lower aspect ratio and consequently decreased aerodynamic performance. In order to achieve high speeds, drag must be minimal. Therefore, the L/D ratio for the airfoil must be considered. The L/D for the Clark Y is about 40 compared to 78 for the FX-63 137 at Re = 300,000.

The trade-off in choosing the increased aerodynamic performance of the FX-63 137 is a large moment coefficient (C_{mo} = -.24) and increased manufacturing difficulties. This large C_{mo} would effect trim characteristics of the airplane. The FX-63 137 was finally selected over the Clark as the airfoil

section solely because the need for high lift was a higher priority than ease of construction. It should be noted that this decision was made prior to the decision to use flaps. Therefore, a different airfoil may have been chosen if flaps were considered.

The FX 63-137 lift curve is shown in Figure 4-1. The maximum C_l is 1.6 and the lift curve slope is approximately .1/deg.

Re = 200,000

C_{mo} = -0.24
C_d = .01 @ 0 degrees

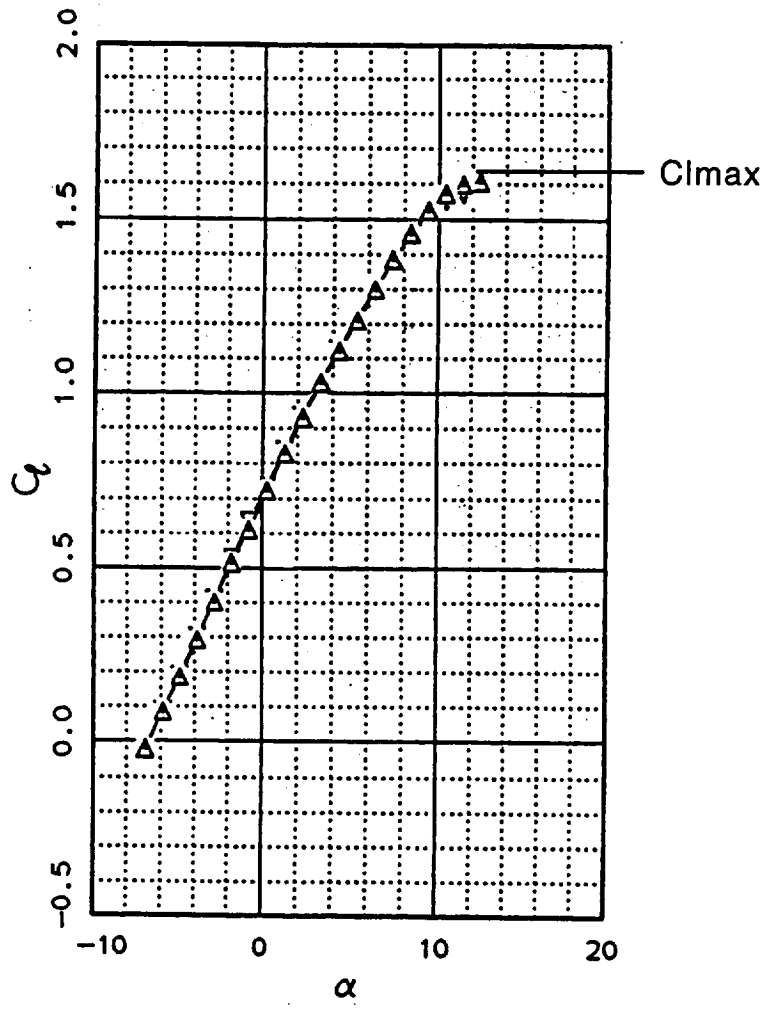

Figure 4-1: FX63-137 Airfoil Lift Curve

4.2 Wing Design

4.2.1 General

The wing design of *The Bullet* was the primary driver in the whole aircraft design. The characteristics of the wing played a crucial role in every aspect of the design decision making process. The primary goal of the wing design was to obtain the smallest wing area possible while still meeting all design requirements and objectives. Because of the requirement that two wings be fabricated for testing purposes, a rectangular planform was chosen with little hesitation due to its simplicity. Simple geometry also translates into less manufacturing time and ultimately less cost.

4.2.2 Wing Sizing

The main requirements that determined the sizing of the wing were

cruise performance
takeoff performance
turn performance
wing loading

AE 441, Inc., requires that the plane be able to execute a level 60 foot radius turn at a speed less than 30 feet/second. A takeoff distance of no greater than 25 feet was also an objective so that all airports in Aeroworld could be serviced by *The Bullet*. The wing loading must also be taken into consideration for the RPV's of Aeroworld. Management recommended that the wing loading should not exceed 12 ounces/foot, to ensure takeoff capabilities and structural soundness within the design.

In order to optimize the wing area, a computer program was written which determined the wing area using the aforementioned factors. A copy of the program is attached as Appendix G. The wing sizing process is a highly iterative

process based on several factors. Therefore, several assumptions were made to determine the wing area. First, and most importantly, a good weight estimate was required. As the design process evolved, the best weight estimate was 4.6 lb. The velocity at takeoff and during turns must also be known. Finally, the value of C_l is necessary to size the wing. C_L for the aircraft can be found by modifying the airfoil lift curve slope to account for three-dimensional down wash effects if the aircraft efficiency factor and angle of attack are known. The efficiency factor, e was assumed to be .8. To assure the passengers a comfortable ride, an angle of attack of 5 degrees was used during turns, while the angle of attack during takeoff was assumed to be 10 degrees without flaps to avoid stall.

Using a weight of 4.6 lb., the program solves for the wing area at both takeoff and during turns while constraining the wing loading to no more than 12 ounces/foot. For the turn performance case, the load factor for a 60 foot level turn at 25 feet/second was found using the relation:

$$n = (\sqrt{\frac{V_{turn}^2}{gR}})^2 + 1$$

Using this load factor the wing area can be found for turns using:

$$S = \frac{nW}{.5C_L\rho V^2}$$

Using a load factor n = 1 for takeoff along with the C_L from the methods described above, the wing area can be found for takeoff assuming $V_{takeoff}$ = 25 feet/second. The larger of the two areas determines the wing size. Prior to using flaps, the wing area converged at 7.2 sq.ft., while it converged to 6.3 sq.ft. using flaps in the design.

The aspect ratio of the wing was then found by imposing the restriction on the airfoil that the batteries be placed in the carry-through structure. Since the airfoil thickness is a function of chord, the chord for *The Bullet* was fixed at .94 feet. Knowing the area and chord, the span was found to be 6.75 feet, which

results in an aspect ratio of 7.2. The aspect ratio is an important design parameter since it determines the efficiency of the wing. As the aspect ratio increases better aerodynamic performance is expected, but the penalty paid results in a weaker wing structure. The aspect ratio of 7.2 imposed on *The Bullet* will not hinder the aerodynamic or structural performance of the design.

It should be noted that the C_{Lmax} for the aircraft was 1.3 without flaps. The value for $C_{L\,max}$ was obtained by multiplying the value of the aircraft lift slope (.077/deg) times the angle of attack of the airfoil, which is the stall angle of the airfoil(12 deg) minus the zero lift angle of the airfoil(-6 deg). Knowing the value of $C_{L\,max}$ to be 1.3 the C_L at takeoff was assumed to be 1.2, which is slightly less than $C_{L\,max}$. Knowing the lift coefficient at takeoff and the aircraft lift curve slope, the necessary angle of attack at takeoff can be determined. For *The Bullet* , the following relationship holds if the ground is the reference line.(i.e. the relative wind is parallel to the ground).

$$C_L = C_{L\alpha}(i_{ground} - \alpha_{Lo} - i_w)$$

where i_{ground} is the angle the fuselage makes with the ground and i_W is the angle at which the wing is mounted to the fuselage. In order to avoid construction difficulties that would arise by mounting a low-wing structure to the fuselage at an angle, i_W was kept at 0. Because the zero-lift angle is constant for the wing at -6 degrees, the angle at which the fuselage sits with respect to the ground becomes important. Since this is a maximum finite angle for a given fuselage length and landing gear length, the necessary C_{Lmax} to reach a takeoff distance of 25 feet could not be achieved without mounting the wing at an angle to the fuselage. Rather than mounting the wing at an angle, the decision to use flaps was implemented.

4.2.3 Flaps

The decision to use flaps was not one of necessity, but rather one of efficiency. As mentioned previously, the decision was made rather late in the design phase for several reasons. Because two of the main goals of the aircraft are to achieve high-cruising speeds and short take off distances, the lift coefficient must be as high as possible during takeoff. This can be achieved by using flaps or highly cambered airfoils. However, when highly cambered airfoils are employed, the wing is less efficient in cruise. Also, since takeoff is the primary controller of wing area, the addition of flaps can reduce wing area and increase efficiency at cruise. Using an aircraft weight of 4.6 lb., Table 4-2 illustrates the benefits when flaps are employed during takeoff.

Weight = 4.6 lb.	Wing Area	L/D @ cruise V = 55 ft/s
Bullet No Flaps	7.2 sq.ft.	3.8
Bullet w/flaps (.2c ,.5b) **(Flaps @ Takeoff only)**	6.3 sq.ft.	8.5

TABLE 4-2 BENEFITS OF FLAPS

Of course, the penalty for flaps is a larger drag at takeoff, increased production costs, and manufacturing difficulty. Also, flaps were a design risk because their effectiveness has been uncertain on previous RPV's in Aeroworld due to increased drag. However, the decision to use flaps was made to resolve the conflicting mission requirements of high cruise speeds and short takeoff distances and decrease wing area.

The sizing of the flaps was determined by takeoff performance as well. The takeoff distance for various flap chord sizes and deflections is illustrated in Figure 4-3.

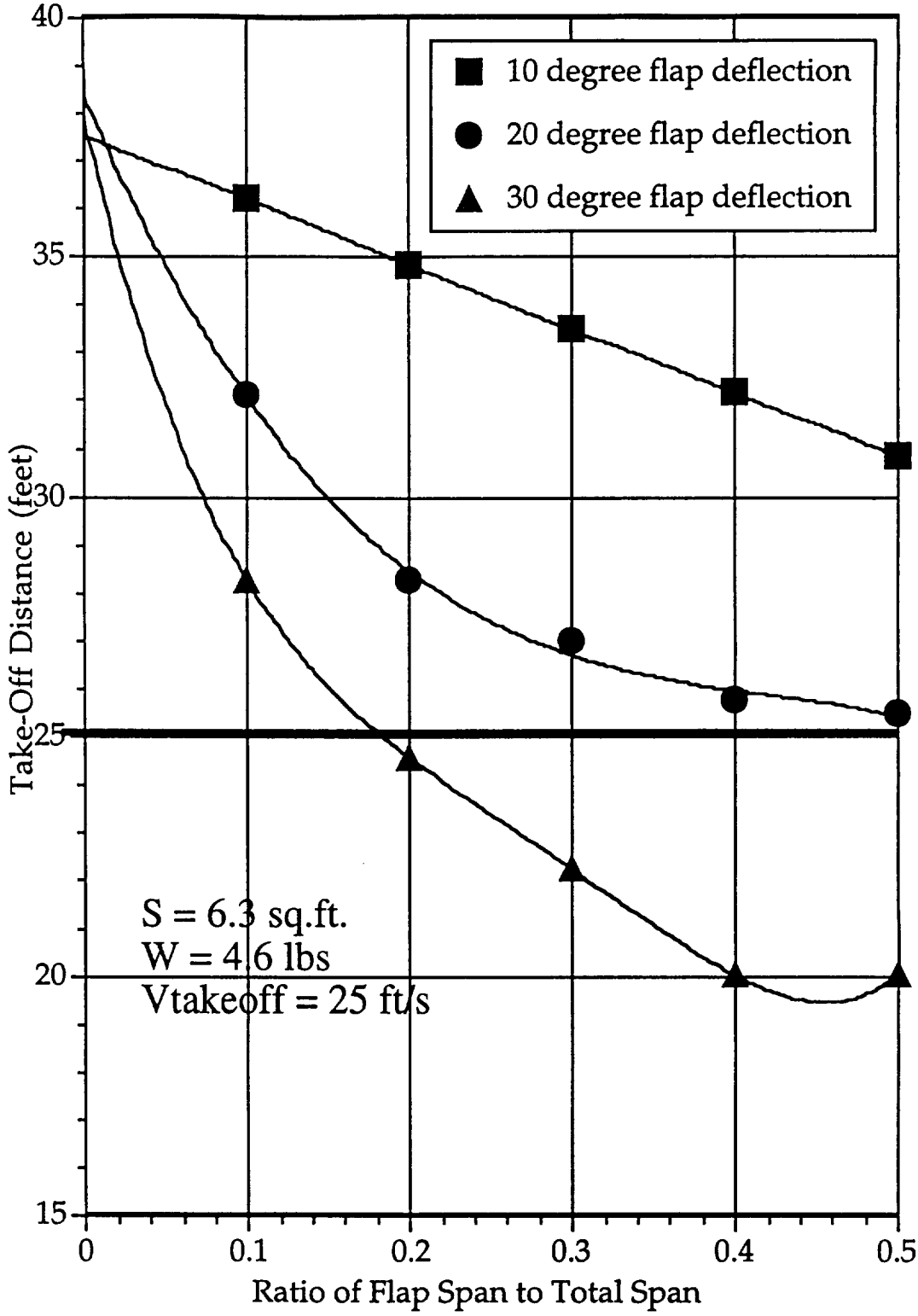

Figure 4-3: Effect of Flaps on Take-Off Distance

A flap size of at least 20% chord was desired for manufacturing reasons and a maximum deflection of 30 degrees was allowed. Takeoff and manufacturing considerations set the flap size at 20% chord and 50% span with a maximum deflection of twenty degrees to achieve the takeoff distance of 25 ft.

With the size of the flaps set at 20% chord and 50% span, their effect on the airfoil was determined for a maximum deflection of 20 degrees. Using the methods presented in Reference #. The flaps were found to increase the C_l of the airfoil by .2. However, the flaps also increase C_d by a factor of .02. The use of flaps does not effect the lift curve slope of the aircraft, but they do shift the curve up and decrease the stall angle. The final aircraft lift curve slope both with and without flaps is shown in Figure 4-5. These results were used in conjunction with the computer program in Appendix G to determine the final wing sizing and aircraft aerodynamic characteristics.

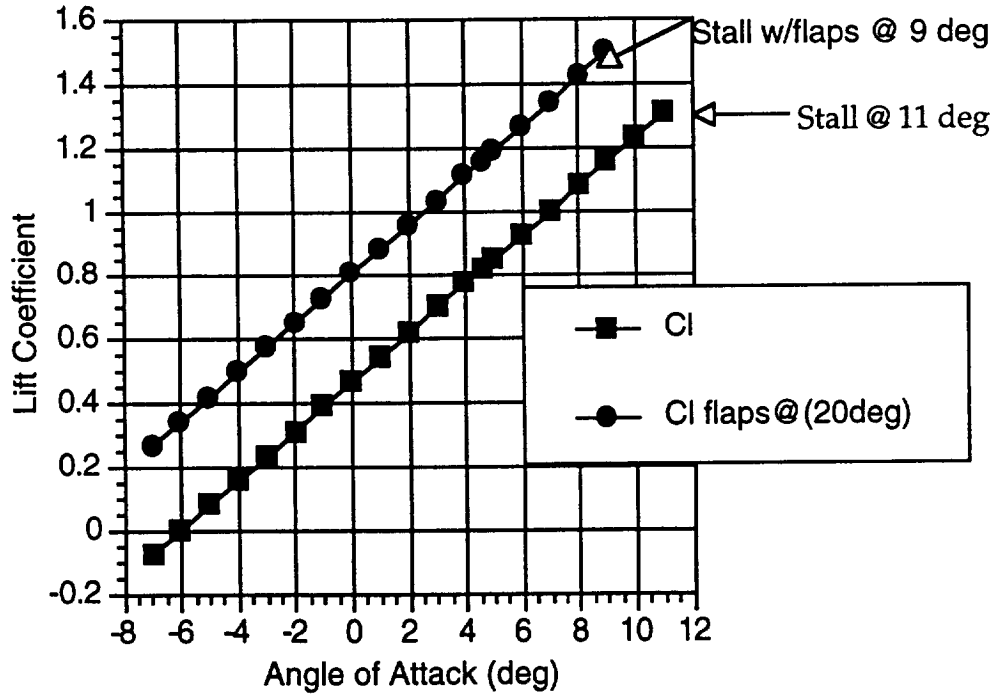

Figure 4-5 Aircraft Lift Curve

4.2.4 Dihedral

The decision to use flaps on a low-wing monoplane meant that ailerons were eliminated from the design, since all four available servos were now in use. The low wing design was chosen to avoid extra structural and cost penalties associated with placing the batteries in a high wing. The consequence of these decisions is that dihedral must be incorporated into the design to provide the necessary roll stability. As shown in Section 7-6, the necessary wing dihedral was 5 degrees.

4.2.5 Load Distribution

With the wing characteristics fixed, the next important parameter is the load distribution. The load distribution is needed during takeoff and at cruise conditions for structural considerations. Takeoff becomes especially important since this is when the wing will experience its greatest loads.

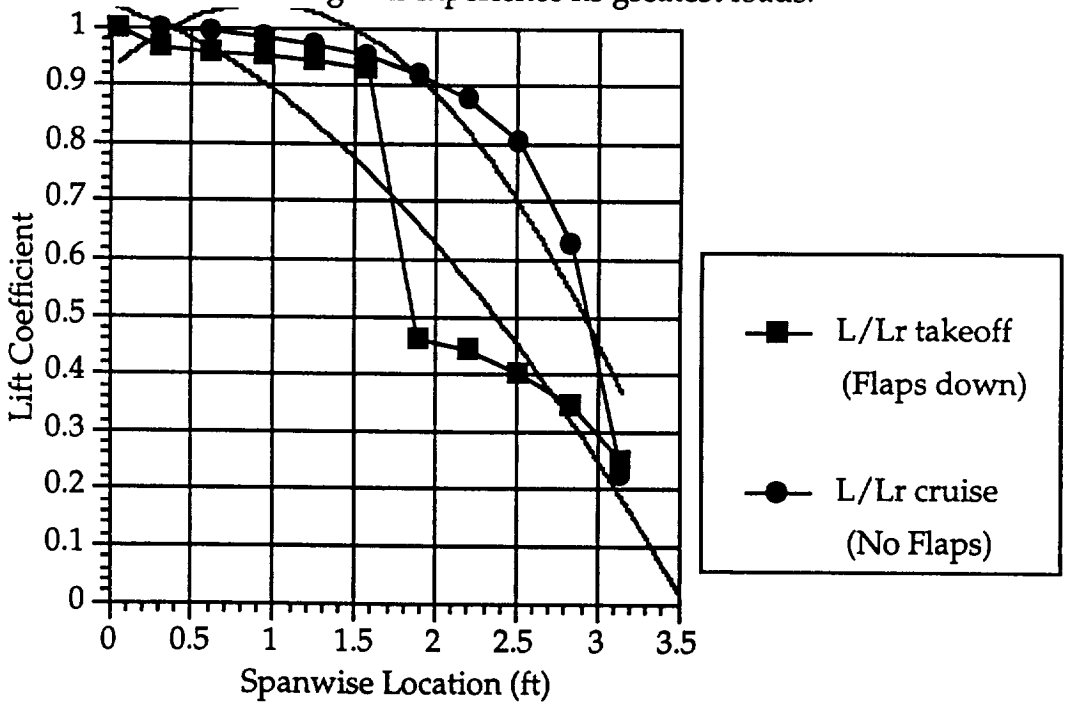

FIGURE 4-6: LOAD DISTRIBUTION

The load distribution was analyzed using a lifting-line code written in Aerodynamics 350. The results show what one would expect. The load distribution is approximately elliptical as shown by the curve fits. It should be noted that the load distribution changes greatly when flaps are deployed. The change in C_L is .2.

4.2.6 Final Wing Characteristics

The final wing characteristics of *The Bullet* are shown in Table 4-4.

Wing Area	6.3 sq.ft
Span	6.75 ft
Aspect Ratio	7.2
Taper Ratio	1.0
Dihedral	5 deg
Chord	.94 ft
e_w	.88
Wing Loading	11.6 oz/sq.ft.

TABLE 4-4: FINAL WING CHARACTERISTICS

4.3 Drag Prediction

The estimation of the drag coefficient is a difficult and challenging task even for the simplest of aircraft such as the RPV's of Aeroworld. The standard method used in determining aircraft drag prediction requires the drag to be split up into the parasite drag and induced drag. The governing equation can be found in most aerodynamic textbooks.

$$C_D = C_{Do} + \frac{C_L}{\pi A \, Re}$$

Although this equation seems simple, the real hurdle is predicting both the parasite and induced drag contribution for each aircraft component. Numerous methods are available with each one having its strengths and weaknesses. In order to obtain the most accurate drag prediction possible, three different methods were applied to our configuration.

4.3.1 Nelson's Method

An initial calculation for C_{Do} was performed using the component buildup method shown in Reference 11.

$$C_{Do} = \sum \frac{C_{D\pi} A_{\pi}}{S_{ref}}$$

The reference area used in the analysis was the wing area S = 6.3 sq. ft. The results are presented in Table 4-4.

Component	CDπ	Aπ (sq. ft)	(Source of Aπ)	CDo
Wing	0.007	6.3	Swing	0.007
Fuselage	0.11	0.0851	Fuselage Max frontal area	0.0015
Horizontal tail	0.008	1.5	Hor. Tail Area	0.0019
Vertical tail	0.008	0.5	Vert. Tail Area	0.0006
Landing Gear	0.014	6.3	Swing	0.014
Interference	15%			
			Total CDo =	**0.0267**

TABLE 4-4: DRAG BREAKDOWN : NELSON METHOD

4.3.2 Jensen's Method

Since Nelson's method applies to real world aircraft, it was necessary to find an alternative method which could account for the low Reynolds number flight regime of Aeroworld planes. Using Daniel T. Jensen's A Drag Prediction Methodology for Low Reynolds Number Flight Vehicles, a more detailed estimate of the drag can be found. The results are presented in Table 4-5 . The C_{Do} from the wing was found using data in Jensen's thesis for the FX-63-137 wing section at a Re of 300,000.

Component	Cfπ	FFπ	Swetπ (sq.ft)	CDo
Fuselage Body	0.003	1.0832	4.06	0.0021
Horizontal tail	0.0032	0.829	1.5	0.0013
Vertical tail	0.0035	0.829	0.5	0.0005
Wing (using	FX-63 137 @	Re=300000)		0.0118
Landing Gear (From Previous Method)				0.014
Interference 15%				0.0024
		TOTAL CDo	=	.0321

TABLE 4-5: DRAG BREAKDOWN: JENSEN METHOD

From Jensen's Method the percent contribution of parasite drag for each component was determined.

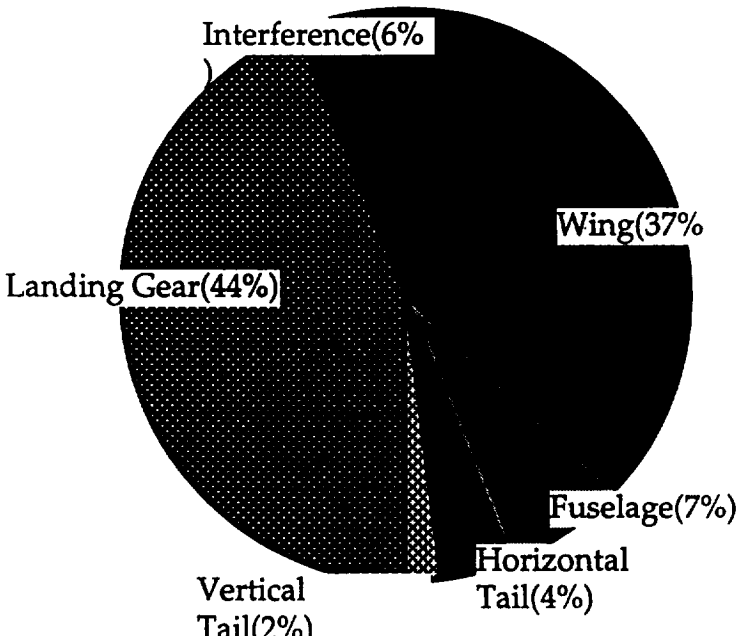

FIGURE 4-7: PARASITE DRAG BREAKDOWN

4.3.3 Landing Gear Buildup Method

As illustrated in Figure 4-2, the landing gear is the largest contributor to the parasite drag. Therefore in order to get a better estimate of the landing gear drag, a simple scheme was devised. The landing gear consists of three struts and three tires. The tires were treated as a combination of spheres (Cd = .4) and cylinders (Cd = 1.0) which gave an average Cd = .7. By modeling the struts as bluff body cylinders of known Cd = 1.0, a better estimate of the landing gear drag could be found as shown in Table 4-6.

Component	Cdo	Aπ (sq.ft)	CDo
Main Struts	1	0.0063	0.001
Nose	1	0.0025	0.0004
Tires(3)	0.7	0.0558	0.0062
Landing Gear Total			0.0076
Rest of Plane (From Nelson Method)			0.0127
Interference 15%			
		Total CDo =	**0.021**

TABLE 4-6: DRAG BREAKDOWN: LANDING GEAR BUILDUP

This final method seems to give the most appropriate C_{Do} , since it combines both low Reynolds number effects and a detailed landing gear drag buildup.

4.3.4 Induced Drag

In order to find the drag polar for the aircraft, only the aspect ratio and Oswald efficiency factor remain to be calculated. The aspect ratio was fixed at 7.2 for reasons previously discussed. The Oswald efficiency factor can be estimated using component buildup techniques similar to those used for the parasite drag.

$$\frac{1}{e_{a.c}} = \frac{1}{e_{wing}} + \frac{1}{e_{fus}} + \frac{1}{e_{other}}$$

Once again, using the methodology given by Jensen, $e_{a.c}$ can be found. The value for e_{wing} can be found from Jensen(Figure 3.3) and is equal to .88. This leaves e_{wing}=.88. The

value for the fuselage efficiency can be found using $e_{fus} = \frac{E_{fus} S_{ref}}{S_{fus}}$. Efus is equal to .6 for aircraft if Jensen (Figure 3.4) is applied. Assuming $e_{other} = 20$, the total aircraft efficiency factor, $e_{ac} = .82$ for *The Bullet.*

4.3.5 Drag Polar

The drag bucket for *The Bullet* is presented in Figure 4-4.

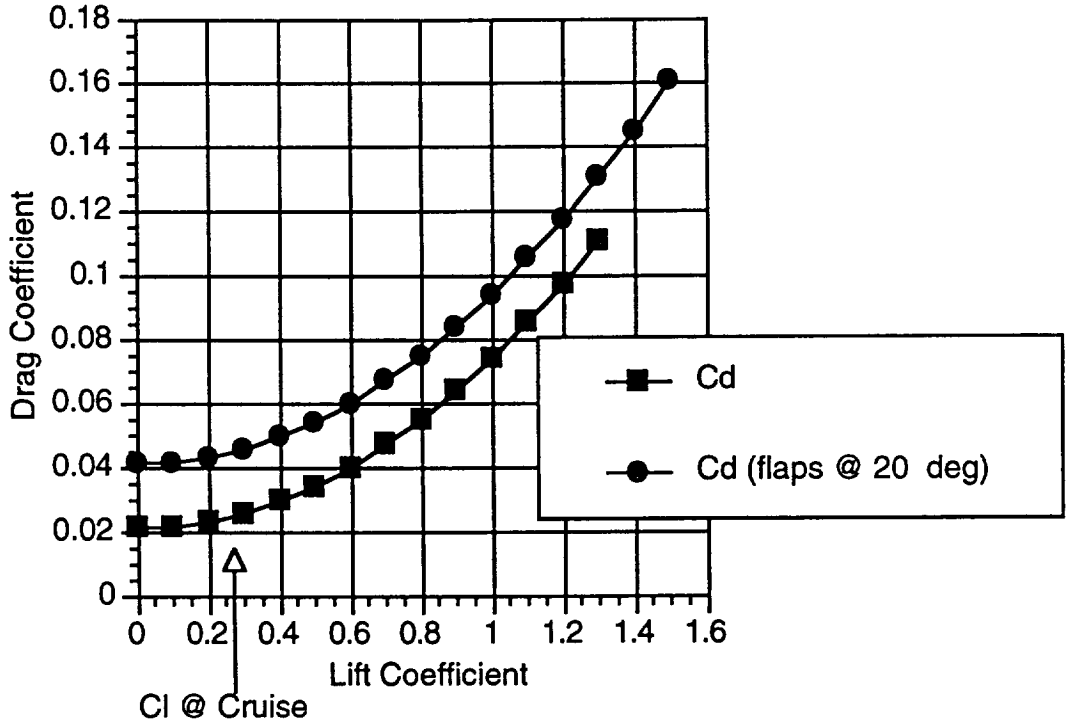

FIGURE 4-4: AIRCRAFT DRAG POLAR

4.3.6 Aircraft L/D Curve

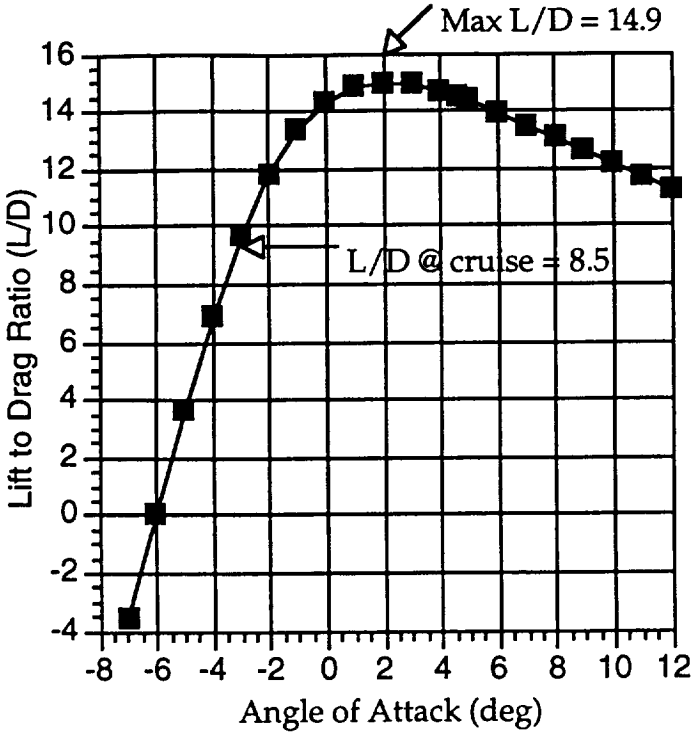

FIGURE 4-4: AIRCRAFT LIFT TO DRAG CURVE

4.3.7 Drag Reduction Possibilities

The drag on the aircraft is a key player in determining whether or not the design cruise speed objective of 55 feet/second could be met. Therefore, drag reduction possibilities were examined with the hope of attaining faster speeds. Three specific techniques were considered:

Splitter plates on struts
Wheel pants or cowlings
Winglets

Because the landing gear accounts for about 50% of the aircraft drag, it was targeted as a possibility for drag reduction. The size of the struts were constrained by structural considerations, and tire size was not flexible since *The Bullet* needed to be equipped for rough field takeoff roll . However, if the struts could be made more aerodynamic in shape by perhaps adding a piece of balsa to act as a splitter plate, the drag could be decreased . This idea may be used in the design of *The Bullet* when flying indoors

rather than outdoors where the plates may fall off in high grass. The idea of changing tires for the indoor and outdoor course was also a possibility, but due to the increased cost of buying an extra set of tires this idea was not deemed feasible. Another option was to use wheel cowlings for the tires. This idea was eliminated solely due to the fact that wheel cowlings are not sold locally, and would most likely hinder takeoff when used on the grass runway. Given more time and analysis, wheel pants technology, or perhaps even a splitter plate technology, could possibly be incorporated into future designs of *The Bullet.*

The Reynolds number at cruise is approximately 350,000 for the aircraft. Because of this relatively low Reynolds number regime the drag is mostly parasite drag rather than induced drag. Therefore, winglets, which reduce the induced drag, would simply add a weight penalty without much drag reduction. Once again, time constraints eliminated an in-depth study of winglet effectiveness.

4.4 Summary of Aerodynamics

The aerodynamic design of *The Bullet,* especially the wing design, was the most difficult task in the design process. In summary, the high-speed versus short takeoff distance was the primary driving factor in the design. The final aerodynamic parameters are summarized in Table 4-7. Although we are confident in our design, there are some potential problems. First, the flaps may not be fully effective due to the large drag increase. Second, the monokote may deform the airfoil shape and degrade performance. Third, many of our predictions are based on educated guesses from analytical data. For example, the lift curve slope of the airfoil is an estimate from the graph, yet it greatly affects all other aspects of the design. Finally, if our weight exceeds 4.6 lb., then the we run the risk of exceeding the takeoff distance objective of 25 feet.

Airfoil		Aircraft		Flaps	
FX 137-63		Max C_L	1.5	size	20% c
Section Cl max	1.6	C_L alpha	.077/deg	length	50% b
Cl alpha	.1/deg	C_{Do}	.021	type	plain
C_{mo}	-.24	e	.82		
		L/D max	14.9		

Table 4-7 Aerodynamic Summary

5.0 PROPULSION

5.1 General Overview

Electrical propulsion systems are considered state-of-the-art in Aeroworld, and will be used to power the RPV. The propulsion system is composed of three main components - engine, propeller, and fuel system (batteries). All components function together, and must be selected as a unit. The driving factors behind the propulsion selection process were maximum obtainable level velocity and satisfactory takeoff performance, while incurring the smallest cost and weight penalties. While these drivers were paramount, the other performance design requirements and objectives could not be neglected.

5.2 Propeller Design

A code, PROP123, was used to predict propeller performance. The code calculates performance using simple blade element theory. Induced velocity and tip loss corrections were available through the program, and both were employed. Reynolds number and Mach corrections were also options for correcting the airfoil section C_l and C_d data, but these refinements were not used. With only Reynolds and Mach corrections the propeller data was found to be the most conservative, and in that sense the best, estimate of propeller performance.

One restriction was placed on the propeller by the design team. The propeller diameter was not to exceed 12 inches. This was imposed to limit the length of the landing gear, and meet the clearance objective for rough field takeoff without incurring substantial drag penalties. Landing gear, especially thick struts, adds significantly to the overall drag, and diminishes the performance of the aircraft.

Propellers ranging in diameter from 9 to 12 inches were studied. These propellers had 2 or 3 blades and pitch values ranging from 4 to 8 inches,

depending on availability. From initial studies of the data it was seen that takeoff and high speed performance improves with increasing propeller diameter, pitch, and number of blades. A chart outlining this trend is presented as Table 5-1 below.

	Advantages	Disadvantages
Larger propeller diameter	takeoff and high speed improvements	length of landing gear increases
Larger propeller pitch	takeoff and high speed improvements	none
More propeller blades	takeoff and high speed improvements	cost and weight increase

Table 5-1: Propeller Selection

An important note from Table 5-1 is that 2-bladed wooden propellers are preferred because they are significantly less expensive ($3.50 as compared to $10.00), and weigh but a fraction of their 3-bladed plastic counterparts (approximately 0.6 ounces less).

The performance of possible propellers was examined, and appears in three graphs. All of the propellers in these charts are 2-bladed except for the 10-8 model which has 3 blades. Figure 5-1 shows the dependence of propeller efficiency on advance ratio. Figures 5-2 and 5-3 depict the effect of advance ratio on C_T and C_P for various possible propellers.

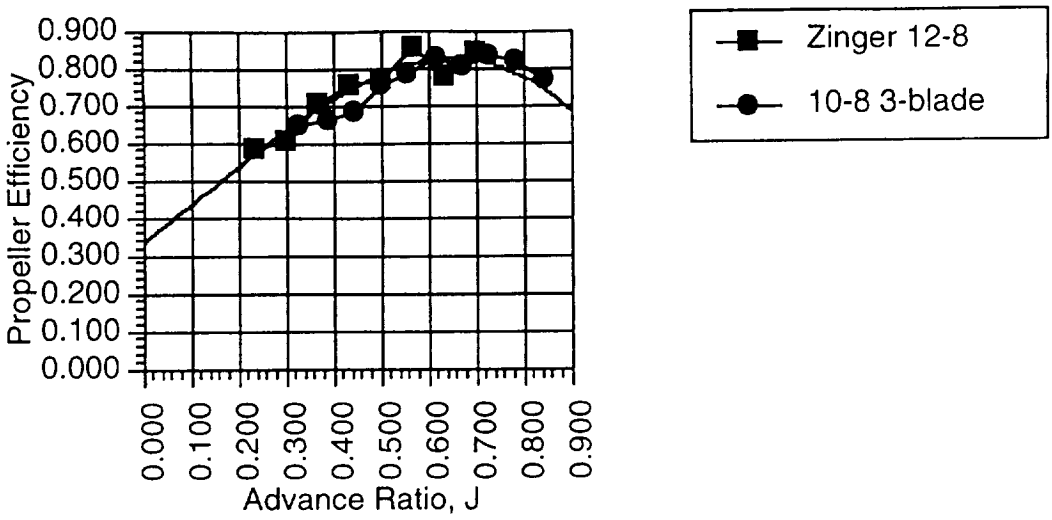

Figure 5-1: Effect of Advance Ratio on Propeller Efficiency

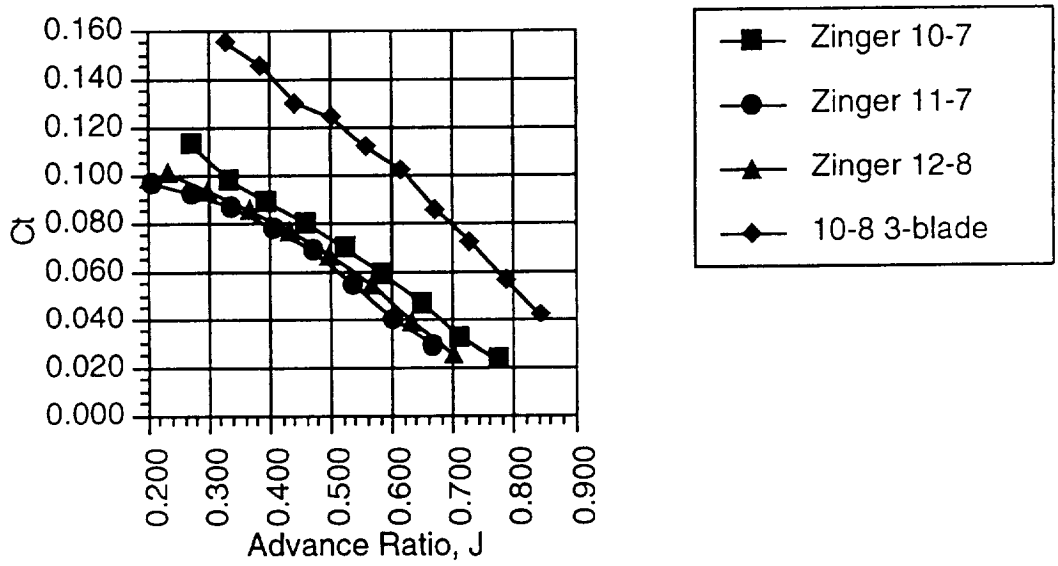

Figure 5-2: Effect of Advance Ratio on C_T

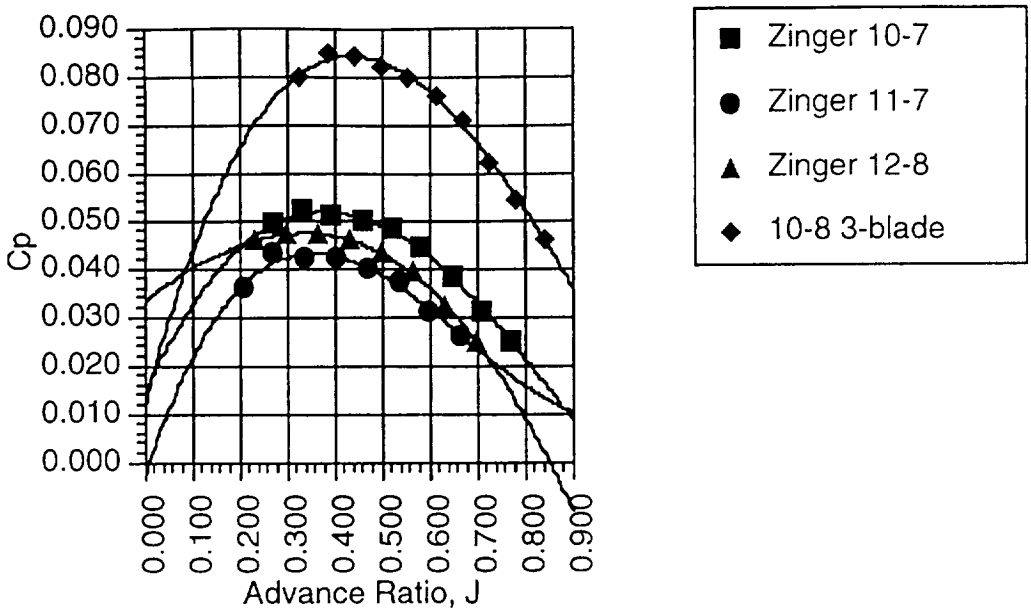

Figure 5-3: Effect of Advance Ratio on C_P

After considerable study, a Zinger 2-bladed wooden propeller was chosen. The propeller is the 12-8 - having a diameter of 12 inches, and a pitch of 8 inches. At first, this might appear to be ill-advised decision. The 3-bladed 10-8 propeller has comparable efficiency to the Zinger 12-8, and larger C_T values for a given advance ratio. It might seem that the 3-bladed 10-8 would be the propeller of choice. However, one must recall that thrust, not C_T, is the measure of merit because it is directly linked to takeoff performance. The equation for thrust is

$$\text{thrust} = C_T \rho n^2 d_{prop}^4.$$

As seen in this equation, the diameter of the propeller greatly affects the resulting thrust at a given RPM and C_T value. In fact, thrust, with all else being equal, is 52% less for the 10 inch propeller than the 12 inch propeller.

The power requirements to turn the propeller must also be studied. C_P values for the 3-bladed 10-8 propeller are approximately twice those of the Zinger 12-8 at a given advance ratio. However, power is defined as

$$\text{Power} = C_p \rho n^3 d_{prop}^5.$$

This equation shows that the power consumed by the propeller is a strong function of RPM and diameter. RPM, or n, in the above equation is assumed to be constant in the analysis. This is not exactly correct (assumes torque of each propeller is the same), but is a good approximation. A small change in propeller diameter, however, can greatly affect the power requirement. As diameter increases, so too does the necessary power. This seems to suggest that a smaller diameter propeller would be desirable from the standpoint of power. One should be careful before arriving at such a rash conclusion.

The power produced by the propeller (power available) is equal to the product of the propeller efficiency and power output of the motor. It is desired to have the lowest power output from the motor, but still enough power so that high speed and climb performance can be improved. The Zinger 12-8 propeller produces enough power to satisfy the high speed requirement, while the 3-bladed 10-8 propeller does not. Therefore, from the standpoint of power, as with thrust, the Zinger 12-8 is a better selection than the 3-bladed 10-8 model.

Graphs of thrust and power, rather than their coefficients, would have been more informative. They were not presented because there was a problem with the PROP123 code. The code was repaired, but time did not permit the reproduction of all graphs. Preliminary studies did reveal increased thrust and power required with the Zinger 12-8 propeller over all others, particularly the 3-bladed 10-8. The preliminary performance estimates, while inaccurate, are believed to accurately predict trends. On the basis of the thrust predictions and propeller power requirements (and resulting power available), it is thought, and

data supports, that the Zinger 12-8 propeller will outperform the 3-bladed 10-8 propeller in the critical areas of takeoff, high speed, and climb.

5.3 Motor Selection

The motors considered for use in the RPV were all Astro motors. Astro models 05, 05 FAI, 15, 25 were stocked, and their use was recommended by upper level management. The Astro 05, and 05 FAI were not studied extensively because their low power rating would not allow the high speed objective to be reached. Therefore, only the Astro 15 and 25 models were researched. A comparison follows.

	Astro 15	Astro 25
Motor Weight (ounces)	7.5	11
Motor Cost (dollars)	107.00	174.00
Cost/Weight Ratio	$14.27/ounce	$15.82/ounce

Table 5-2: Motor Comparison

Preliminary study proved that the Astro 15 outperforms the Astro 25 in the areas of takeoff and high speed for the size of propeller used in the design. Only with propellers which produce a large torque load (large diameter, large pitch, and increased number of blades) will the larger Astro 25 motor produce a higher maximum velocity than the Astro 15. Besides better high speed performance, the Astro 15 is also less expensive, and weighs much less than the Astro 25 (See Table 5-2). The Astro 15 is also capable or providing sufficient takeoff performance, and the range requirement can be easily met. These performance features will be explicitly delineated in section 8.0. For these reasons, the Astro 15 was clearly the engine of choice. Two models of the Astro 15 were readily available: one with a gear ratio of 31:14, and the other with a gear ratio of 31:13.

The model equipped with a gear ratio of 31:14 was chosen because it delivers a slightly higher propeller RPM, and maximum speed. See Table 5-3 for the specifications of the Astro 15 motor.

Name	Astro 15
Maximum Power	200 Watts
Internal Resistance	0.12 Ohms
K_v	1.098 inch-ounce/amp
K_t	7.94E-4 Volts/RPM
T_{loss}	1.37 inch-ounce
Gear Ratio	31:14

Table 5-3: Motor Specifications

5.4 Engine Control and Fuel

The fuel for the aircraft consists of 13 nickel-cadmium batteries with a capacity of 1000 mah. Each battery has a nominal voltage of 1.2 Volts, bringing the total voltage to 15.6 Volts (this is maximum allowable voltage for the Astro 15). The high voltage of the batteries provides for a higher maximum velocity, improved climb capabilities, and better takeoff performance. The effect of number of batteries on the maximum velocity and takeoff performance is shown in Figure 5-4. The effect of number of batteries on maximum rate of climb is plotted in Figure 5-5.

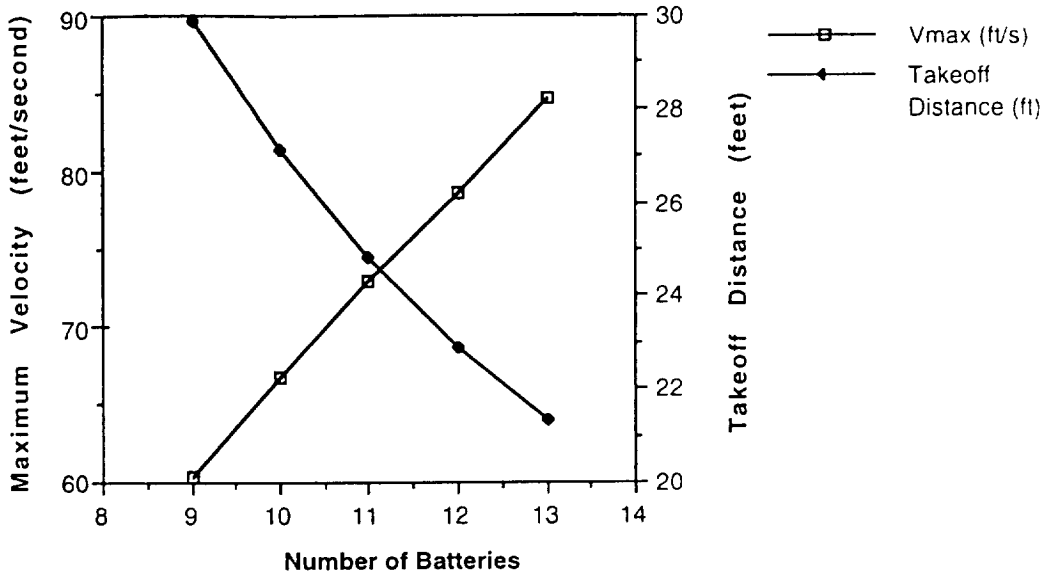

Figure 5-4: Effect of Number of Batteries on Maximum Velocity and Takeoff Distance

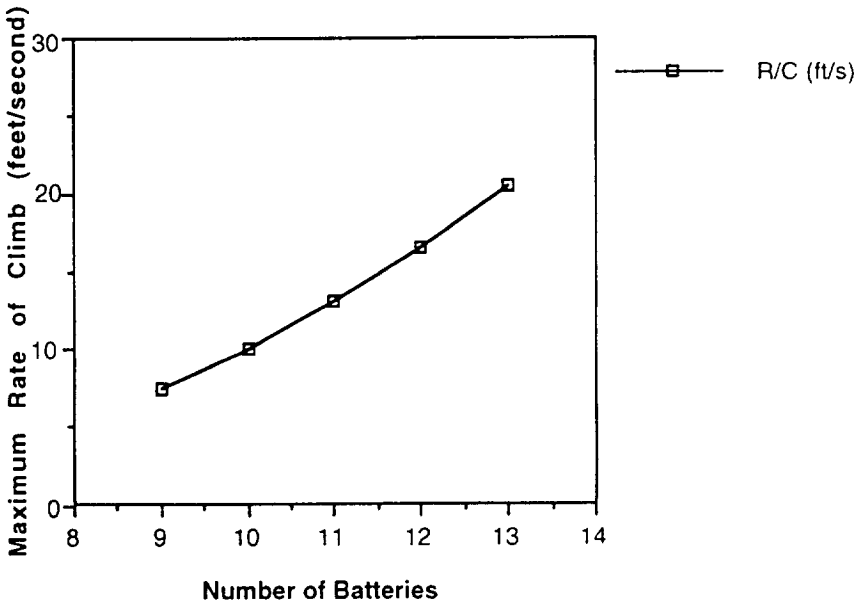

Figure 5-5: Effect of Number of Batteries on Maximum Rate of Climb

The capacity (1000 mah) only affects the range and endurance of the aircraft. The range requirements for the aircraft were not difficult to achieve (16000 feet), and could have been achieved with batteries of smaller capacitance (600 mah). These batteries would have been smaller, and a possible weight savings could have been garnished. However, the 1000 mah batteries were the smallest available, and will be used in the technology demonstrator.

The voltage input to the motor will be controlled with a Tekin speed controller. The maximum voltage of 15.6 Volts will be used in the takeoff, climb, and maximum velocity flight configurations. However, the voltage supplied to the motor will have decreased so that level flight can be achieved at speeds between V_{stall} and V_{max}. Only then will the power available and required terms match - the necessary condition for level flight.

At cruise, for example, the aircraft will not require the 15.6 available Volts. In fact, only 9.82 Volts are necessary. This is approximately 63% of the available throttle. Such information is valuable, and allows the pilot to select the necessary throttle setting on the radio controller to achieve the cruise condition.

5.5 Manufacturing and Installation

It is required than the complete propulsion system be removed or installed in less than 20 minutes. This is so that the equipment can be used by several RPVs in the same air show. In order to achieve this goal, the batteries and engine will be made readily accessible. The batteries will be contained with heat-shrink plastic and reside in the wing carry-through structure below an access hatch located on the top of the aircraft. The battery pack will be attached with Velcro, rather than screws to facilitate removal and installation. The Velcro connection will be strong to help minimize any battery translation. Any motion

could have pronounced effects on the aircraft because the batteries represent a large weight item (over one pound).

The engine is also accessible at the nose of the aircraft. There will be room between the fuselage and engine to allow for air circulation, and necessary cooling. The nose cone section which houses the engine will also be hinged to streamline motor installation. An engine mount will be securely fashioned to the frame of the fuselage, bolted into a sturdy plywood bulkhead. The motor can be installed or removed from the mount with a turn of a fastener. In summary, the propulsion system will be manufactured so that it can be installed or removed within 20 minutes. The integrity of all propulsion attachments will not be sacrificed to achieve this goal.

6.0 WEIGHTS AND BALANCE

6.1 Weight Breakdown

6.1.1 Preliminary Estimate

When the basic concept for *The Bullet* was chosen, the preliminary sizing for the plane was made, and an initial weight estimate was calculated. Because the weights of the avionics, the different engines, and the available batteries, were known constants, the actual structure of the plane was the largest unknown. The decision to use the Astro 15 engine, along with the voltage and current requirements, led to the selection of 12 1000 mAh batteries as the power supply. The preliminary estimate for the weight of the structural components was made by looking at the component weights of several previous airplanes. This data can be found in Appendix B. For example, for each wing, the weight per unit area was calculated, and the average of these values was found. This was then used to calculate an estimate of the weight of *The Bullet's* wings based on the preliminary value for the surface area. A similar method was used to calculate the weights for the fuselage, the vertical and horizontal tails, and the landing gear. However, because the mission requirements for *The Bullet* differed from previous years, the weight estimates arrived at using this method were not expected to be very exact.

6.1.2 Secondary Estimate

In order to make reasonable estimates for the amount of wing area needed and the structural load requirements, a refined value for the weight of the airplane was needed. Using the initial weight estimate, a preliminary structural design was created. From this, the volumes of the monokote, balsa, and spruce

needed to build the fuselage, wings, and tail, and volume of the steel needed to build the landing gear were approximated. Since the densities of each of the building materials was known, individual component weights were calculated by multiplying the volume of each material included in the component by its density. As can be seen from Table 6.1, in most cases, these values turned out

Airplane Component	Initial Weight (pounds)	Revised Weight (pounds)	% of Revised Total Weight
Propulsion	0.704	0.735	16.02
Engine	0.438	0.469	10.21
Gear Box	0.094	0.094	2.04
Engine Mount	0.073	0.073	1.58
Propeller	0.100	0.100	2.18
Batteries	1.095	1.056	23.02
Avionics	0.408	0.433	9.43
Servos (3)	0.113	0.113	2.45
Speed Controller	0.111	0.111	2.41
System Batteries	0.125	0.125	2.72
Receiver	0.059	0.059	1.29
Fuselage	0.563	0.280	6.10
Wing	0.781	0.800	17.44
Tail	0.250	0.205	4.46
Horizontal	0.125	0.149	3.25
Vertical	0.125	0.056	1.21
Landing Gear	0.375	0.621	13.53
Main Gear	0.250	0.410	8.93
Nose Gear	0.125	0.211	4.60
Glue, etc.	****	0.200	4.35
Error Factor	5%	5%	****
Total Unloaded	**4.384**	**4.546**	****
Payload	0.035	0.050	1.08
Total Loaded	**4.419**	**4.596**	****

Table 6.1: Weight Estimation

to be fairly close to the preliminary weight estimates. The only major discrepancies occurred in the weights of the fuselage and the landing gear. The reason for the difference in the estimates for the fuselage weight was the fact that

the fuselage weight to volume ratio turned out to be considerably less than the original sizing. The difference in the landing gear weights was a result of the longer struts necessary to accommodate the increased tip clearance requirement. Because the design for *The Bullet* called for a lightweight plane with high ground clearance, the weight percentages shown in Figure 6.1 for the components differed from previous designs in the obvious areas, the landing gear, the fuselage, and the wing.

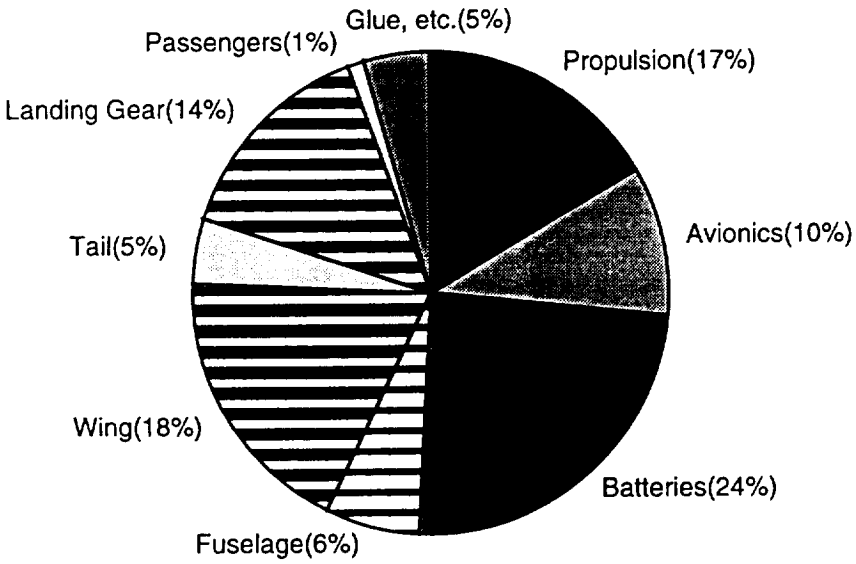

Figure 6.1: Component Weight Percentages

The weight of the components was combined with the weights of the propulsion system, the batteries, and the avionics package to complete the estimate. While all of these weights were given, there were several minor changes between the preliminary and secondary values. In order to provide a more exact estimate, the value for the engine weight was changed to the that found when an available Astro 15 was weighed. The number of batteries in the secondary estimate was boosted to 13 from the original 12. However, while the number of batteries changed, the weight per battery for the 1000 mAh battery

given by the new catalog was 1.3 ounces as opposed to the 1.46 ounce weight given by the old catalog. Therefore, the total weight of the batteries actually dropped in the secondary estimate. Also, weight was added to the avionics package to account for the wire connections and to the total to account for glue and fasteners.

6.2 Center of Gravity Location

Once a reasonable weight estimate was made for each of the components, the location of the center of gravity for *The Bullet* had to be found. In order to do this, a detailed internal layout of the plane was made, showing the positions of each of the components relative to the nose. Ideally, both the forward (unloaded) and the aft (fully loaded) center of gravity positions should be placed so that the static margin of the airplane falls between 20 and 25 percent of the chord. The static margin was calculated from

$$\text{static margin} = \frac{X_{NP}}{c} - \frac{X_{cg}}{c} \tag{6.1}$$

where X_{NP} is the position of the neutral point as given in section 7.3 and c is the chord of the wing. In order to achieve the desired static margin with a neutral point location of 0.492c, the center of gravity location had to fall between 0.292c and 0.242c. Therefore, the wing had to be placed so that the airplane center of gravity was slightly aft of the quarter chord location of the aerodynamic center of the wing.

To find the configuration that would provide the desired center of gravity location, the positions of the separate components were varied over limited ranges. The main constraints that had to be considered were the lengths of wire available to connect different components, the fact that the batteries were required to be housed in the wing carry-through, and the lengths available for the servo push rods. Because the wing and batteries essentially must be moved

together, and the sum of the two makes up approximately 40% of the total weight of the airplane, this was the combination that was most influential in changing the position of the center of gravity. The final configuration, detailed in Table 6.2 and Figure 6.2, resulted in a center of gravity location of 9.76 inches for the unloaded plane, and 10.03 inches for the fully loaded plane. These values, as was desired, are both slightly aft of the quarter chord position of 9.5 inches.

Airplane Component	Weight (pounds)	X Position (inches) from Nose
Engine, Gear Box, Engine Mount	0.635	2.0
Propeller	0.100	-0.5
Batteries	1.056	10.3
Flap Servo	0.038	13.25
Rudder Servo	0.038	15.5
Elevator Servo	0.038	15.5
Speed Controller	0.111	5.75
System Batteries	0.125	8.0
Receiver	0.059	8.25
Fuselage	0.280	14.5
Wing	0.800	9.5
Horizontal Tail	0.149	35.5
Vertical Tail	0.056	35.5
Main Gear	0.410	12.5
Nose Gear	0.211	4.0
Unloaded	**4.546**	**9.76**
Payload	0.050	23.0
Fully Loaded	**4.596**	**10.03**

Table 6.2: Center of Gravity Locations

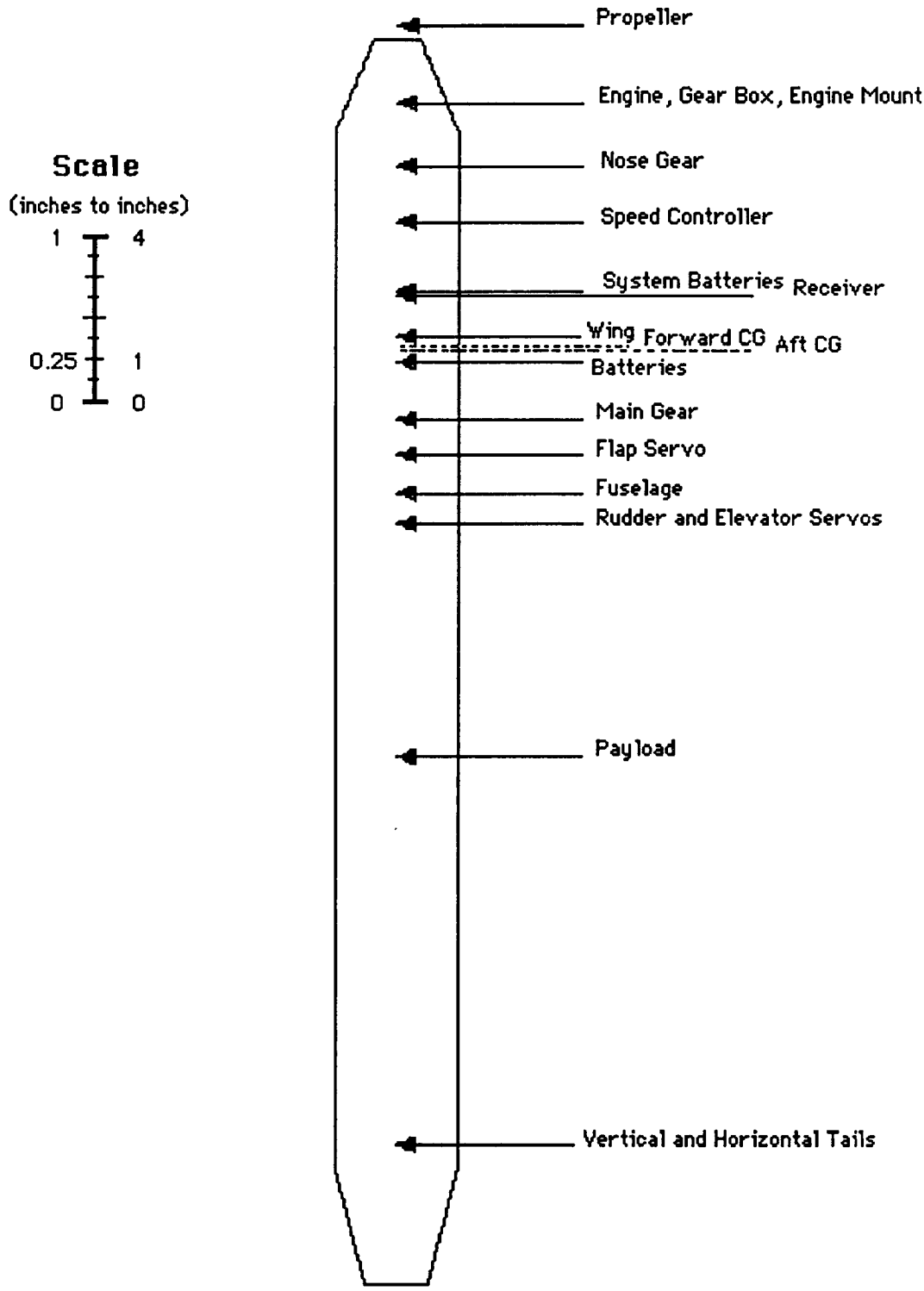

Figure 6.2: Center of Gravity Locations

7.0 STABILITY AND CONTROL

7.1 Stability and Control Requirements

The stability and control requirements of this aircraft were among its most crucial. However, because the desired stability and control characteristics can be achieved with many different configurations, the location and sizing of the stability and control surfaces was engineered last in order to fit within aerodynamic and structural parameters. The aircraft was required to be stable and controllable in the three coordinate directions, namely yaw, pitch, and roll. These definitions led to the specific requirements for *The Balsa Bullet:*

- Pitch, or Longitudinal, stability would be accomplished through the use of a horizontal stabilizer aft of the wing and pitch control through deflection of an elevator on the horizontal stabilizer.
- Yaw, or Lateral, stability would be accomplished through the use of a vertical tail aft of the wing and yaw control through deflection of a rudder on the vertical tail.
- Roll stability would be accomplished through the use of dihedral on the wing and roll control through the combination of deflection of the rudder and the dihedral of the wing.
- The yaw and roll control devices needed to allow the aircraft to perform a 60 ft. radius turn at flight speeds of less than 30 ft/s.

7.2 Pitch Stability

The need for pitch stability required that if the aircraft was pitched up, it would correct itself by pitching back down to its previous equilibrium position. The pitch angle, θ, was measured from the horizontal to the

fuselage reference line of the aircraft and, because there was no wing incidence, was equal to the angle of attack. Because a pitch-up moment which caused an increase in angle of attack was defined as positive, the slope of the pitching moment coefficient versus angle of attack curve was required to be negative for a stable aircraft. The pitching moment coefficient at zero degrees angle of attack (Cm_0) was also needed in order to find the total moment so that the aircraft could be trimmed at any flight condition. The desired magnitude of the slope (Cm_α) was chosen using data from previous designs and from data found in Appendix B of Reference 12. The desired value of Cm_α at cruise (i.e. fully loaded) was chosen to be -1.0 ± 0.1. There were three major components of the aircraft which contribute to the Cm_0 and Cm_α. They were the fuselage, the wing, and the horizontal stabilizer.

One of the most important measures of pitch stability was the static margin. The static margin was defined as the difference between the neutral point and the center of gravity location as a fraction of the mean aerodynamic chord. The neutral point was the point at which Cm_α was equal to zero meaning the slope of the Cm versus α curve was zero. The aircraft was stable for a neutral point aft of the center of gravity. Therefore, a static margin greater than zero was found on a longitudinally stable aircraft. The target value for the static margin of *The Balsa Bullet* was about 0.25.

7.2.1 Fuselage Contribution

The fuselage was a destabilizing component of pitch characteristics meaning that its Cm_α was positive while its Cm_0 contribution was negative. To find these components, Reference 12 suggested Multhopp's method which breaks the fuselage into discreet sections and applies empirically determined

relationships to each section. The following formulas were employed in this method.

$$C_{m_{0_f}} = \frac{k_2 - k_1}{36.5S\bar{c}} \sum_{x=0}^{x=l_f} w_f^2(\alpha_{0w} + i_f)\Delta x \tag{7.1}$$

$$C_{m_{\alpha_f}} = \frac{1}{36.5S\bar{c}} \sum_{x=0}^{x=l_f} w_f^2 \frac{\partial \varepsilon_u}{\partial \alpha} \Delta x \tag{7.2}$$

Because the fuselage was essentially entirely rectangular, the contributions of all the sections were taken to be uniform. The width of the fuselage was constant at 3.5 inches and the zero lift angle of attack was constant at -6 degrees. These formulas were applied at the aft center of gravity location. The coefficients found by applying this method were

$$C_{m_{0_f}} = -1.23 \times 10^{-4}$$

$$C_{m_{\alpha_f}} = 3.28 \times 10^{-3} \quad \text{per radian}$$

7.2.2 Wing Contribution

Assuming that the aerodynamic center of the wing was in front of the center of gravity as was the case in all aircraft studied in the data base, the wing contribution to Cm_α was positive and to Cm_0 was negative. The following formulas found in Reference 12 show that Cm_α and Cm_0 depended upon the lift generated by the wing and the moment arm from the lift vector to the center of gravity.

$$C_{m_{0_w}} = C_{m_{ac_w}} + C_{L_{0_w}} \left(\frac{x_{cg}}{\bar{c}} - \frac{x_{ac}}{\bar{c}} \right) \tag{7.3}$$

$$C_{m_{\alpha_w}} = C_{L_{\alpha_w}} \left(\frac{x_{cg}}{\bar{c}} - \frac{x_{ac}}{\bar{c}} \right) \tag{7.4}$$

From inspection of these formulas it was easy to see that there were three factors which influenced the wing contributions to pitch stability. They were the airfoil section, the wing geometry, and the placement of the wing relative to the center of gravity. The chosen airfoil section, the FX63-113, had

a Cm_{ac} = -0.12. The chosen wing geometry altered the lift curve slope of the wing from that of the airfoil as shown in Section 4. The distance from the aerodynamic center of the wing to the center of gravity of the aircraft was the moment arm for the aerodynamic forces. The coefficients were

$$C_{m_{0_w}} = -9.87 \times 10^{-2}$$

$$C_{m_{\alpha_w}} = 0.203 \qquad \text{per radian}$$

for this aircraft.

7.2.3 Horizontal Stabilizer Contribution

The device which provided the pitch stability and whose size and placement was driven by the stability and control requirements of the aircraft was the horizontal stabilizer. It provided a negative contribution to Cm_α and a positive contribution to Cm_0. The effect that the tail had upon these coefficients depended upon the airfoil section and geometry of the stabilizer as well as distance from center of gravity of the aircraft to the aerodynamic center of the stabilizer. The interference due to the wing also affected the horizontal stabilizer contribution. Reference 12 provided development of the following formulas for the contribution of the horizontal stabilizer to Cm_α and Cm_0.

$$C_{m_{0_t}} = \eta V_H C_{L_{\alpha_t}} (\varepsilon_0 + i_w - i_t) \tag{7.5}$$

$$C_{m_{\alpha_t}} = -\eta V_H C_{L_{\alpha_t}} \left(1 - \frac{d\varepsilon}{d\alpha}\right) \tag{7.6}$$

where

$$\varepsilon_0 = \frac{2C_{L_{\alpha_w}} (i_w - \alpha_{LO})}{\pi e AR} \tag{7.7}$$

$$\frac{d\varepsilon}{d\alpha} = \frac{2C_{L_{\alpha_w}}}{\pi e AR} \tag{7.8}$$

$$V_H = \frac{S_t l_t}{S_w \bar{c}} \tag{7.9}$$

The values for these coefficients were as follows:

$$C_{m_{0_t}} = 0.142$$

$$C_{m_{\alpha_t}} = -1.109 \qquad \text{per radian}$$

The two major parameters in the horizontal stabilizer contribution are l_t and S_t because they are the most controllable from the design standpoint. The position of the center of gravity relative to the aerodynamic centers of the wing and horizontal stabilizers has a tremendous effect of the stability of a specific design because it affects the wing and horizontal tail contributions. Therefore, it is important to have an accurate estimate of the center of gravity location before stability and control analysis is attempted. The sizing of the horizontal stabilizer depends upon the constraints placed upon it by aerodynamic, structural, weight, center of gravity, as well as stability concerns. The pitching moment coefficients for the entire aircraft were found by summing the coefficients of the individual parts.

The initial location of the aerodynamic center of the horizontal stabilizer was at thirty-six inches. However, the span of the stabilizer would have had to be over four feet in order to meet the stability criteria. This was deemed unacceptable due to structural concerns. When the location was moved to forty inches, the span decreased to approximately 2.74 feet which was acceptable. Figure A-6 shows the pitching moment coefficient versus angle of attack curve for the aircraft at the forward and aft center of gravity locations and indicates the angles of attack required in order to have no pitching moment on the aircraft in the absence of an elevator deflection. The required cruise speeds would then be forty-three feet/second for the forward center of gravity location and thirty-nine feet/second for the aft center of gravity location. This curve was crucial in determining pitch behavior of the aircraft at the extreme conditions.

7.3 Pitch Control

7.3.1 Sizing and Actuation

Pitch control for the aircraft was delivered through the use of an elevator located on the horizontal stabilizer. When the elevator was deflected, the lift on the horizontal stabilizer was altered, changing the pitching moment coefficient for the aircraft. Pitch was used in climbing and diving two obviously important maneuvers. Reference 12 developed equations for determining the effect of the elevator deflection on the moment coefficient. This was accomplished through formulas for determining the slope of the change in pitching moment coefficient versus elevator deflection (δ_e).

$$C_{m_{\delta_e}} = -V_H \eta \tau C_{L_{\alpha_t}} \tag{7.10}$$

This coefficient was negative, and the range of its magnitude was determined from examining Appendix B of Reference 12 as 0.9±0.2.

In order to facilitate ease of manufacturing, it was determined that the elevator would run the whole length of the span of the horizontal stabilizer. The percentage of the stabilizer chord which was elevator and was determined such that the control coefficient was within the acceptable range and such that the elevator wasn't too small to raise serious structural and manufacturing concerns. The maximum elevator deflection angle was determined such that the aircraft could be trimmed at any angle of attack in the normal operating flight regime. The elevator would be controlled by a single flexible control rod extending from the servo in the wing carry-through, traveling through the inside of the fuselage, exiting the through the rear of the fuselage, and attaching to the underside of the elevator. Figures 7-1 and 7-2 show the pitch moment coefficient versus angle of attack at

multiple elevator deflection angles for the forward and aft center of gravity locations, respectively.

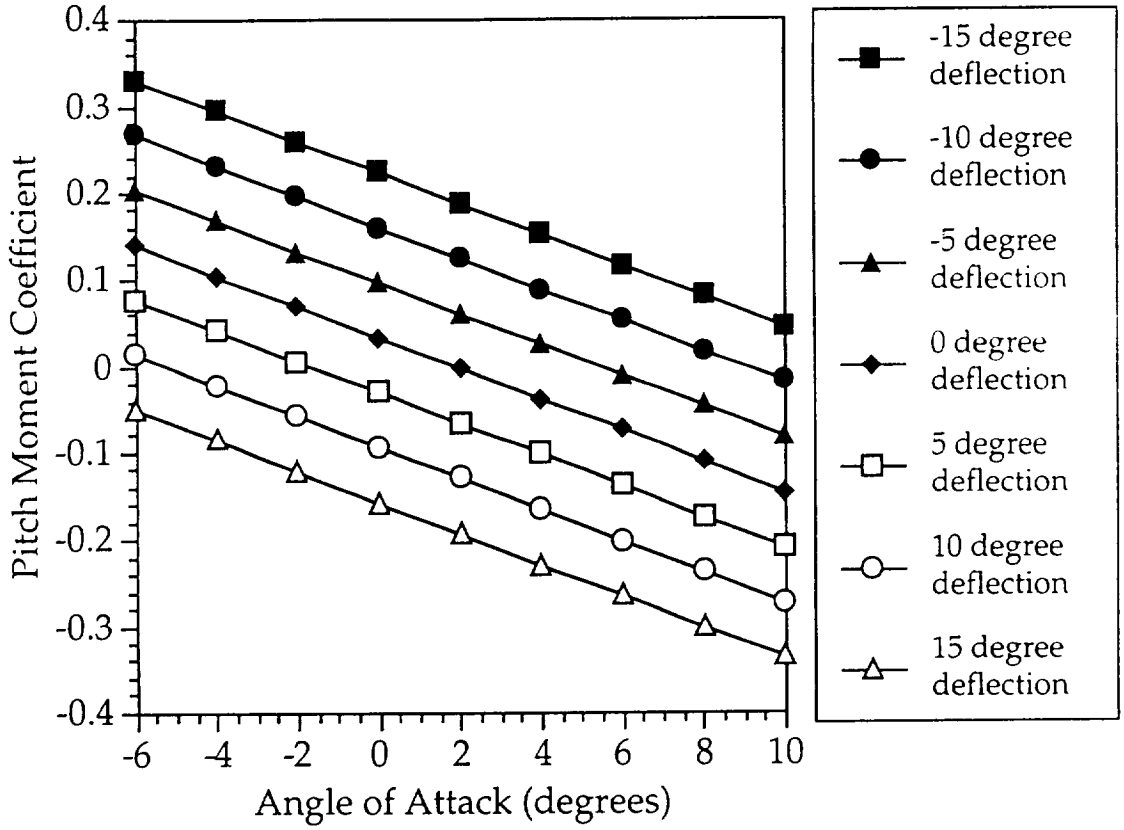

Figure 7-1: Effect of Angle of Attack and Elevator Deflection on Pitch Moment Coefficient at the Forward Center of Gravity Position

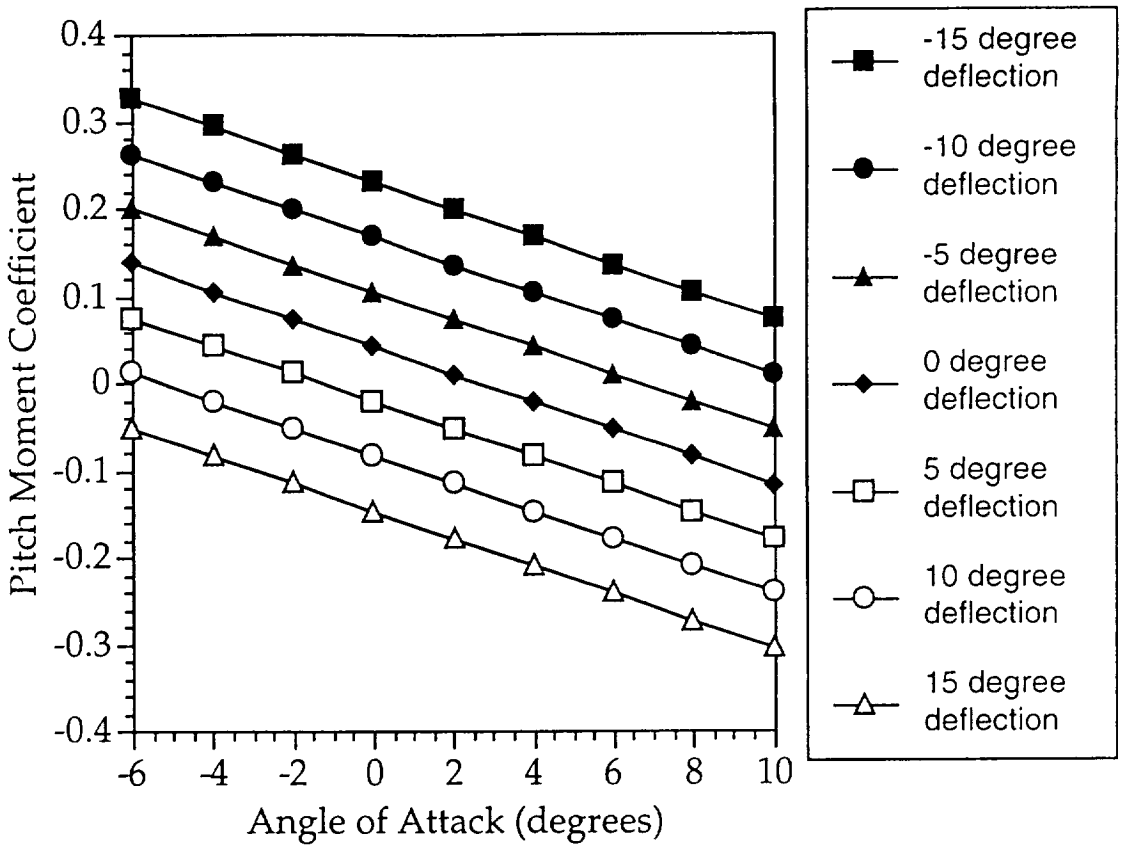

Figure 7-2: Effect of Angle of Attack and Elevator Deflection on Pitch Moment Coefficient at the Aft Center of Gravity Position

7.3.2 Trimming the Aircraft

Perhaps the most important use of the elevator was trimming the aircraft. To trim the aircraft means to actuate control surfaces such that the pitching moment is zero at the desired flight conditions. Trimming the aircraft was necessary to maintain these conditions. Unlike yaw and roll, it was necessary to maintain a cruise pitch angle which in the absence of a rudder deflection would result in a non-zero pitching moment. This was due to the fact that angle of attack played a crucial role in the magnitude of the lift on the aircraft. Reference 12 developed equations for the determination of the appropriate elevator deflection angle to trim the aircraft. Another

coefficient was defined to aid in this process. It was the slope of the change in stabilizer lift coefficient versus elevator deflection angle.

$$C_{L_{\delta_e}} = \frac{S_t}{S_w}\eta\tau C_{L_{\alpha_t}} \tag{7.11}$$

This allows for a tidy form for the elevator deflection to trim (δ_{trim}).

$$\delta_{trim} = -\frac{C_{m_0}C_{L_\alpha} + C_{m_\alpha}C_{L_{trim}}}{C_{m_{\delta_e}}C_{L_\alpha} - C_{m_\alpha}C_{L_{\delta_e}}} \tag{7.12}$$

where C_{Ltrim} is the aircraft lift coefficient at which trim was desired.

To trim the aircraft at cruise, the elevator was required to overcome the pitching moment at an angle of attack of -3.3 degrees because it was at this angle of attack that lift was equal to the weight for the designed cruise speed. Because the design center of gravity location was the aft location, the cruise elevator deflection angle was determined using that location. The angle of incidence of the horizontal tail was set such that the elevator deflection angle to trim at cruise was as close to zero degrees as possible in order to reduce drag. The aircraft can be trimmed at any angle of attack, but the cruise conditions were used in determining the appropriate angles because cruise conditions are encountered the majority of the flight.

7.3.3 Rotation at Take-Off

Takeoff rotation was crucial in determining the incidence angle of the tail, the angle the fuselage makes with the ground, and angle of attack. Figure 7-3 shows the forces acting on the aircraft at takeoff.

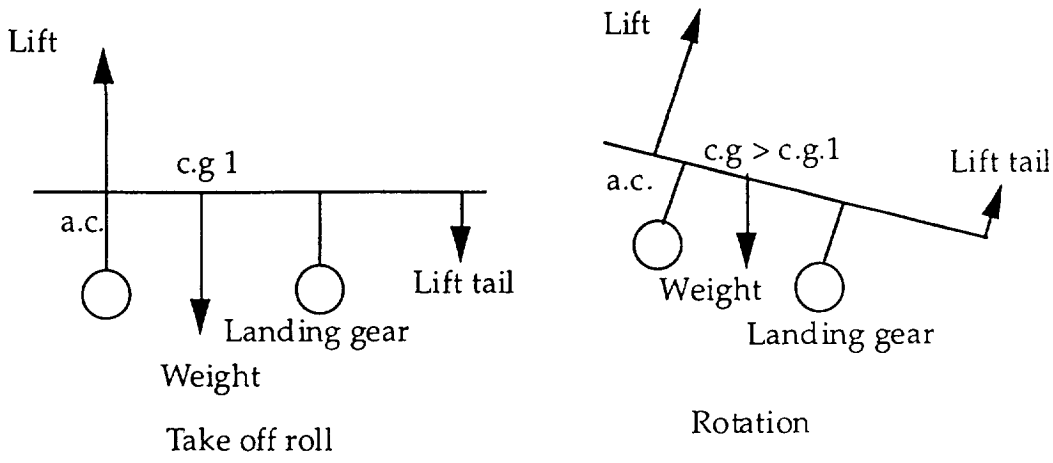

Figure 7-3: Aerodynamic Forces During Rotation

From the diagram, one notices that the lift on the tail will create a pitch up moment on the aircraft during roll since it is mounted at a negative incidence angle. As the angle of attack changes relative to the ground, the angle of attack of the tail plane changes. When the angle of attack becomes great enough that the lift on the tail changes direction to oppose the increased moment due to the increased lift, rotation will occur. The takeoff rotation analysis sets the incidence angle of the tail as well as the position of the landing gear (See Section 9.4). One other note is that the center of gravity location will move back slightly from its original position from the nose at rotation.

S_t	1.5 square feet
AR_t	5.0
Airfoil Section	NACA 0009
Planform Shape	Rectangular
Se	0.3 square feet
δ_e (max)	±15 degrees
δ_e (trim at cruise)	0.05 degrees

Table 7-1 : Horizontal Stabilizer Data

$C_{m_\bullet}$	4.307×10^{-2} per radian
C_{m_α}	-0.903 per radian
$C_{m_{\delta_e}}$	-0.721 per radian
$C_{L_{\delta_e}}$	0.319 per radian
Neutral Point	49.2% MAC
Static Margin	22.3 % MAC

Table 7-2 : Pitch Coefficients

7.4 Yaw Stability

An aircraft is determined to be laterally stable if, when perturbed sideways, the aircraft resumes it original position. The yaw angle, β, was measured from the body x-axis to the velocity vector of the aircraft in the x-y plane and was positive in the clockwise direction. A positive yaw moment is one which causes the aircraft to rotate clockwise. This means that an aircraft is stable if the slope of the yaw coefficient (C_n) versus yaw angle curve is positive. The range for the magnitude of the slope was determined by

looking at previous designs as well as the aircraft data found in Appendix B of Reference 12. Two aircraft components contributed to this stability coefficient: the fuselage, which was destabilizing, and the vertical tail, which was stabilizing.

7.4.1 Wing and Fuselage Contribution

The wing and fuselage provided a destabilizing component to the yaw coefficient. The magnitude of the contribution was found through a combination of the geometry of the aircraft and empirical interference and correction factors. The method used was that laid out in Reference 12. The following was the formula for the fuselage contribution to the yaw coefficient versus yaw angle slope.

$$C_{n_{\beta_{wf}}} = -k_n k_{R_l} \frac{S_{fs}}{S_w} \frac{l_f}{b_w} \text{ (per degree)} \tag{7.13}$$

For this aircraft design the coefficient was:

$$C_{n_{\beta_{wf}}} = -4.33 \times 10^{-4} \text{ (per degree)}$$

7.4.2 Vertical Tail Contribution

The aircraft device used to provide yaw stability was the vertical tail. Its size and distance from the center of gravity were primarily based upon the stability requirements of the aircraft. The wing interfered with the flow near the vertical tail, and the magnitude of this interference depended upon the wing size and geometry. Reference 12 developed the formulas for the vertical tail contribution to slope of the yaw coefficient versus yaw angle curve.

$$C_{n_{\beta_v}} = V_v \eta C_{L_{\alpha_v}} \left(1 + \frac{d\sigma}{d\beta}\right) \tag{7.14}$$

where

$$V_v = \frac{S_v l_v}{S_w b_w} \tag{7.15}$$

$$\eta\left(1+\frac{d\sigma}{d\beta}\right)=0.724+3.06\frac{S_v/S_w}{1+\cos\Lambda_{c/4w}}+0.4\frac{z_w}{d}+0.009AR_w \quad (7.16)$$

The latter factor accounted for the difference in flow velocity between the wing and the vertical tail as well as the side swish due to vortices from the wings. For *The Balsa Bullet* , the vertical tail contribution was:

$$C_{n_{\beta_v}}=0.0760$$

Again the total coefficient for the aircraft was found from summing the individual components.

The location of the center of gravity of the vertical tail was taken to be forty inches like the horizontal stabilizer. The size of the vertical tail was determined such that the stability coefficient was within the acceptable range and was acceptable to the structures group. The desired range was again found by analyzing values from past designs as well as from data taken from Appendix B of Reference 12. The range of acceptable values was determined to be 0.05±0.01.

7.5 Yaw Control

Yaw control was accomplished through deflecting a rudder on the vertical tail. The rudder was used to overcome forces in various conditions such as cross wind landings, asymmetric power situations, and spins. The rudder was also used in conjunction with wing dihedral to produce roll control especially during turning maneuvers. Rolling during turning provided a more efficient and more comfortable turn. The measure of yaw control was the slope of the change in yaw moments versus rudder deflection angle curve. The method for obtaining this slope was developed in Reference 12. The calculations result in the following relation.

$$C_{n_{\delta_r}}=-\eta V_v \tau C_{L_{\alpha_v}} \quad (7.17)$$

Again for manufacturing ease, the rudder it was determined that the rudder would run the entire height of the vertical tail. The percentage of the chord which was rudder was determined such that the control coefficient was within the predetermined acceptable range and met structural requirements. As with the previous stability and control coefficients, the range of $Cn_{\delta r}$ was determined from previous designs and Appendix B of Reference 12 as 0.06±0.02. The rudder would be controlled by a single control flexible rod extending from the servo in the wing carry-through, traveling through the fuselage, exiting the side of the fuselage, and attaching to the side of the rudder. Figure 7-4 shows the effect of rudder deflection on the yaw moment coefficient.

S_V	0.5 square feet
AR_V	3.0
Airfoil Section	NACA 0009
Planform Shape	Rectangular
Sr	0.25 square feet
δ_r (max)	±30 degrees

Table 7-3 : Vertical Tail Data

C_{n_β}	5.12×10^{-2} per radian
$C_{n_{\delta_r}}$	-4.61×10^{-2} per radian

Table 7-4 : Yaw Coefficients

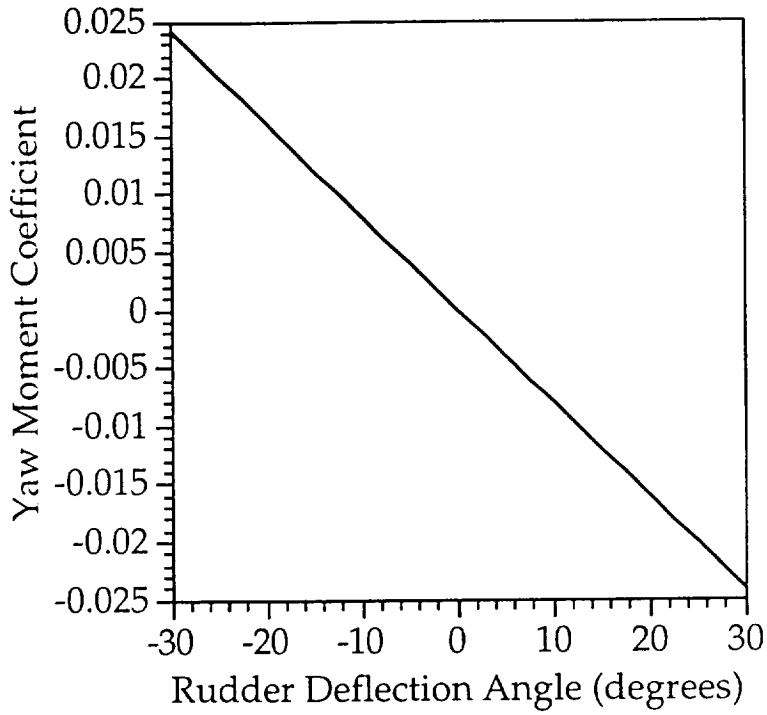

Figure 7-4: Effect of Rudder Deflection on Yaw Moment Coefficient

7.6 Roll Stability

Unlike pitch and yaw stability, roll stability was not attributed to a surface separate from the lifting surface. Instead, roll stability was a function of the wing placement on the fuselage and dihedral. The fuselage of the aircraft could either be stabilizing, if the wings are mounted on the top of the fuselage, or destabilizing, if the wings are mounted on the bottom of the fuselage. This was due to how the lift on each semi-span on the wing is changed during roll. Figure 2.33 of Reference 12 shows the effect the fuselage has on roll stability.

In Reference 12 the measure of roll stability was defined as the slope of the change in roll moment versus side slip angle curve. If this slope (Cl_β) was negative then the aircraft is stable. This is because a positive roll moment induces a positive side slip, so a negative roll moment is needed to return the

aircraft to its equilibrium condition. Reference 11 provided a formula for this slope.

$$C_{l_\beta} = -2\frac{\Gamma}{S_w b_w}\int_0^{b/2} C_{L_{\alpha_w}} cydy \tag{7.18}$$

where Γ was the wing dihedral in radians. The amount of wing dihedral was determined such that the angle would be small enough to have a negligible effect on lift and large enough to provide a roll stability coefficient within the acceptable range. The target range of values for this coefficient was found from data in Appendix B of Reference 12. The chosen range was -0.08±0.02.

7.7 Roll Control

Roll control was necessary in order to bank the aircraft during a turn. It could be provided either by ailerons or by a combination of rudder deflection and wind dihedral. The latter method was chosen for use in *The Balsa Bullet* because of the limitation of three servos and the choice to use high-lift devices. Reference 12 provides an equation which quantified the roll control of an aircraft as the slope of the change in roll moment versus rudder deflection curve. The formula is provided below.

$$C_{l_{\delta_r}} = \frac{S_v}{S_w}\frac{z_v}{b_w}\tau C_{L_{\alpha_v}} \tag{7.19}$$

The magnitude of this coefficient was not as important as its sign. This was because roll control would not need to produce very much power. Any value under between 0.01 and 0.1 was acceptable. Figure 7-5 shows the effect of rudder deflection on the roll moment coefficient.

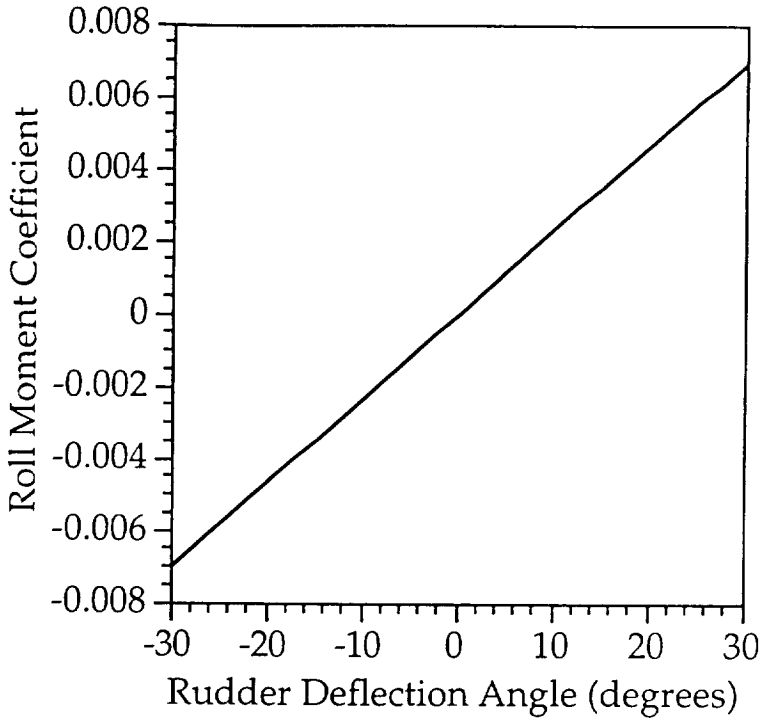

Figure 7-5: Effect of Rudder Deflection on Roll Moment Coefficient

C_{l_β}	-9.49×10^{-2} per radian
$C_{l_{\delta_r}}$	1.33×10^{-2} per radian

Table 7-5 : Roll Coefficients

8.0 PERFORMANCE

8.1 Takeoff

Takeoff performance was a difficult parameter to accurately predict because of the uncertainty in the propeller data. Takeoff was predicted using propeller data obtained from the PROP123 program coupled with a program called TAKEOFF. The TAKEOFF program uses thrust values derived from actual motor performance calculations. Ground roll was also calculated using corrected simple blade element theory predictions (Reference 11-10) with a personally developed FORTRAN code. The code was aptly named GROUND ROLL. In GROUND ROLL, the engine thrust was estimated using the same simple blade element theory with knowledge of the maximum power produced by the engine. Both takeoff codes utilized the equations of motion, and a numerical integration sequence. It was hoped that the calculated ground roll distances of the two methods would be comparable, thus increasing the confidence in the results. Table 8.1 shows the comparison (calculated with $\mu = 0.15$), and lends confidence that the aircraft will be able to meet the takeoff distance requirement of a 25 foot roll from a prepared field.

	TAKEOFF Predictions	GROUND ROLL Predictions
Static Thrust (pounds)	3.12	2.94
Takeoff Velocity (feet/second)	25.3	24.5
Time to Takeoff (seconds)	1.4	1.7
Roll Distance (feet)	16.5	21.3

Table 8-1: Takeoff Performance

It is important to note that the takeoff performance of the TAKEOFF program is believed to be somewhat optimistic. This is because the propeller performance predicted by PROP123 is better than that produced in an experiment conducted at the University of Notre Dame which used an identical propulsion system. Experimental data revealed that the static thrust would equal 2.94, not 3.12 pounds. Despite the discrepancy, there is reasonable certainty that the plane will fulfill its design objective, and liftoff in under 25 feet.

The rough field takeoff requirement was not as restrictive as the indoor requirement. When the value of μ is doubled (to represent long grass), the ground roll distance is increased by only 5 feet. The takeoff distance from long grass was found to be 26.3 feet, much less than the requirement of a 60 foot maximum ground roll.

8.2 Cruise

After climbing to 25 feet, the aircraft will cruise at a velocity of 55 feet/second. This velocity is higher than planes in the current Aeroworld fleet, and provides customers with a high speed alternative. The necessary C_L for the cruise configuration is calculated from the equation:

$$\text{Lift} = \text{Weight} = \frac{1}{2}\rho V_{cruise}^{2} S C_L,$$

and is found to be 0.202. This C_L can be obtained at an angle of attack of -3.3 degrees. This is a small angle, and allows for a relatively level attitude in the cruise configuration. This attitude will provide passengers and pilot a comfortable ride. Also, the cruise condition can be obtained with a voltage setting of 9.82 Volts. This is only 63% of the 15.6 available Volts, and gives

the aircraft sufficient excess power to climb or maneuver. The current draw in the cruise configuration is 7.05 amps.

In the cruise condition, the L/D of the plane is 8.5. The maximum L/D for the aircraft is 14.98 and occurs at a velocity of 31.5 feet/second. From a purely aerodynamic standpoint, the airplane would achieve lower fuel costs if the maximum L/D condition existed at cruise. However, by flying at 55 feet/second the airplane achieves attractive improvements in speed, and economic improvements (in area of depreciation) as well (See 10.0: Economic Analysis). Therefore, a cruise speed of 55 feet/second can be justified.

Higher cruise speeds could also be obtained. At higher cruise speeds, however, the range capability would be lessened, and higher capacity batteries would be necessary. In *The Balsa Bullet* demonstrator, the range requirement was grossly exceeded because appropriate batteries were not available at time of construction. It is hoped that eventually the design batteries (600 mah) will become available. If the proper batteries are installed, the design cruise velocity of 55 feet/second will be appropriate. As it now stands, higher cruise velocities would not cause exception to the design requirements and objectives, and are recommended.

8.3 Turns

The aircraft, a low wing design, will use rudder deflection coupled with a 5 degree wing dihedral to achieve the banking necessary to negotiate a turn. In order to meet the requirement of a 60 foot radius turn at 30 feet/second, the calculated bank angle must be 25 degrees. This angle was found with the aid of the following relation:

$$\tan\phi = \frac{V_{turn}^{\ 2}}{gR}.$$

where ϕ is the bank angle, and R is the turn radius.

In order to evaluate turn performance, it was necessary to study the roll capability of the aircraft. No formula was found which estimates the roll rate as a function of rudder deflection and dihedral. To crudely approximate the steady state roll rate, P_{SS}, an equation involving ailerons was modified and appears below (References 11-7, 11-12):

$$P_{ss} = \frac{12 Cl_{\delta r} \Delta \delta r}{Cl_{\alpha} b}.$$

The calculated roll control of 0.0133/rad ($Cl_{\partial r}$), and a maximum rudder roll deflection of 30 degrees, the aircraft can roll to the necessary bank angle in 5.15 seconds. This is a very long roll time; it is much greater than similar Aeroworld designs of the past. On this basis, it is believed that the roll capability of *The Balsa Bullet* will be markedly better than that predicted by the crude formula above.

The minimum level turn radius of the aircraft was also computed using

$$R_{min} = \frac{V_{turn}^{\ 2}}{g(n_{ult} - 1)}.$$

Using this equation the minimum turn radius was found to be 28 feet. This turn radius is much smaller than the 60 foot maximum imposed for the V_{turn} of 30 feet/second.

8.4 Landing

The landing performance for the aircraft was estimated using techniques similar to those employed for takeoff. The roll distance was

calculated using the same equations with appropriate initial conditions and the thrust set equal to zero. To validate the landing roll code, results were compared to those predicted by

$$X = \frac{W}{2gB} \ln\left[1 + \left(\frac{B}{A}\right) V_{land}^{\ 2}\right],$$

where,

$$B = \frac{1}{2} C_D \rho S \qquad A = \mu W.$$

This equation was found in reference 11-10. The landing roll distance calculated from the two methods were 52.5 and 52.6 feet respectively with a friction coefficient of 0.15, and V_{land} = 24.5 feet/second. The close agreement of the two solutions produces confidence in the results.

The plane must be able to stop in a distance of 40 feet to service any Aeroworld airports. Obviously, with calculated roll distances of over 50 feet, the plane does not meet the objective. However, the RPV is not required to meet this objective because it lacks braking or reverse thrusting capabilities. In the actual production these features will be incorporated, and the landing performance will satisfy the objective. It should be noted that brakes will add to the overall weight of the aircraft, and will adversely affect the range of the aircraft.

8.5 Power Available and Required

A graph of power available and required contains a lot of information. The graph shows not only the maximum obtainable level velocity, but also the voltage necessary to cruise at various speeds in the flight envelope. This is done by realizing that level flight is achieved when the power available and

required curves intersect. From Figure 8-1, the maximum obtainable speed of the aircraft is approximately 84.6 feet/second.

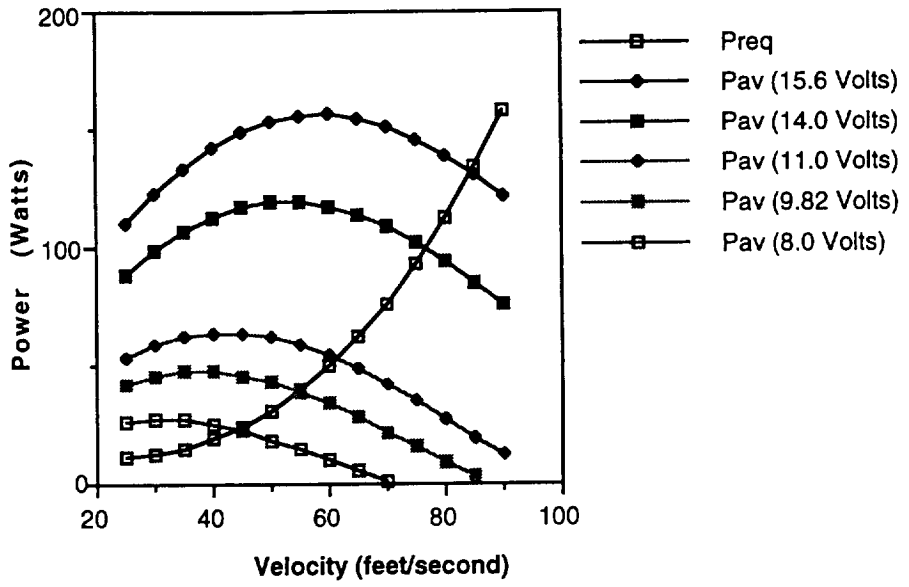

Figure 8-1: Effect of Velocity on Power Available and Required

8.6 Climbing and Gliding

Upon takeoff, the initial rate of climb is 15.8 feet/second. The maximum rate of climb occurs at a velocity of 45 feet/second, and its value is 20 feet/second. Using the lowest value of rate of climb for the ascent profile, the plane reaches its design altitude of 25 feet in a time of 1.6 seconds. Figure 8-2 shows how rate of climb varies with velocity at the maximum voltage setting of 15.6 Volts.

The plane, starting from rest, must also be able to clear a 50 foot obstacle in under 200 feet. With ground roll and climb, *The Balsa Bullet* will obtain a height of 50 feet after only 89.4 feet have been covered. Therefore, the plane easily meets the climb requirement.

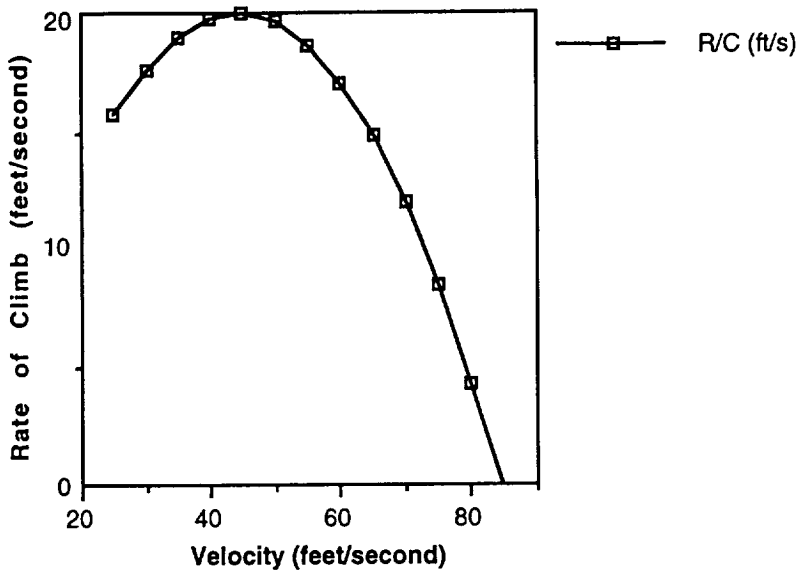

Figure 8-2: Effect of Velocity on Rate of Climb

Another graph was also produced using rate of climb data (V_{actual} = 15.6 Volts). Figure 8-3 was made because it provides very useful performance information. By graphically showing the effect of horizontal velocity on rate of climb (R/C), the largest possible climb angle and the climb angle which produces the greatest rate of climb can be found. These angles were found using the following relation:

$$\theta_c = \tan^{-1}\left(\frac{R/C}{H.Velocity}\right).$$

The maximum angle of climb was found to be 38.4 degrees, and occurs at a horizontal velocity of 20 feet/second. At a horizontal velocity of 40 feet/second the angle of maximum climb is calculated to be 26.6 degrees. Besides providing data regarding the climb angle, Figure 8-3 also shows the maximum obtainable level velocity. The highest velocity is the horizontal velocity when the rate of climb is zero. This occurs at a velocity of

approximately 84.6 feet/second, and is in close agreement with velocity information obtained from power available and required curves.

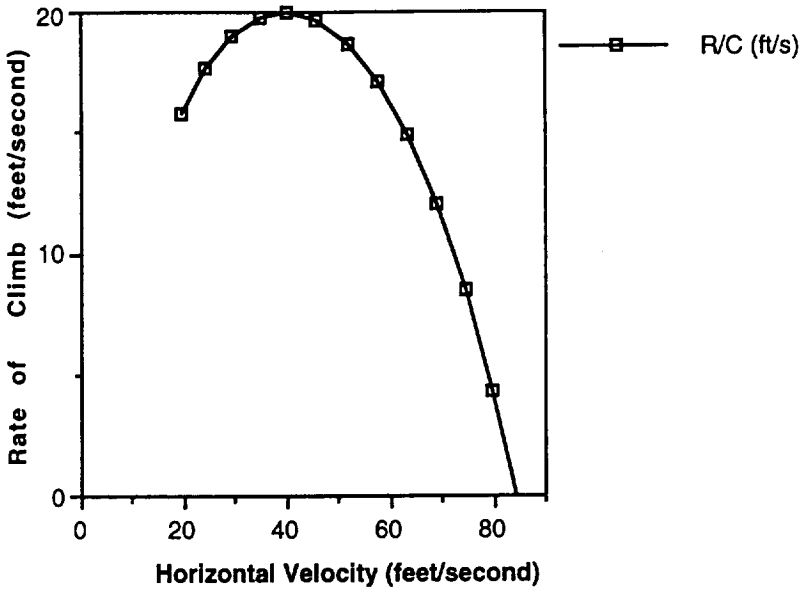

Figure 8-3: Effect of Horizontal Velocity on Rate of Climb

In the event of catastrophic engine failure, it is imperative that the valuable components of the aircraft survive. Excellent glide performance will help ensure this. The minimum glide angle was calculated using the following:

$$\tan(\gamma_{min}) = \frac{1}{(L/D)_{max}}.$$

where γ is the glide angle. With the maximum L/D ratio of 14.98, the minimum glide angle was found to be 3.82 degrees. With this glide slope angle the plane is able to negotiate a horizontal distance of 15 feet for every foot of vertical height. With this glide capability, the airplane can easily avoid any serious damage which might otherwise be incurred to the propulsion system or avionics package.

8.7 Range and Endurance

Simplified equations were used to calculate the endurance and corresponding range. Endurance was found by using

$$\text{Endurance} = \frac{970\text{mah}}{i_a},$$

where 970 mah is the capacity of the battery pack allowing for 30 mah to be drained during taxi. i_a represents the current draw for the cruise velocity of 55 feet/second. Range is calculated using the endurance as

$$\text{Range} = \text{Endurance} * V_{cruise}.$$

The effect of velocity on range and endurance is shown in Figure 8-4.

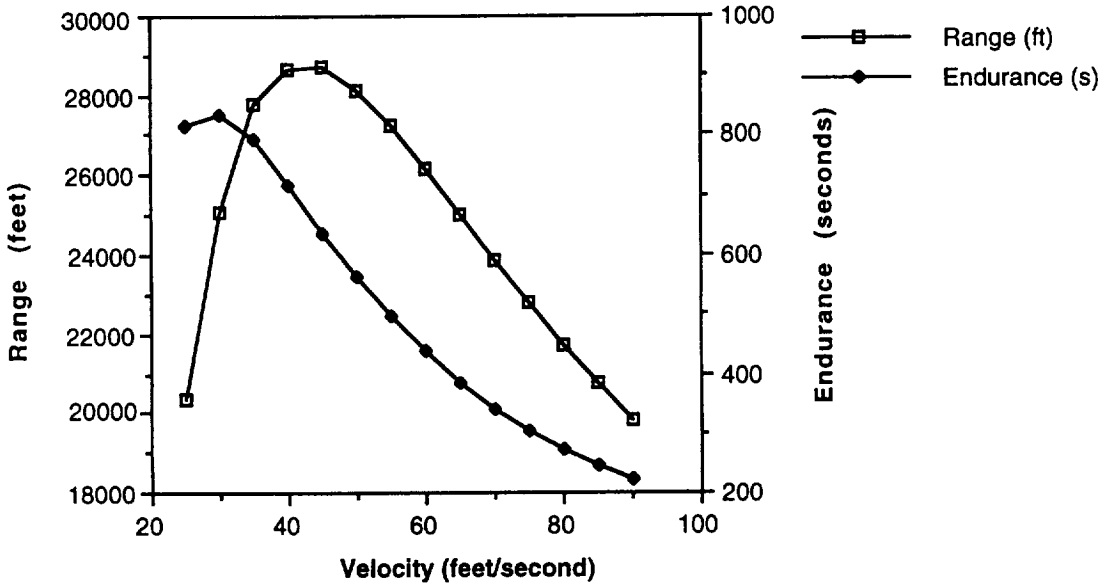

Figure 8-4: Effect of Velocity on Range and Endurance

For the cruise configuration the range was found to equal 27241.5 feet, and the plane could remain airborne for 8.26 minutes. The maximum values for

endurance and range were found by calculating both quantities at every velocity of the plane's flight envelope; from V_{stall} to V_{max}. The results appear in Table 8-1.

Velocity (feet/second)	Range (feet)	Endurance (minutes)
30 (Maximum Endurance)	25055.1	13.92
45 (Maximum Range)	28692.2	10.63
55 (Cruise Condition)	27241.5	8.26

Table 8-1: Range and Endurance Values

A more detailed calculation of range and endurance for the actual flight profile was also performed. The results follow in Table 8-2.

Flight Regime	Time (minutes)	Range (feet)	Current Draw (Amps)
Takeoff	0.023	0	16.70 (6.5 mah)
Climb (25 ft/s)	0.026	63.1	18.41 (7.9 mah)
Cruise (55 ft/s)	7.510	24783	7.05 (881.8 mah)
Loiter (30 ft/s)	1.000	1800	4.43 (73.8 mah)
Landing (25 ft/s)	0.000	0	0 (0.00 mah)
Totals	**8.55 minutes**	**26646.1 feet**	970 mah (30 mah-taxi)

Table 8-2: Detailed Range and Endurance for Flight

From this table is seen that the maximum endurance for a flight involving takeoff, climb, cruise velocity, and one minute loiter is 8.55 minutes. In the flight, the plane will travel 26646.1 feet. These values are comparable to those calculated under the assumption that the cruise condition was maintained for the entire flight.

8.8 Ceiling

The absolute and service ceilings for the aircraft were also calculated. In Aeroworld there are no large mountains to negotiate, and it is assumed to be at sea level. However, it is important to know the altitudes at which the airplane can effectively function. From Figure 8.5, the absolute ceiling is seen to be 52177 feet, and the service ceiling (where R/C = 1.65 feet/second) is at 47872 feet.

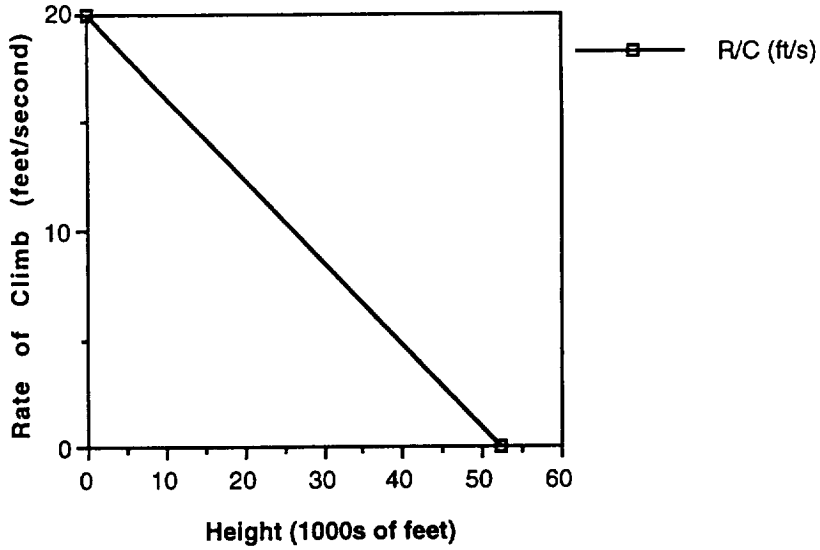

Figure 8-5: Effect of Height on Rate of Climb

9.0 STRUCTURAL DESIGN

The *Long Shot Aeronautics* structural design philosophy was to provide for the structural needs and requirements of *The Balsa Bullet* with a factor of safety of 1.5, while attempting to achieve the lowest structural weight in a relatively simple-to-construct design. Cost was also an issue. Because manufacturing labor expenses are a larger percentage of the total cost of the aircraft than raw materials, the emphasis of the design was placed on ease of manufacturing and not on raw material cost.

9.1 Loading

9.1.1 Flight Loading

The most strenuous maneuver which *The Balsa Bullet* was designed to accomplish was a sixty foot radius turn at a speed of thirty feet per second. This maneuver would place the aircraft at a twenty-eight degree bank angle from level flight, and incurs a load factor of 1.13 on the aircraft. Using a factor of safety of 1.5, this would have made the limit maneuvering load factor 1.7, which can be associated with a bank angle of fifty-four degrees. A sixty degree bank angle corresponds to a load factor of 2.0, and this was viewed as a more conservative estimate of the limit maneuvering load factor which *The Balsa Bullet* might encounter in flight. A negative limit maneuvering load factor of one was adopted, guided in part through the knowledge that *The Balsa Bullet* was not designed to fly in extreme dive maneuvers, and in part by standard Federal Air Regulations (F.A.R.). The resulting V-n diagram for *The Balsa Bullet* is shown in figure 9-1. Gust loads were not examined for *The Balsa Bullet*. Future designs should analyze these, as they may prove significant for outdoor flight.

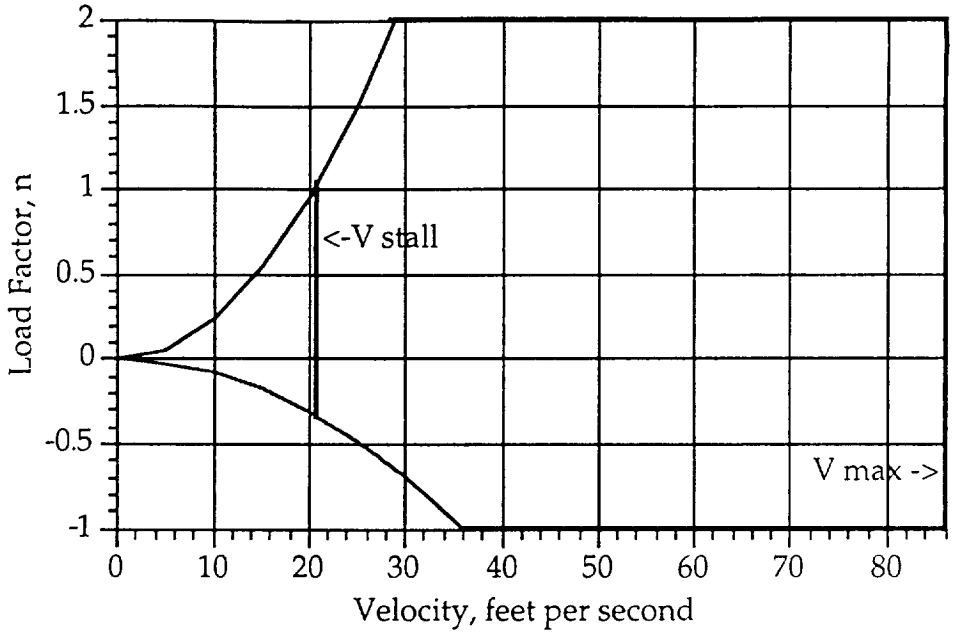

Figure 9-1: V-n Diagram

For this flight envelope, the maximum bending moment in the wing was computed to be 165.6 inch-pounds, occurring at the root of the wing. Additionally, the maximum bending moment in the fuselage was found to be 25.5 inch-pounds occurring at the wing/fuselage joint location.

9.1.2 Ground Loading

The free body diagram in figure 9-2 shows the ground forces on The Balsa Bullet in a stationary, fully loaded configuration. The force occurring on the main landing gear is assumed to be distributed evenly on each of the two wheels (1.5 pounds on each wheel).

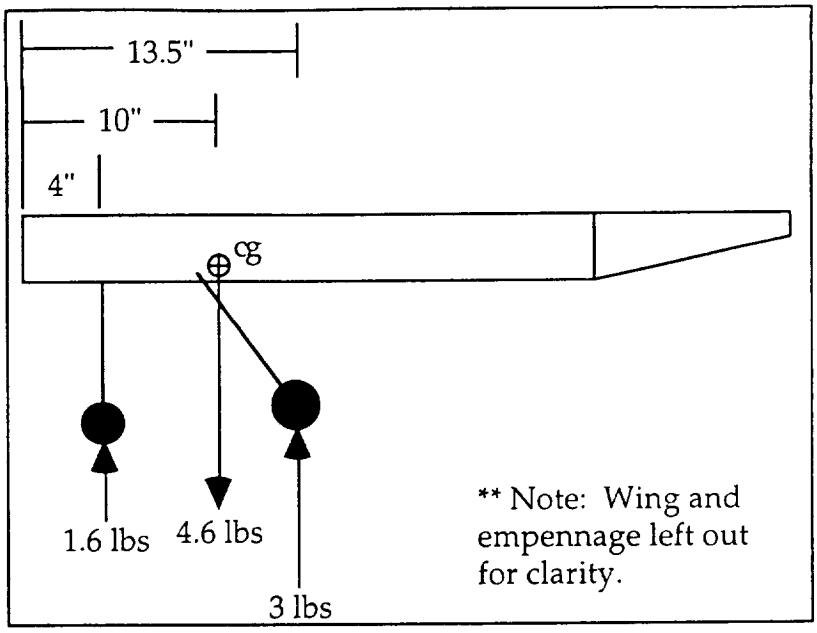

Figure 9-2: Aircraft Free Body Diagram -- Ground Loads

Based on previous Aeroworld design techniques, a landing load factor of three was adopted for the design of the landing gear for The Balsa Bullet. If the configuration in figure 9-2 is considered to be a landing load factor of one, a landing load factor of three would be three times each force acting on each respective landing gear assembly (that is 4.5 pounds on each of the main gear assemblies). The factor of safety of 1.5 required each main landing gear assembly to be designed to withstand a load of 6.75 pounds. Landing loads were assumed to occur on the two main landing gear assemblies only. (That is, a two point landing was the only scenario considered.)

9.2 Materials

Materials selection was based on the strength requirements for primary members and on weight and cost for non-critical members. Spruce, balsa, carbon fiber, and steel were selected for use in structural applications. Aluminum was also considered as a candidate, however the availability and more simple

manufacturing qualities of carbon fiber showed it to be a superior candidate in high strength situations. Table 9-1 provides a comparison of all materials considered.

Material	σ Compression (psi)	σ Tension (psi)	ρ (lb/in3)	E (psi) x 10^6
Balsa	400	600	0.009	0.065
Spruce	6200	4000	0.016	1.3
Carbon	130000	126000	0.058	24
Steel*	21000 (shear)	36000 (y) 58000 (u)	0.284	29
Aluminum	20000	15000	0.100	10

*Note: (y)-->yield, (u)-->ultimate

Table 9-1: Properties of Selected Materials

9.3 Wing Design

The design of the wing for *The Balsa Bullet* was driven by the high speed objective at cruise and the take-off distance requirement. Compromising the two factors necessitated the use of half-span flaps, and resulted in a relatively high wing loading.

With the half span flaps using 20% of the chord, there was an opportunity to make a three spar wing construction, with spars located at the leading edge, 25% chord, and 80% chord locations. Because the FX 63-137 airfoil section is thin at the 80% chord location, a two spar design was attempted, as the spar at the 25% chord location had a much larger potential cross-sectional moment of inertia, and would likely be able to carry the primary loads by itself. In addition, the two spar design was less complicated in both analysis and construction. (A half-span bulkhead was designed for use at the 80% chord in order to provide for flap attachment.)

For the wing design, the primary load bearing member was the 25% chord main spar. Figure 9-3 presents the wing lift, shear, and bending moment distributions in the spar at a load factor of 2.

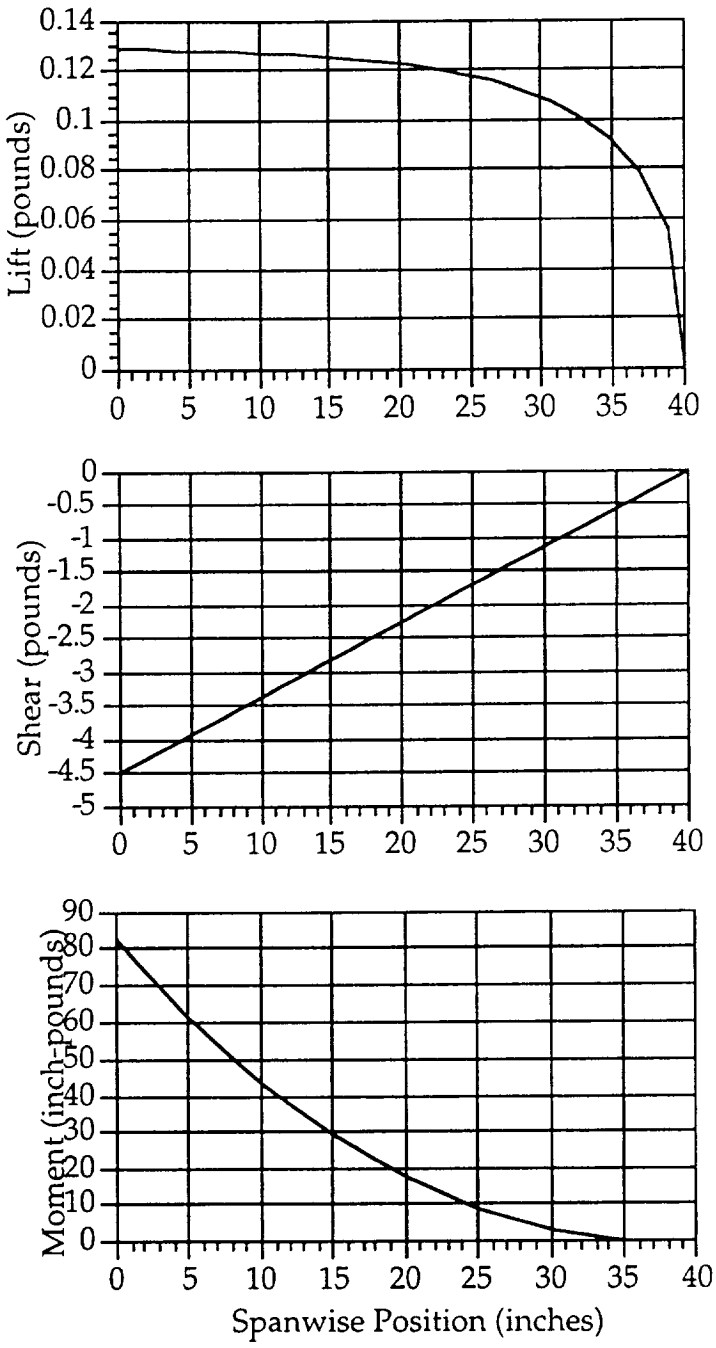

Figure 9-3: Half Span Wing Loading for Load Factor n=2

Figure 9-4 shows the main spar cross section chosen for use in the wing of *The Balsa Bullet*. With a factor of safety of 1.5, the spar was designed to withstand a bending moment of 248.4 inch-pounds at the root. The carbon fiber spar caps were selected for use in stiffening the wing. Figure 9-5 shows partial results of a trade study conducted on the main spar design. Note that at the design point, where the spar cap thickness is 0.25 inches, wing tip deflection was reduced by 80% due to the carbon fiber. The main spar has a margin of safety of 5, due to the significant strength improvement given by the carbon fiber.

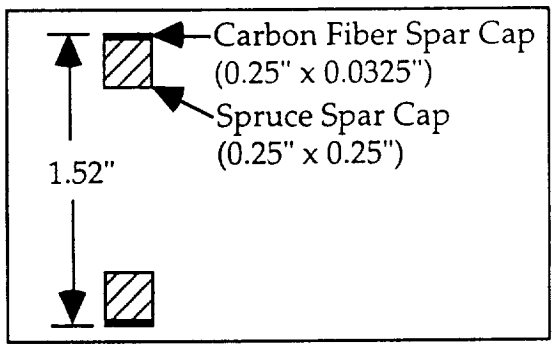

Figure 9-4: Main Spar Cross Section

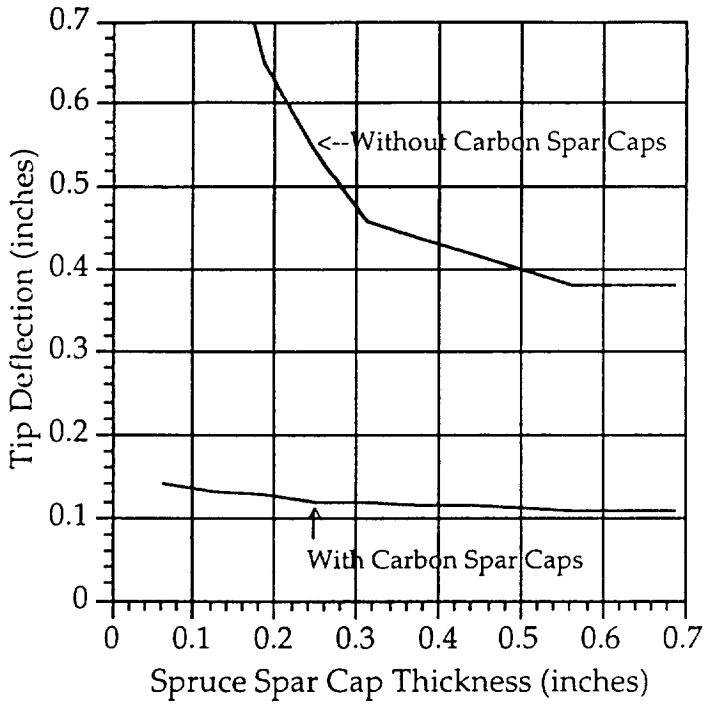

Figure 9-5: Wing Tip Deflection Analysis

9.4 Landing Gear

9.4.1 Considerations

The design philosophy regarding *The Balsa Bullet's* maneuverable nose wheel tricycle landing gear was to create main gear struts that would yield without failing in an extreme landing situation. Minimization of both drag and weight were considered critical. Landing gear design was constrained by the rough field requirement (three inch grass) in terms of strut length (constrained by tip clearance and propeller diameter), and wheel diameter, as well as the elimination of using of a shock absorbing tensile wire between the main struts. A rough field was also thought to interfere with the ground operation of a tail-dragger configuration. The fixed diameters available for steel strut rods further limited the design choices.

9.4.2 Strut Selection

Stand-alone struts were selected for the main landing gear design, as opposed to landing gear struts connected by a shock absorbing spring or wire. This was due primarily to the three inch clearance requirement. A shock absorbing wire was thought to cause maneuvering difficulties in rough grass.

Because the density of steel is high, a seemingly small increase in the main strut diameter resulted in a large weight increase. This caused the design landing load factor of three to be called into question. A specific concern was whether a design based on a load factor of three in addition to the required factor of safety of 1.5 would create landing gear which would be too stiff. The extreme landing case was also questioned on the grounds of probability -- what are the chances that an aircraft would actually impact at a load factor of three? Although the questions raised were not examined in detail (perhaps they should be), significant landing impacts have been observed in Aeroworld (*Diamond Back*, 1993). Due to these occurrences and the desire to be cautious in the event of an upset, the decision was made to design the landing gear at the previously decided load factor of three.

A steel strut of diameter 5/32 inch was found to yield without failing under the required loading conditions, providing a margin of safety of -0.24. This negative margin is justifiable, as the landing gear has been designed to deflect and absorb some of the forces of a hard landing, much like a spring, rather than transmit the force of impact through to the main spar. Figure 9-6 shows a sketch of the main landing gear attachment to the main lower spar cap.

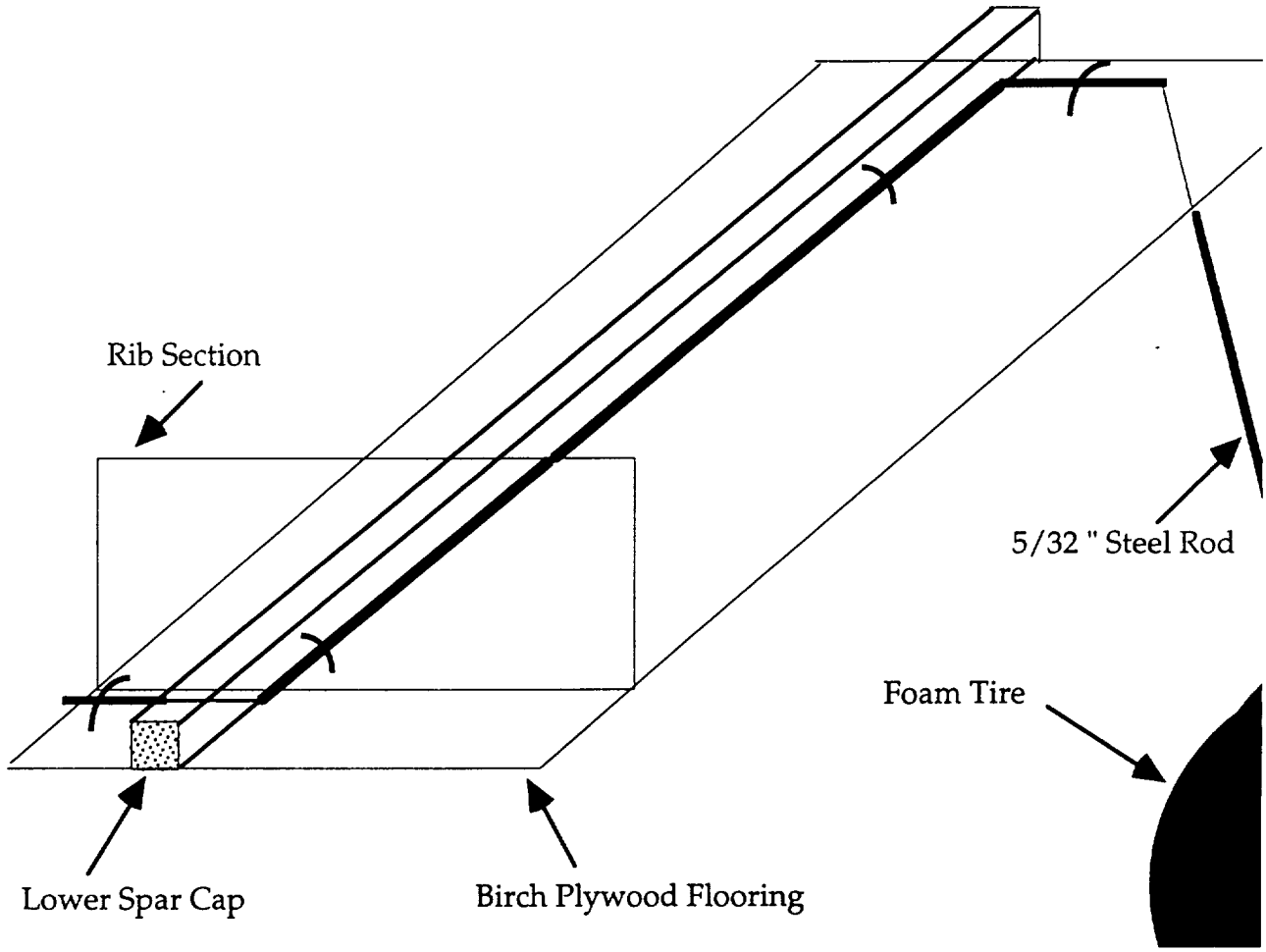

Figure 9-6: Landing Gear Detail

The nose strut was selected to be a 5/32 inch diameter steel rod. The steering assembly and strut will be off-the-shelf and will attach to the main plywood floor of the aircraft, just aft of the motor mount bulkhead. These "pre-fabricated" components were selected with and eye towards the associated time (and hence cost) savings which they should provide. Steering control will be provided by the rudder control servo.

9.4.3 Wheel Selection

The primary drivers in wheel selection were weight, drag considerations, and the wheel's ability to roll in three inch grass. While the third factor was

largely intuitive, it did serve to narrow down the tire choices. A two inch diameter wheel was believed to be able to roll in three inch grass, however it was not believed to be able to overcome the starting friction in the grass. A 2.5 inch diameter wheel was the smallest diameter tire which was believed to be able to overcome the initial friction of the rough field and was selected for use on all three struts. Foam tires were selected, as they are 15% lighter than rubber tires with similar diameters. Larger diameter tires were desirable for easier take-off and ground handling characteristics, however, a tire diameter reduction of 0.75 inches (from 3.25 inches to 2.5 inches) reduced the total aircraft drag by approximately 5%.

9.5 Fuselage

Figure 9-7 shows the fuselage for *The Balsa Bullet*. The length was limited by the necessary payload volume on one extreme, and by the necessary length for stability and control on the other (while maintaining reasonably sized empennage surfaces). Weight was also a consideration, and spruce was limited to high stress areas.

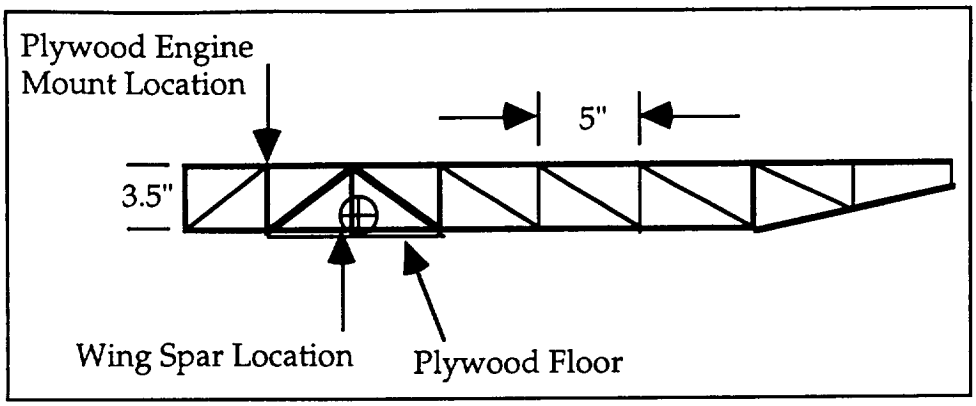

a) Side View

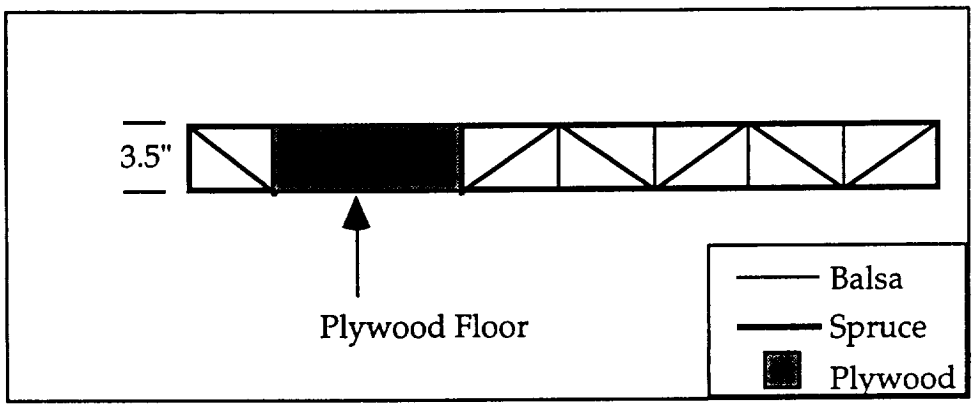

b) Bottom View

Figure 9-7: Fuselage

The main longerons of the fuselage were designed to withstand a bending moment of 38.25 inch-pounds. The 1/4 by 1/4 inch spruce longerons selected provide a margin of safety of 2.0 in this loading configuration.

9.6 Empennage

The empennage design featured the use of NACA 0009 airfoil sections for both vertical and horizontal surfaces. For manufacturing simplicity, the control surfaces were ideally designed to be solid balsa sections with cut out holes for weight savings. Due to availability concerns, though, the rudder design had to utilize spar and rib construction. Figures 9-8 and 9-9 show the vertical

tail/rudder and the stabilizer assemblies respectively. Due to control horn mounting considerations as well as rib/spar joining considerations, thicker balsa spars were used in place of slimmer spruce spars. Both sections use all balsa designs.

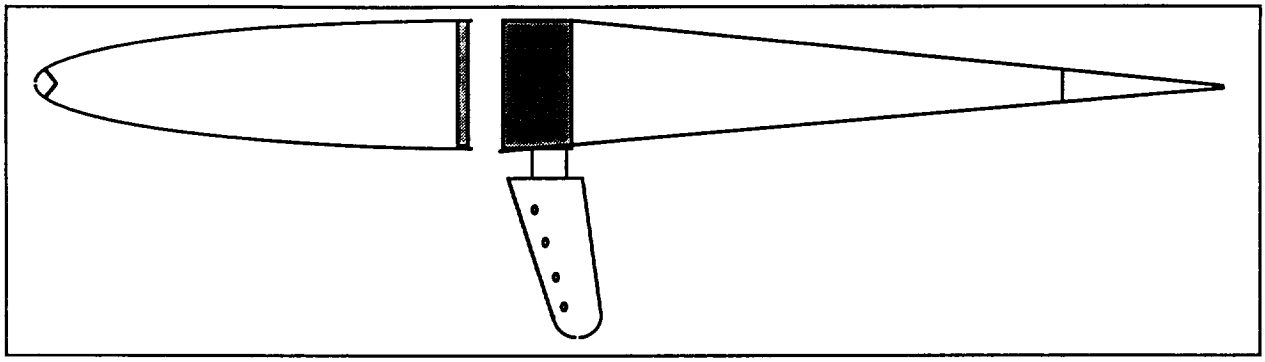

a) Top View

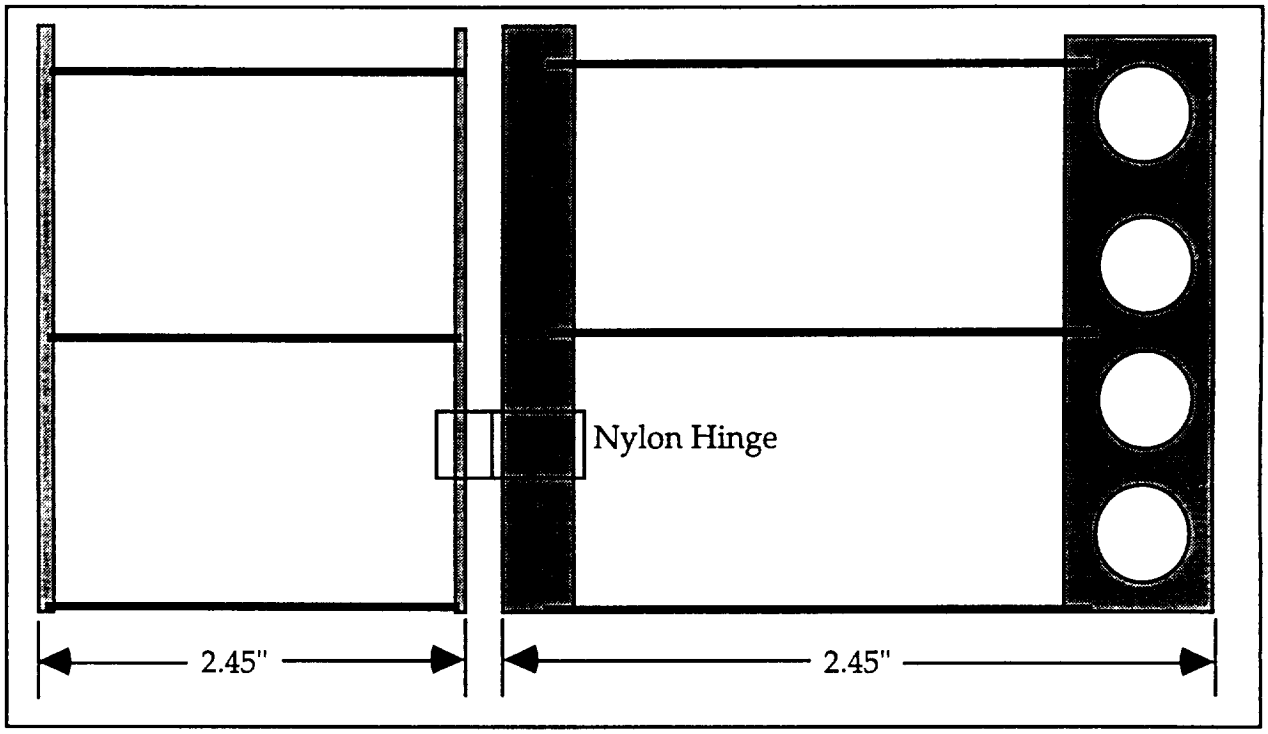

b) Side View

Figure 9-8: Vertical Tail Assembly

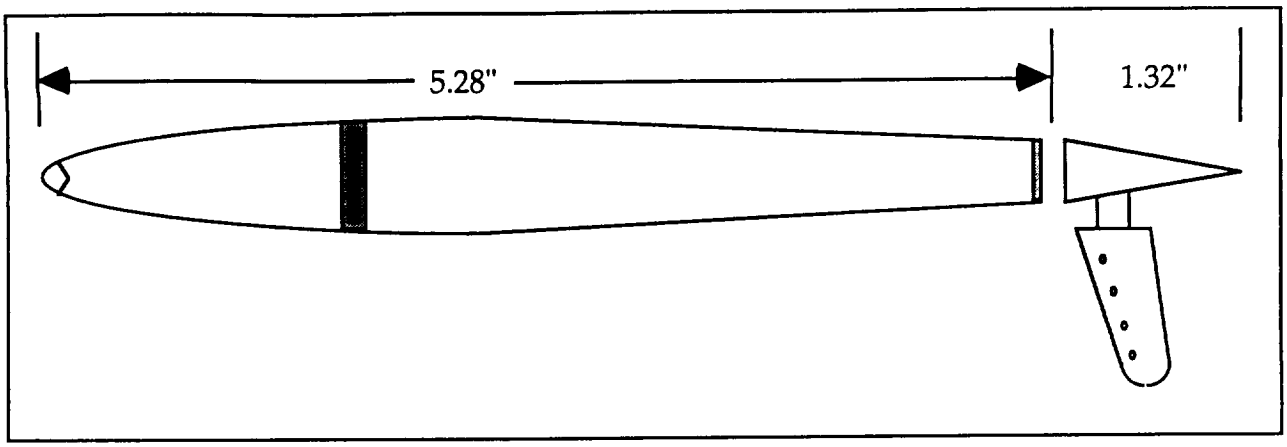

a) Side View

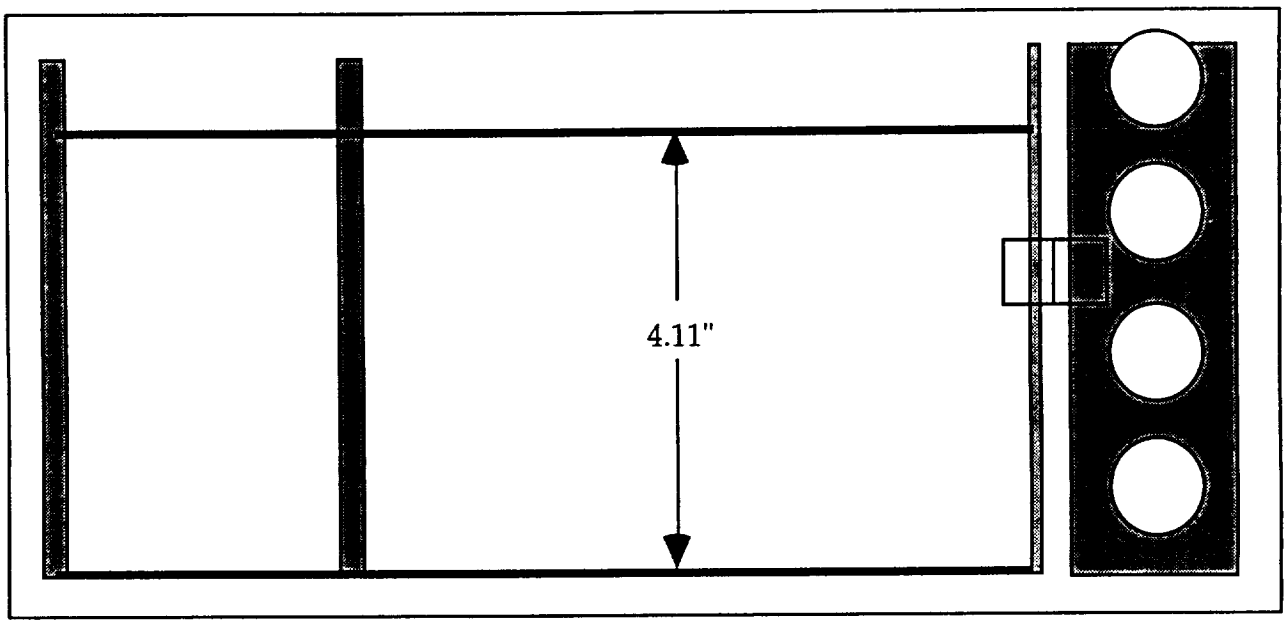

b) Top View

Figure 9-9: Stabilizer Assembly

10.0 Economic Analysis

10.1 Economic Requirements and Objectives

Long Shot Aeronautics began with the goal to create a high-speed, low cost plane to compete in an Aeroworld market that was sagging. In order to compete in this market, the total aircraft cost to the consumer became a primary objective for *The Bullet* design. The primary goal was to create an affordable aircraft that could be mass produced without sacrificing cruise and takeoff performance. The specific economic requirements and objectives as determined by *Long Shot Aeronautics* were:

- Maximum manufacturing cost of $1600
-Maximum labor cost of $900 (90 hrs of construction)
- minimize waste and associate costs
- maximum limit of $290.00 on raw materials
-minimize cost per flight

10.2 Cost Estimates

The total estimated cost for *The Bullet* is laid out in Table 10-1. Based on this estimate, all the economic objectives were met. However, this is contingent upon labor costs totaling no more than $900. As illustrated in Figure 10-1, the largest costs occur in the manufacturing process (55%).

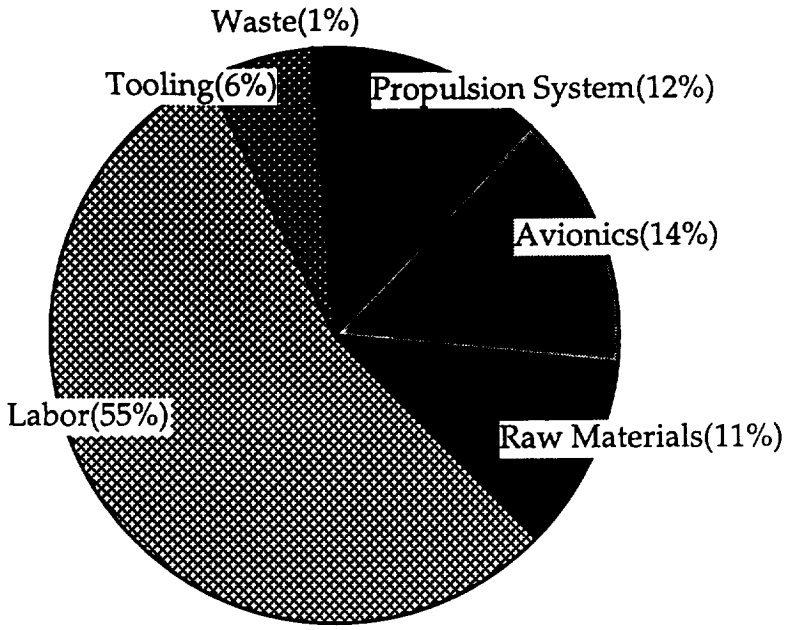

FIGURE 10-1: COST BREAKDOWN OF THE BALSA BULLET

In order to meet the labor cost objective, a very detailed and efficient manufacturing plan must be developed. Otherwise, the cost of the aircraft will increase approximately $16.00 for every extra hour of work. Thus, ease of construction became a catalyst in our drive to keep labor costs down.

10.3 Direct Operating Costs

The direct operating costs per flight are composed of the depreciation costs, operation costs, and fuel costs. The breakdown of direct operating costs for *The Bullet* are shown in Table 10-1. These values were calculated using the procedures set forth in Reference 1. Early on in the design process, a range of 16,000 feet was selected as a design requirement. This allows *The Bullet* to service over 50% of the flights to any two airports in Aeroworld with a one minute loiter. The decision to choose a relatively short range was very cost effective. Not only could money be saved by using a lower amphour battery, but also the direct operating costs of the Bullet were reduced. For a design range of

16,000 ft and cruise velocity of 55 feet/second, the design flight time is only 4.8 minutes. The resulting number of flights possible is 1238, which means the depreciation costs per flight are only $2.07. Fuel costs were directly proportional to the current draw, which increases with velocity, and inversely proportional to the lift to drag ratio which decreases with velocity. The fuel costs range from $1.57 to $1.93, depending on the price of an amp-hour. The resulting costs per flight range from $3.82 to $4.18. The breakdown of the cost per flight as a function of cruising velocity is shown in Figure 10-2.

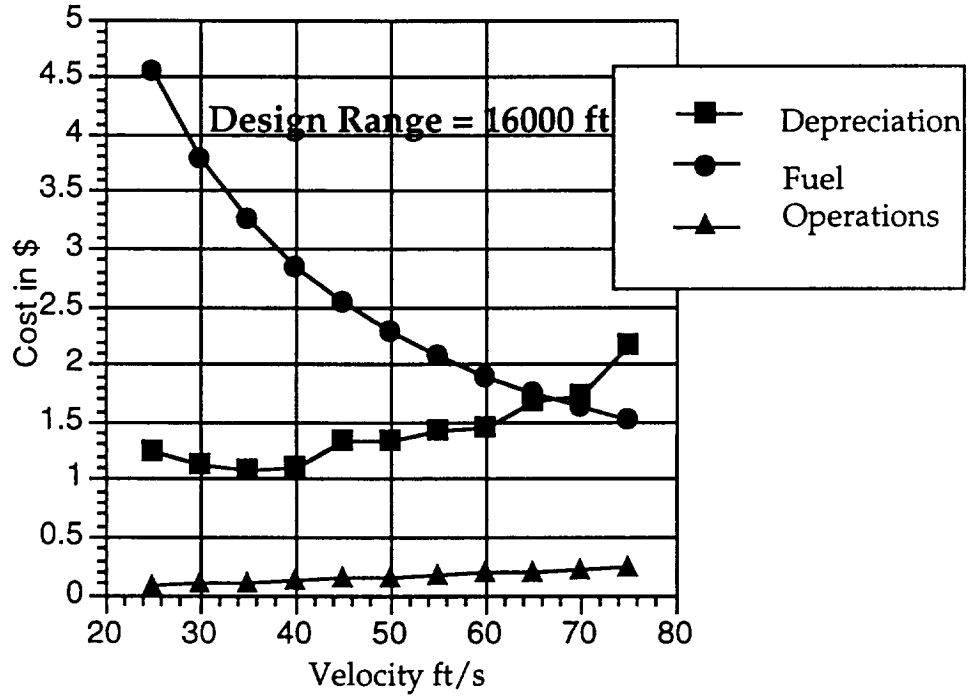

FIGURE 10-2:

DIRECT OPERATING COSTS AS A FUNCTION OF VELOCITY

10.3 Costing Factors

The three primary cost factors that will determine the marketability of the Bullet in the Aeroworld market are

-cost per flight (CPF)
-cost per 1000 ft (CPKFT)
-cost per minute (CPFM)

The specific formulas to determine these cost factors can be found in Reference 1. The CPF for the bullet is $3.93, the CPKFT is $.23, and the CPFM is $.76. The economic objective to be competitive in Aeroworld facilitates the need to minimize these cost factors. In order to achieve this goal, one would think that *The Bullet* should fly at its most aerodynamically efficient cruise speed to reduce fuel costs. This occurs are 31 feet/second, where the lift to drag ratio is a minimum. However, upon further analysis as shown in Figure 10-3, this is not the case.

In fact, the optimum cruising speed in terms of cost per flight is 60 feet/second, which even betters the design cruise speed objective of 55 feet/second. Although the cost per flight minute is higher at this speed, the rationale is that the people of Aeroworld are willing to pay a little extra if they can get to their destination a little quicker.

It should also be noted that the maximum attainable range for *The Bullet* is 27,000 feet due to the fact that smaller batteries could not be purchased. However, this allows for flexibility in the costing factors of *The Bullet* . If the maximum range of 27000 feet is used in calculating the costing factors, the CPF turns out to be $5.93, the CPKFT = $.22, and the CPFM = $.1. Comparing these values with the values found using a design range of 16,000 feet, it is clear that for a little extra cost per flight ($2.00 more), the prospective customer can now make over 80% of the flights in Aeroworld. At the same time, the CPFM, is reduced drastically. This flexibility in the aircraft can satisfy a larger portion of the prospective buyers in the Aeroworld market. *The Bullet* can either be used for short quick flights, or longer more time consuming flights, without an enormous increase in cost.

10.4 Economic Summary

Low cost was a main focus in the design of *The Bullet*. However, as the design process evolved, low cost was not deemed as important as meeting high-speed performance and takeoff requirements. Therefore, several decisions made in the design process may not seem very economical. For example, the decision to use flaps, was not very economical. The use of flaps added fixed costs in terms of an extra servo ($35), and they also pose a major construction risk. The decision to use flaps may require extra labor costs as well. Also, the selection of the FX-63-137 airfoil may pose some economic problems since it may also be difficult to manufacture. The thinking behind these decisions was that the increased aerodynamic performance will actually save the company in the long run both in terms of cost per flight and fuel costs which makes *The Bullet* more marketable.

Fixed Subsystems			
Propulsion			
	motor		$107
	speed control		$50
	batteries (13 panasonic 1000 maph)		$39
	propeller(Zinger 12-8)		$5
Controls			
	radio receiver		$35
	radio transmitter		$75
	avionics battery pack		$10
	switch harness		$5
	servos(3)		$105
	wiring		$4
		Subtotal	$435
Raw Materials			
	balsa		$30
	spruce		$30
	plywood		$5
	carbon strips		$50
	monokote		$30
	glue		$10
	miscellaneous		$10
	landing gear struts		$2
	wheels		$12
		Subtotal	$179
Manufacturing			
	labor		$900
	tooling		$100
Waste Disposal			$20
	Company's Cost		**1,634**
	Overhead	x 1.4	2287.6
	Profit	x 1.12	2562.11
	Selling Price		**$2,562.11**
Vcruise = 55 ft/s	Number of Flights		1,238
Range = 16000 ft	Depreciation Costs		$2.07/flight
	Operation Costs		$.177/flight
	Fuel Costs		
	$1.50/maph		$1.57/flight
	$3.00/maph		$1.93/flight
	Total Cost Per Flight		**$3.82-$4.18**

TABLE 10-1: TOTAL COST BREAKDOWN

11.0 References

1. Batill, Stephen. "AE441 Lecture Notes." University of Notre Dame, 1994.

2. Beer, Ferdinand P. and E. Russell Johnston, Jr. Mechanics of Materials. McGraw-Hill: New York , 1981.

3. Design Proposal for *The Airplane* . University of Notre Dame, 1993.

4. Design Proposal for *The Bunny* . University of Notre Dame, 1993.

5. Design Proposal for *Diamondback* . University of Notre Dame, 1993.

6. Design Proposal for *Gold Rush* . University of Notre Dame, 1993.

7. Design Proposal for *The RTL-46* . University of Notre Dame, 1993.

8. Dunn, Patrick F. "AE454 Lecture Notes." University of Notre Dame, 1993.

9. Jensen, Daniel T. "A Drag Prediction Methodology for Low Reynolds Number FLight Vehicles." University of Notre Dame, 1990.

10. McCormick, Barnes W. Aerodynamics, Aeronautics, and Flight Mechanics. John Wiley and Sons: New York, 1979.

11. Nelson, Robert C. "AE444 Lecture Notes." University of Notre Dame, 1993.

12. Nelson, Robert C. Flight Stability and Automatic Control. McGraw-Hill: New York, 1989.

13. Selig, Michael S., John F. Donovan, and David Fraser. Airfoils at Low Speeds. HA Stokely Publishing: Virginia, 1989.

Appendix A: Deliverable Items

Figure A-1: Effect of Weight on Range

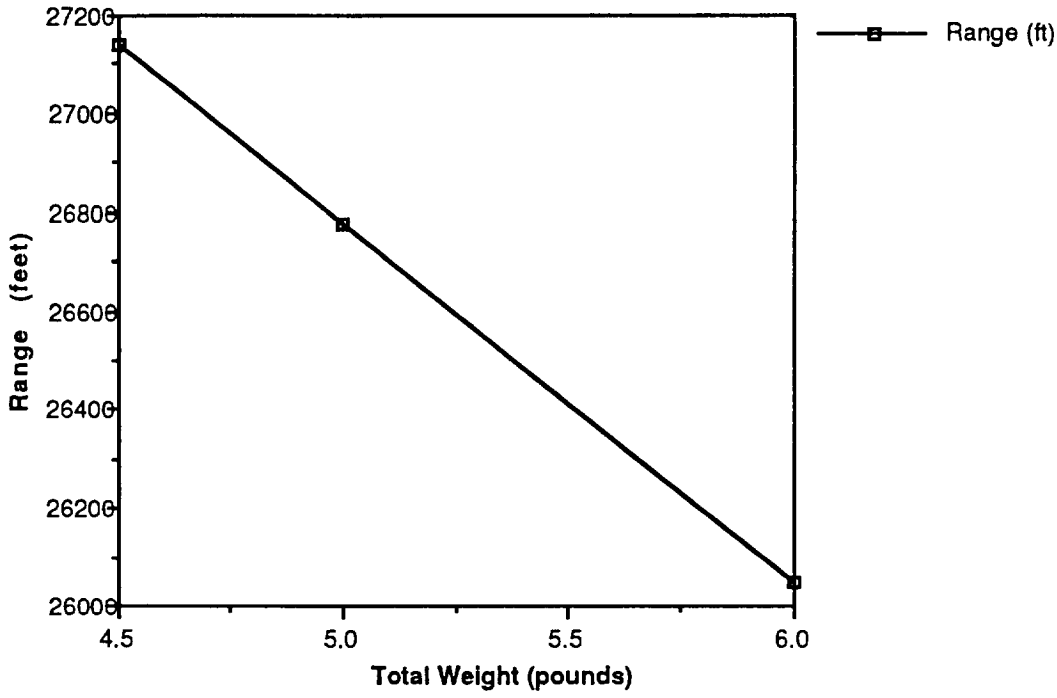

Figure A-2: FX63-137 Airfoil Lift Curve

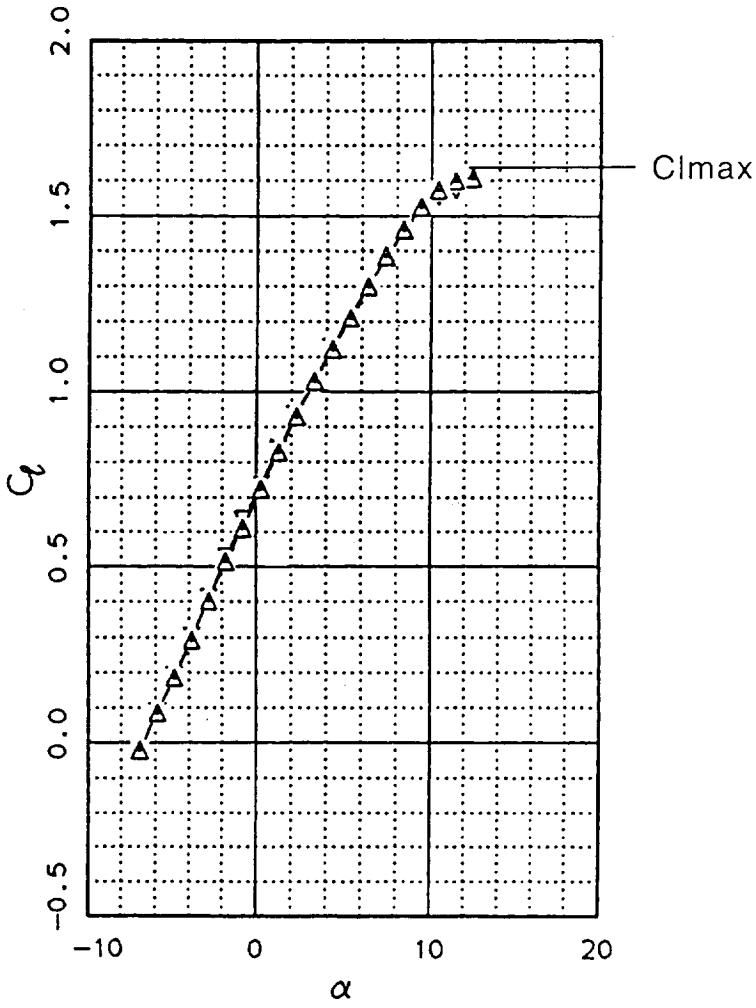

Figure A-3: Aircraft Lift Curve With and Without High Lift Devices

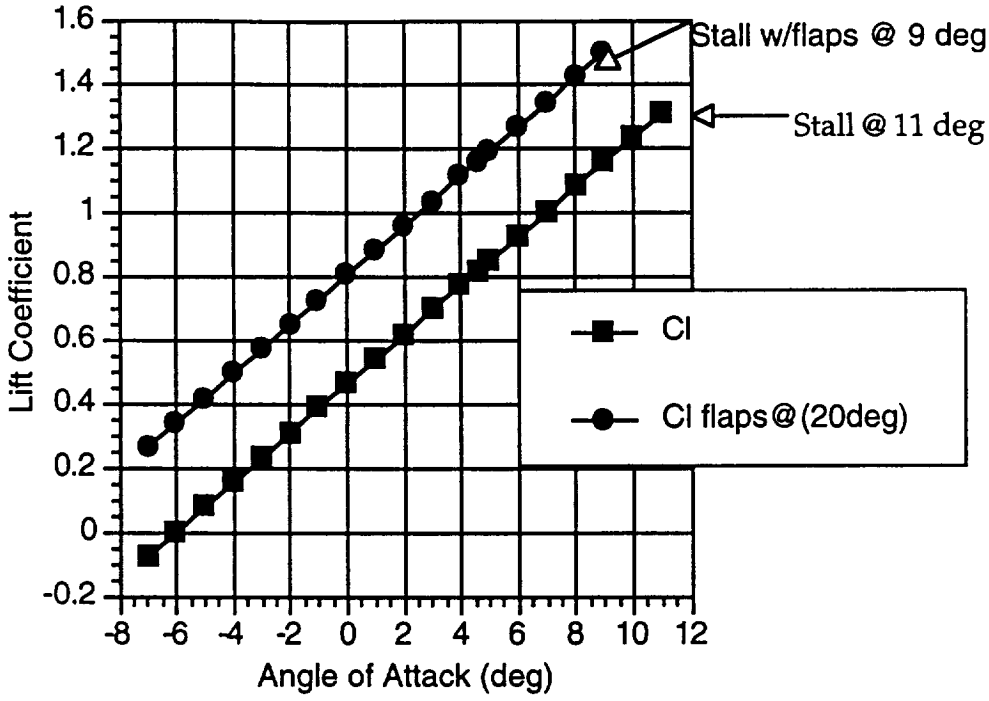

Figure A-4 Aircraft Drag Polar With and Without High Lift Devices

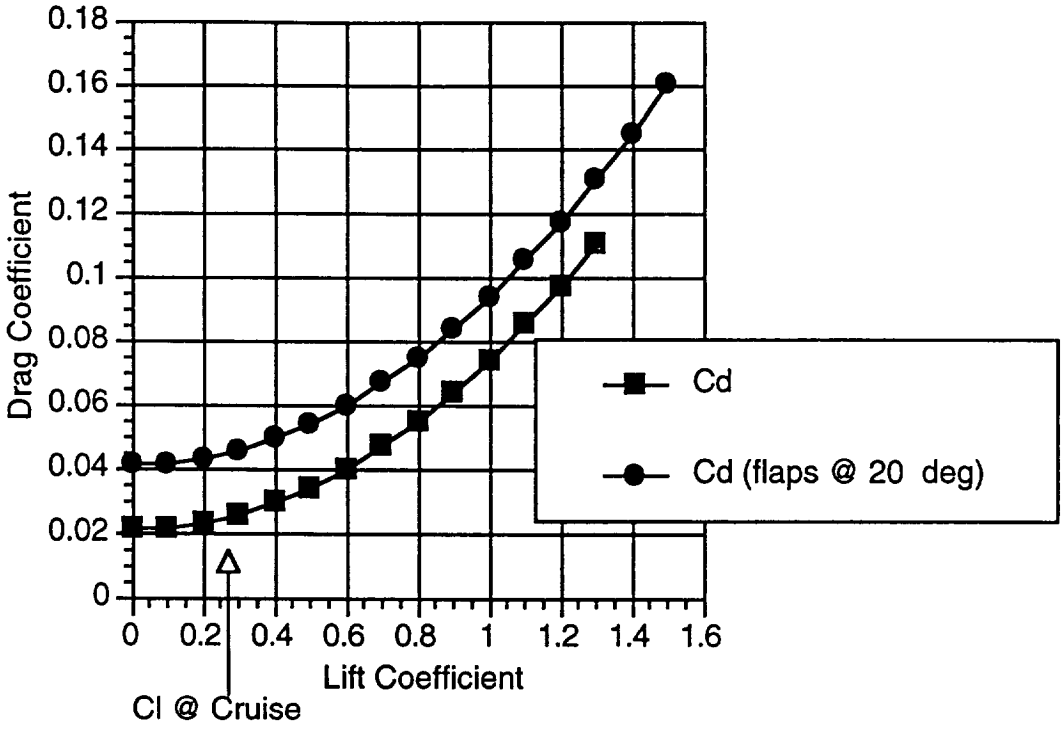

Figure A-5: Lift to Drag Ratio Dependence Upon Aircraft Angle of Attack

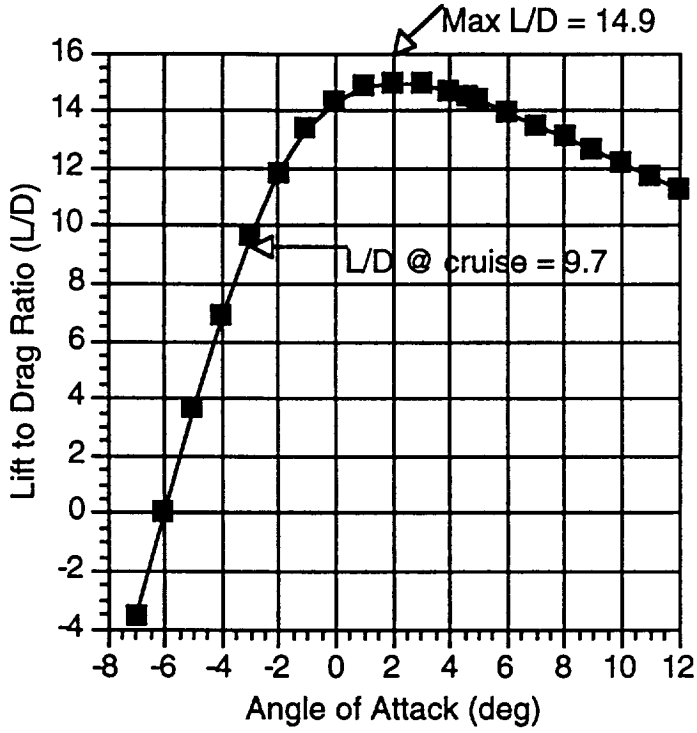

Figure A-6: Effect of Angle of Attack on Pitch Moment Coefficient at the Forward and Aft Center of Gravity Locations

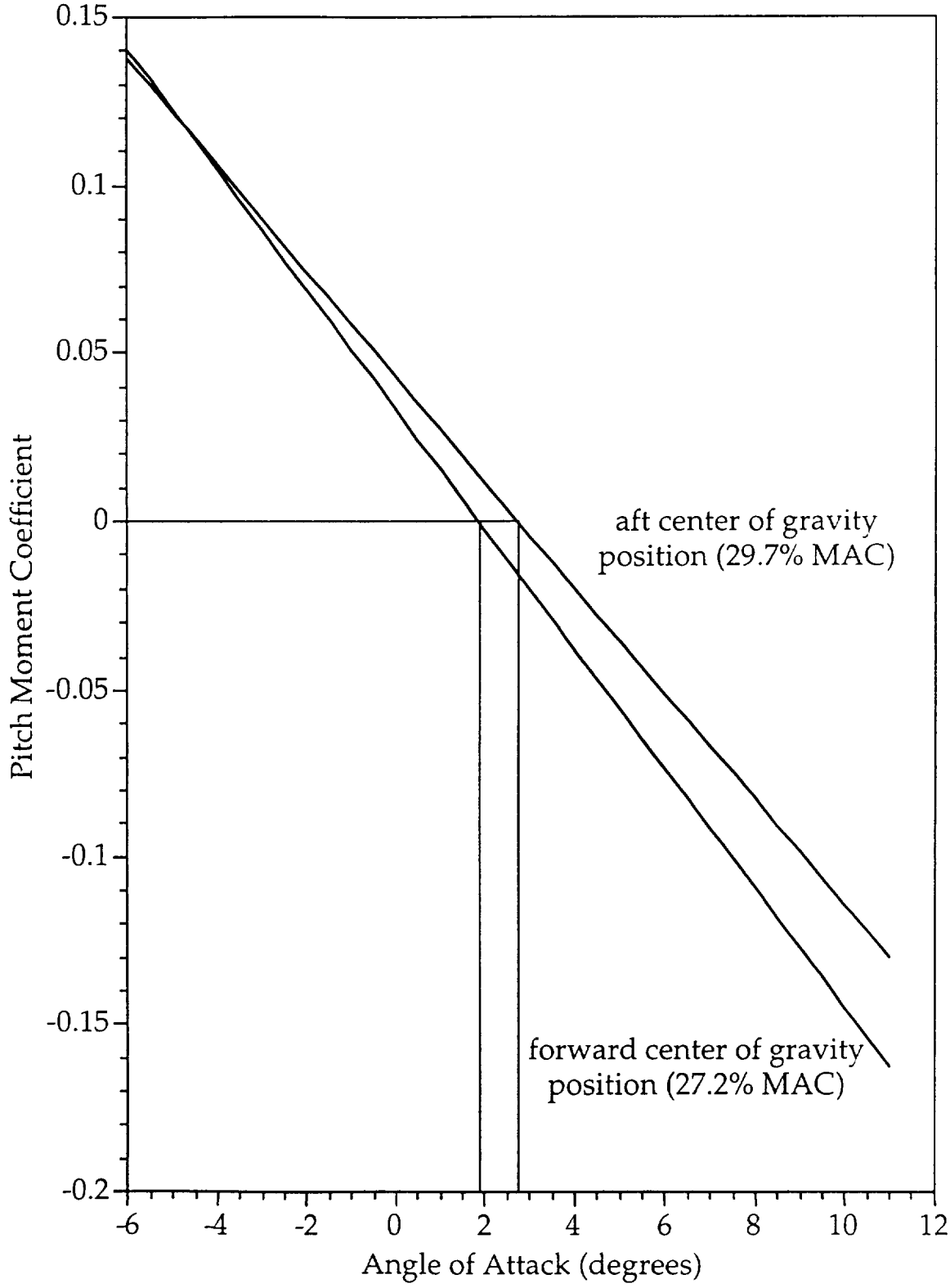

Figure A-7: Effect of Velocity on Power Available and Required

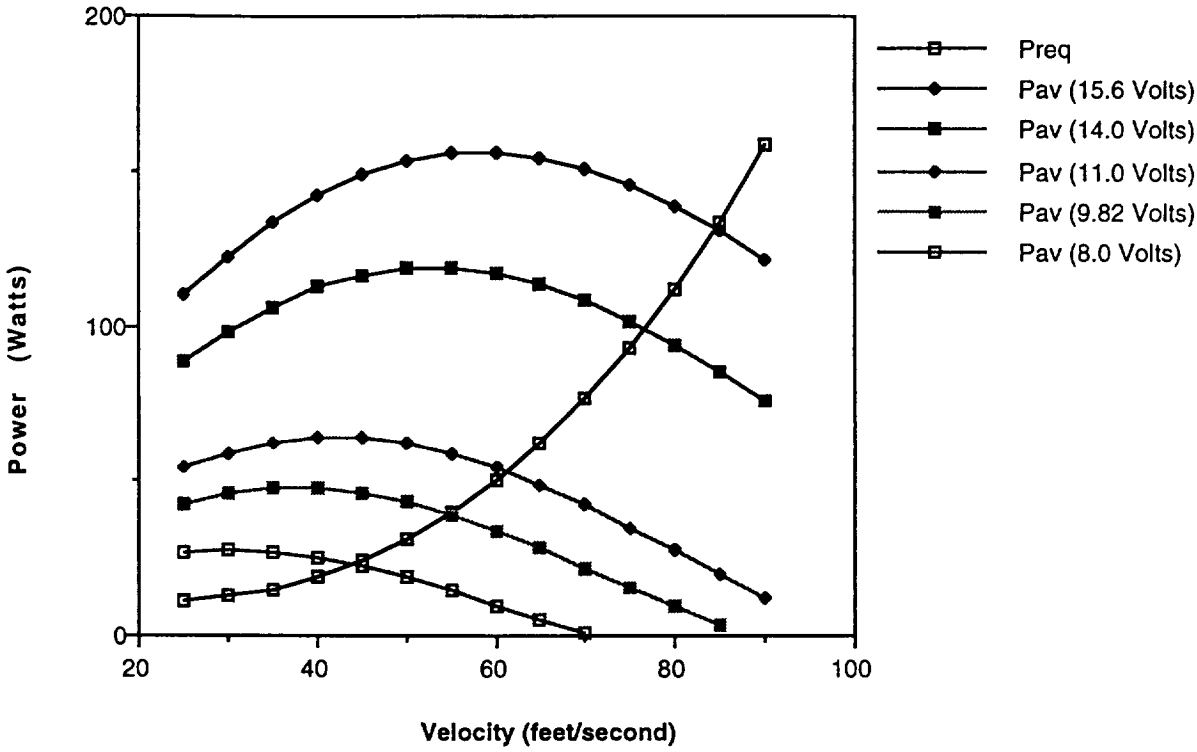

Figure A-8: Effect of Advance Ratio on Propeller Efficiency

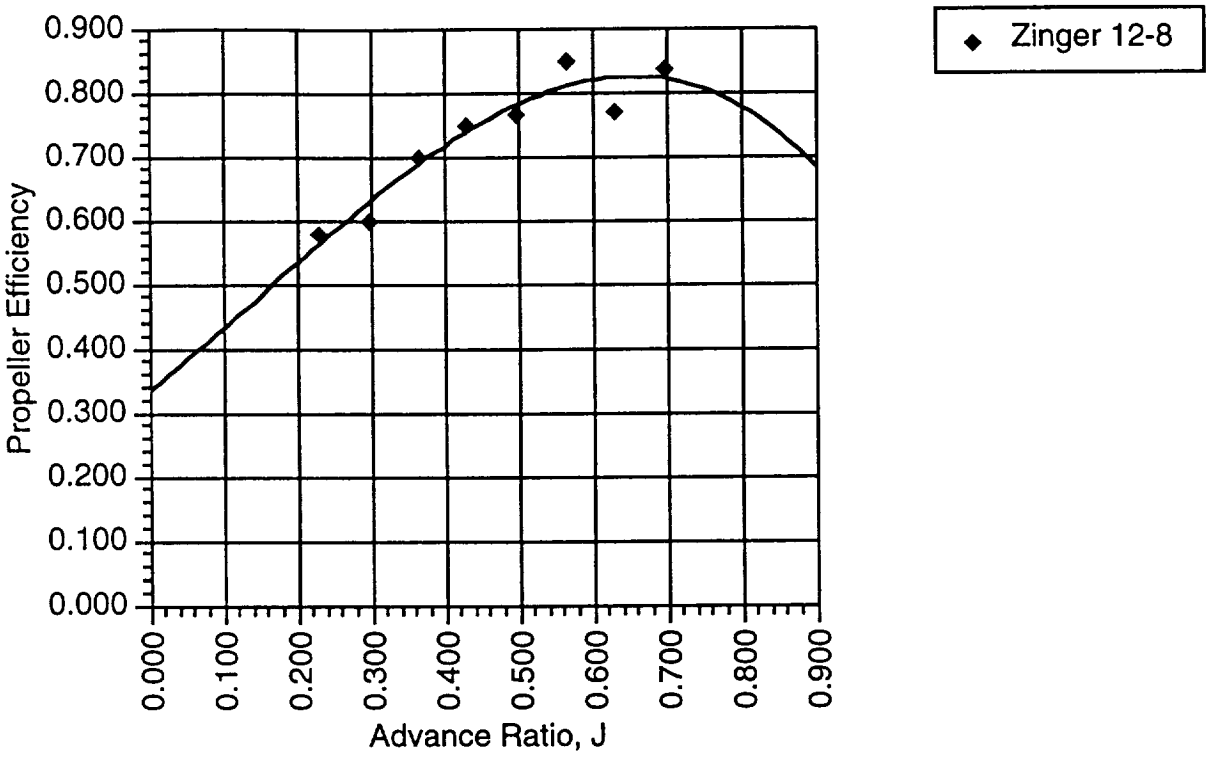

Figure A-9: Weight and Balance Diagram

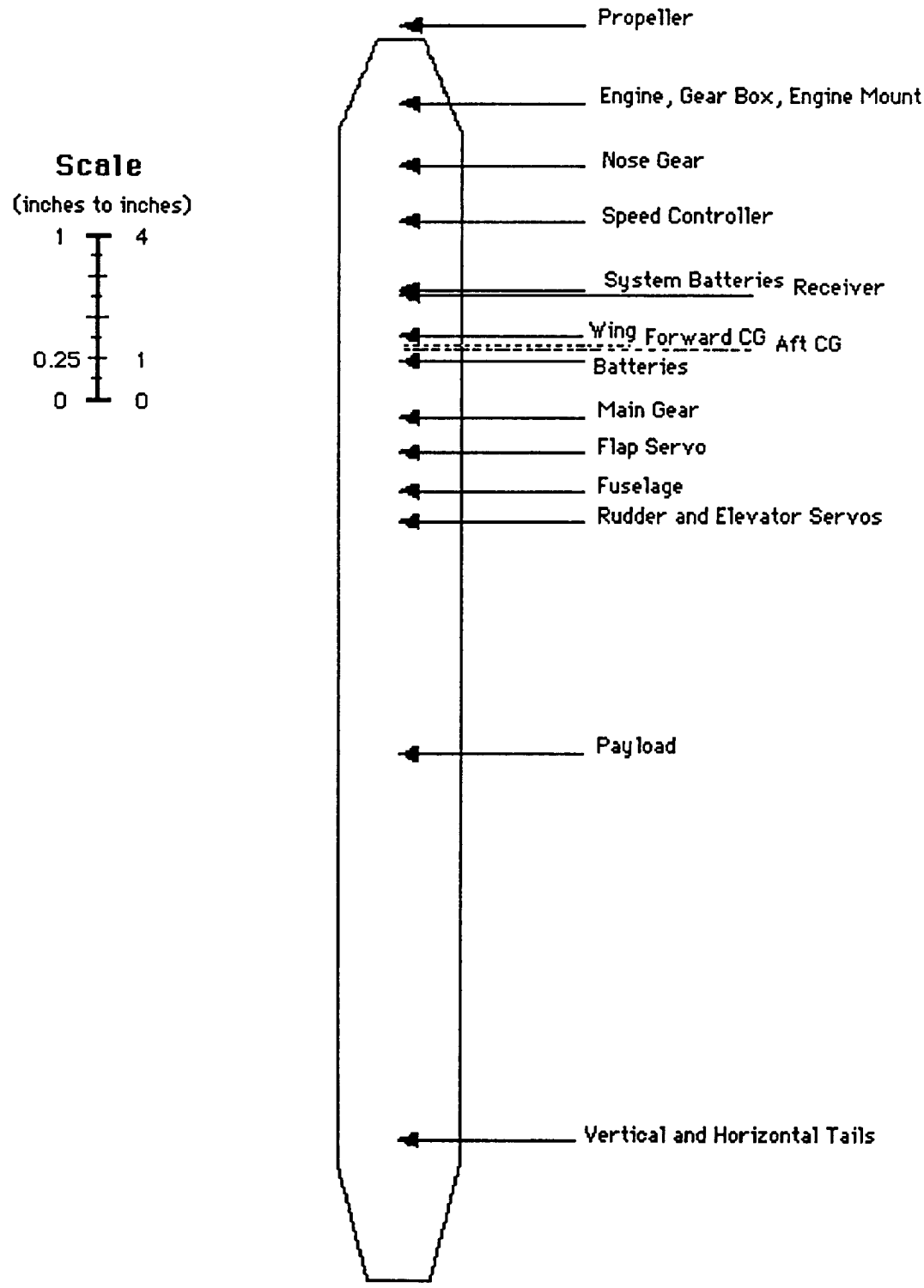

Table A-10: Weight Estimation

Airplane Component	Initial Weight (pounds)	Revised Weight (pounds)	% of Revised Total Weight
Propulsion	0.704	0.735	16.02
Engine	0.438	0.469	10.21
Gear Box	0.094	0.094	2.04
Engine Mount	0.073	0.073	1.58
Propeller	0.100	0.100	2.18
Batteries	1.095	1.056	23.02
Avionics	0.408	0.433	9.43
Servos (3)	0.113	0.113	2.45
Speed Controller	0.111	0.111	2.41
System Batteries	0.125	0.125	2.72
Receiver	0.059	0.059	1.29
Fuselage	0.563	0.280	6.10
Wing	0.781	0.800	17.44
Tail	0.250	0.205	4.46
Horizontal	0.125	0.149	3.25
Vertical	0.125	0.056	1.21
Landing Gear	0.375	0.621	13.53
Main Gear	0.250	0.410	8.93
Nose Gear	0.125	0.211	4.60
Glue, etc.	****	0.200	4.35
Error Factor	5%	5%	****
Total Unloaded	**4.384**	**4.546**	****
Payload	0.035	0.050	1.08
Total Loaded	**4.419**	**4.596**	****

Figure A-11: V-n Diagram

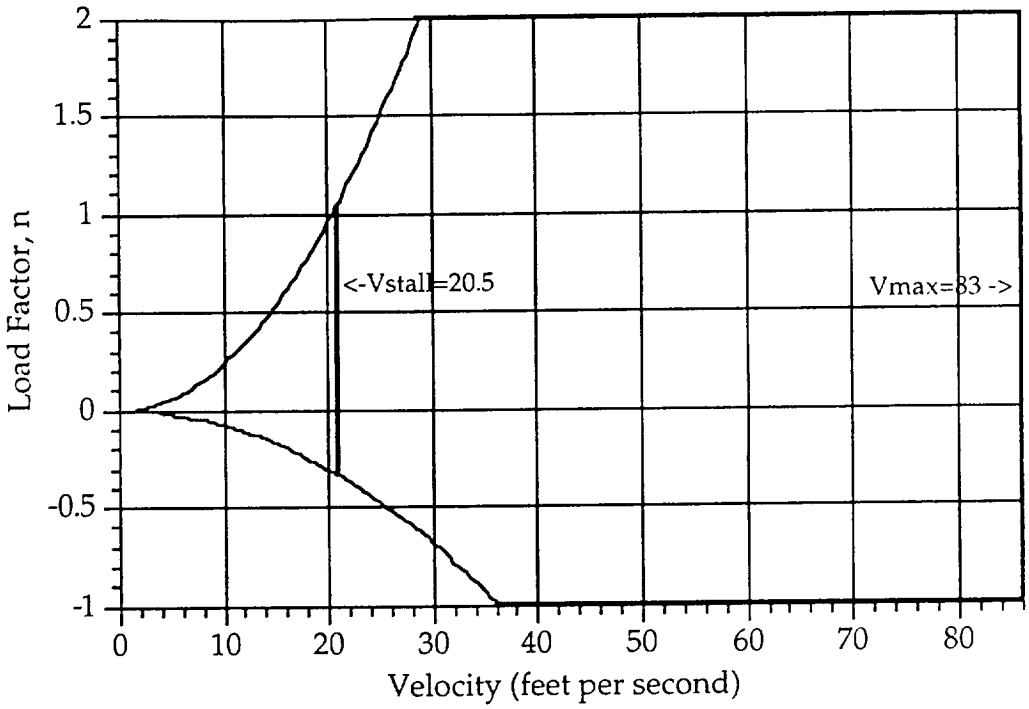

Figure A -12: Three View External Sketch

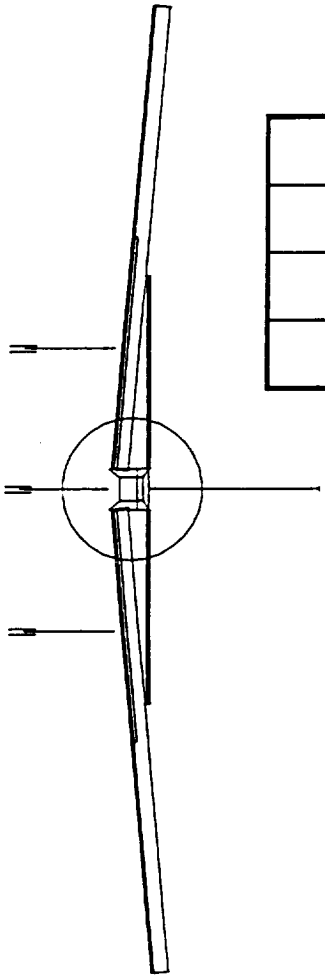

S_W = 6.33 ft^2	S_V = .50 ft^2
c_W = .96 ft	c_V = .41 ft
S_h = 1.50 ft^2	length = 3.54 ft
b_h = 2.74 ft	Zinger 12 - 8 propeller

Scale: 1 inch = 1.74 feet

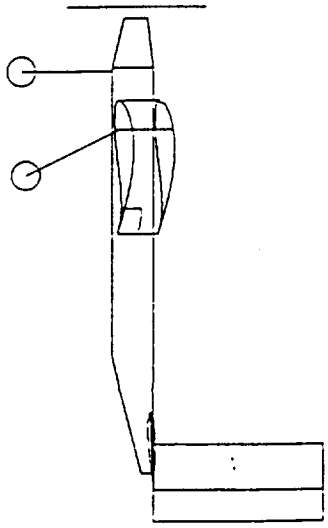

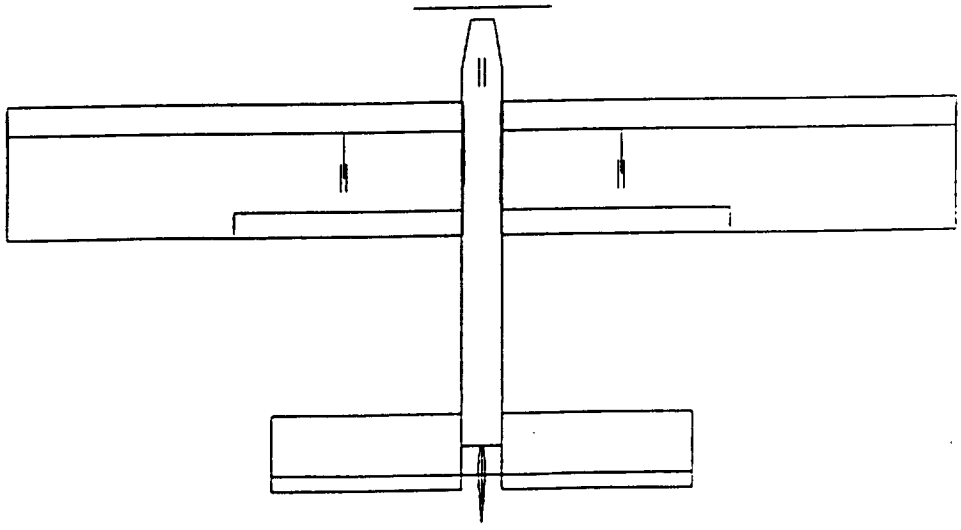

Figure A - 13: Internal Configuration

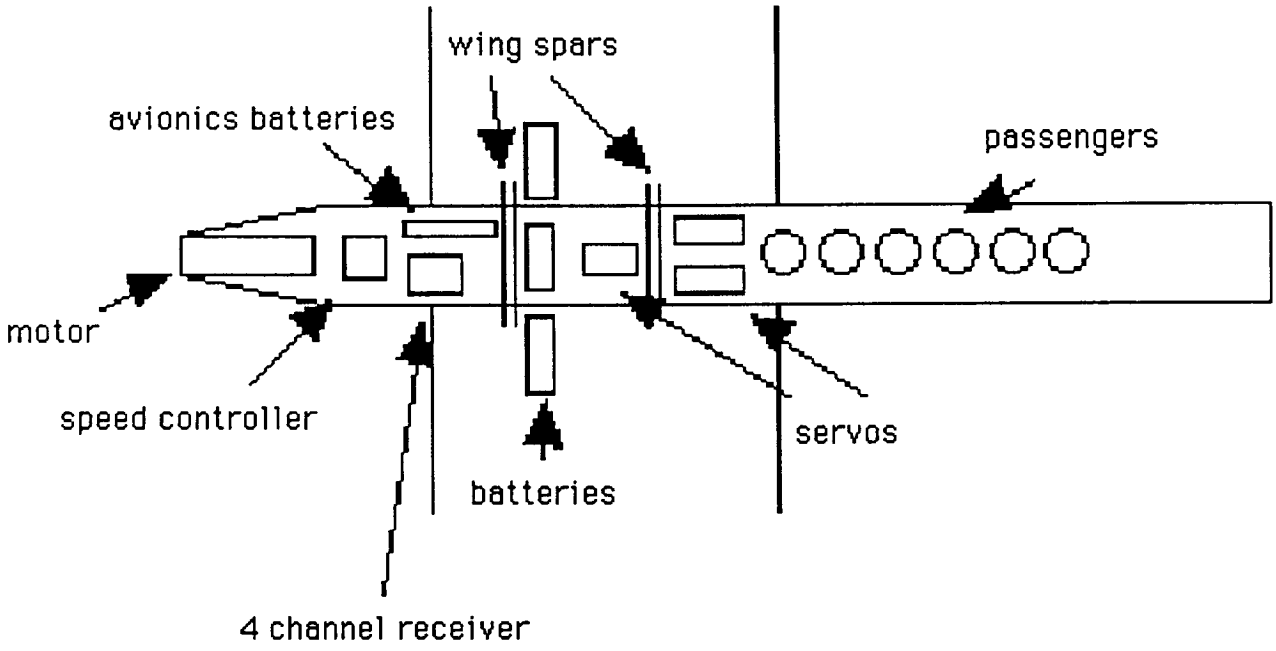

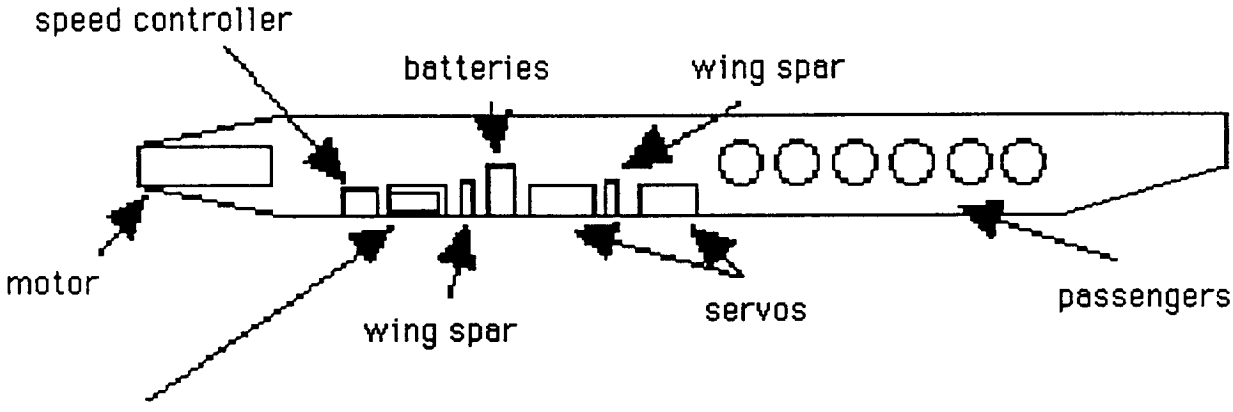

4 channel receiver and avionics batteries

Appendix B: Critical Data Summary

Parameter	Initials of RI:	Date: 24 Mar
*[all distances relative		
to aircraft nose		
and in common units]*		
DESIGN GOALS:		
V cruise	DK	55 ft/s
No. of passengers/crew	DK	6
Max Range at Wmax	DK	16000 ft
Maximum TO Weight-WMTO	DK	5.5 lb
BASIC CONFIG.		
Wing Area	jr	6.33 sq ft
Maximum TO Weight - WMTO	sg	4.6 lbs
Empty Flight Weight	sg	4.54 lbs
Wing loading(WMTO)	sg	11.63 oz/sq ft
max length	jr	40 in
max span	jr	6.75 ft
max height	dk	24.6 in
Total Wetted Area	dk	2048 sq in
WING		
Aspect Ratio	jr	7.2
Span	jr	6.75 ft
Area	jr	6.33 sq ft
Root Chord	jr	0.937 ft
Tip Chord	jr	0.937 ft
taper Ratio	jr	1
C mac - MAC	jr	-0.12
leading edge Sweep	jr	0
1/4 chord Sweep *	jr	0
Dihedral	jr	5 deg
Twist (washout)	jr	0
Airfoil section	jr	FX 63-137
Design Reynolds number	jr	328,000
t/c	jr	13.60%
Incidence angle (root)	jr	0 deg

Hor. pos of 1/4 MAC	jr	0.917 ft
Ver. pos of 1/4 MAC	jr	0.71 ft
e- Oswald efficiency	jr	0.8
CDo -wing	jr	0.007
CLo - wing	jr	0.456
CLalpha -wing	jr	4.35 /rad
FUSELAGE		
Length		40 in
Cross section shape		square
Nominal Cross Section Area		0.0625 sq ft
Finess ratio		12.4
Payload volume		0.54 sq in
Planform area		0.972 sq ft
Frontal area		12.25 sq in
CDo - fuselage		0.005
EMPENNAGE		
Horizontal tail		
Area	jr	1.5 sq ft
span	jr	2.74 ft
aspect ratio	jr	5
root chord	jr	0.548 ft
tip chord	jr	0.548 ft
average chord	jr	0.548 ft
taper ratio	jr	1
l.e. sweep	jr	0
1/4 chord sweep	jr	0
incidence angle	jr	-2.25 deg
hor. pos. of 1/4 MAC	jr	2.958 ft
ver. pos. of 1/4 MAC	jr	0.71 ft
Airfoil section	jr	NACA 0009
e - Oswald efficiency	jr	0.8
CDo -horizontal	jr	0.0019
CLo-horizontal	jr	0
CLalpha - horizontal	jr	4.46 /rad
CLde - horizontal	jr	0.518
CM mac - horizontal	jr	0
Vertical Tail		
Area	jr	0.5 sq ft
Aspect Ratio	jr	3
root chord	jr	0.41 ft

tip chord	jr	0.41 ft
average chord	jr	0.41 ft
taper ratio	jr	1
l.e. sweep	jr	0
1/4 chord sweep	jr	0
hor. pos. of 1/4 MAC	jr	2.958
vert. pos. of 1/4 MAC	jr	1.41 ft
Airfoil section	jr	NACA 0009
SUMMARY AERODYNAMICS		
Cl max (airfoil)	jr	1.7
Cmo (airfoil)	jr	-0.12
CL max (aircraft)	jr	1.46
lift curve slope (aircraft)	jr	4.30 /rad
CDo (aircraft)	jr	0.0288
efficiency - e (aircraft)	jr	0.76
Alpha stall (aircraft)	jr	11 deg
Alpha zero lift (aircraft)	jr	-6 deg
L/D max (aircraft)	jr	12.22
Alpha L/D max (aircraft)	jr	2.6 deg
WEIGHTS		
Weight total (empty)	sg	4.54 lbs
C.G. most forward-x&y	sg	9.76 in
C.G. most aft- x&y	sg	10.03 in
Avionics	sg	0.433 lb
Payload-Pass.&lugg.-max	sg	0.05 lb
Engine & Engine Controls	sg	0.636 lb
Propeller	sg	0.1 lb
Fuel (battery)	sg	1.056 lb
Structure	sg	1.906 lb
Wing	sg	0.8 lb
Fuselage/emp.	sg	0.485 lb
Landing gear	sg	0.621 lb
PROPULSION		
Type of engines	JS	ASTRO 15
number	DK	1
placement	DK	5 in
Pavil max at cruise	JS	155.93 Watts
Preq cruise	JS	39.385 Watts
max. current draw at TO	JS	16.7 amps

cruise current draw	JS	7.05 amps
Propeller type	JS	Zinger
Propeller diameter	DK	12 in
Propeller pitch	DK	8 in
Number of blades	DK	2
max. prop. rpm	JS	7271.7
cruise prop. rpm	JS	4793.8
max. thrust	JS	3.12 lb
cruise thrust	JS	0.528 lb
battery type	JS	P-100SCR
number	JS	13
individual capacity	JS	1000 mah
individual voltage	JS	1.2 V
pack capacity	JS	1000 mah
pack voltage	JS	15.6 V
STAB AND CONTROL		
Neutral point	jr	0.492 c
Static margin %MAC	jr	22.3
Hor. tail volume ratio	jr	0.51
Vert. tail volume ratio	jr	0.17
Elevator area	jr	0.75 sq ft
Elevator max deflection	jr	30 deg
Rudder Area	jr	0.25 sq ft
Rudder max deflection	jr	30 deg
Aileron Area	jr	0
Aileron max deflection	jr	0
Cm alpha	jr	-0.971
Cn beta	jr	0.521
Cl alpha tail	jr	0.518
Cl delta e tail	jr	0.319
PERFORMANCE		
Vmin at WMTO	JS	20.45 ft/s
Vmax at WMTO	JS	84.6 ft/s
Vstall at WMTO	JS	20.45 ft/s
Range max at WMTO	sg	28692.2 ft
Endurance @ Rmax	sg	10.63 min
Endurance Max at WMTO	sg	13.92 min
Range at @Emax	sg	25055.1 ft
Range max at Wmin	sg	28842.7 ft
ROC max at WMTO	sg	20.0 ft/s
Abs. Ceiling	JS	52177 ft

Min Glide angle	JS	3.82 degrees
T/O distance at WMTO	JS	21.3 ft
SYSTEMS		
Landing gear type	DK	tricycle
Main gear position	DK	13.45
Main gear length	DK	7.62
Main gear tire size	DK	2.5 in dia
nose gear position	DK	4
nose gear length	DK	8
nose gear tire size	DK	2.5 in dia
engine speed control	js	tekin
Control surfaces	jr	rudder, elevator
ECONOMICS:	ke	
raw materials cost	ke	$179
propulsion system cost	ke	$201
avionics system cost	ke	$234
production manhours	ke	90 hours
personnel costs	ke	$900
tooling costs	ke	$100
total cost per aircraft	ke	$2562.11

Appendix C: Aircraft Data Base

Plane Name	Wto (lb)	Fus. shape	lfus (in)	Wfus (oz)	S (ft^2)	b (ft)
FX/90, 1990	2.75	Rec	17	10	4.38	5.84
Blue Emu, 1993	5.6	Rec	58.8	10.44	10	10
Gold Rush, 1993	5.4	Rec	60	13.76	10.94	8.75
The Airplane, 1993	5.25	Rec	64	17	9.5	9.5
The Penguin, 1990	3.125	Rec, tapered	42	9.6	4.67	7
The Screem-J4D, 1990	3	Rec, tapered	37	10.9	5.47	8
The Drag-n-Fly	3.05	Rec, tapered	41		6	8.5
The RTL-46, 1993	5.1	Rec	66		9.93	9.17
The Diamondback, 1993	6.41	Rec	67		9.65	9.65
The Bunny, 1993	5.3	Trap	58	19.67	10	9.22

Plane Name	Wing Loading (lb/ft^2)	Wing Weight (lb)	Weight/S
FX/90, 1990	0.616	0.656	0.150
Blue Emu, 1993	0.5625	1.96	0.196
Gold Rush, 1993	0.49	0.84	0.078
The Airplane, 1993	0.58125	1	0.105
The Penguin, 1990	0.6692	0.781	0.167
The Screem-J4D, 1990	0.548	0.648	0.118
The Drag-n-Fly	0.444	0.525	0.088
The RTL-46, 1993	0.514	1.31	0.131
The Diamondback, 1993	0.664	0.81	0.084
The Bunny, 1993	0.503	0.9	0.090

Plane Name	Weight/b	Airfoil	Clmax	AR
FX/90, 1990	0.112	FX-63-137B-Pt	1.23	7.79
Blue Emu, 1993	0.196	Wortman	1.1	10
Gold Rush, 1993	0.096	FX63-137	1.6	7
The Airplane, 1993	0.105	SPICA	1.28	9.5
The Penguin, 1990	0.112	Wortmann FX-63-137	1.1	10.5
The Screem-J4D, 1990	0.081	NACA 4415	1.3	11.7
The Drag-n-Fly	0.062	SPICA	1	12
The RTL-46, 1993	0.143	SD7062	1.8	8.46
The Diamondback, 1993	0.084	Clark-Y	1.17	9.65
The Bunny, 1993	0.098	FX63-137	1.45	8.5

Plane Name	High/Low, Dihedral	Lt ver (ft)	Sv (in^2)	bv (in)	ARv	Lt hor (ft)
FX/90, 1990	H, 13 deg	2.05	50.46	8.4	1.4	2.05
Blue Emu, 1993	H, 8 deg	3	105.12	13.4	1.7	2.77
Gold Rush, 1993	H, 15 deg	4.25	144	12	1	4.475
The Airplane, 1993	H, 8 deg	5.167	180	30	5	5.167
The Penguin, 1990	H, 3 deg	2.86	60.48	12	2.4	2.86
The Screem-J4D, 1990	L, 10 deg	2.06	54.72	8.7	1.4	2.21
The Drag-n-Fly	H, 10.5 deg	2.3	72	12	2	2.3
The RTL-46, 1993	L, 10 deg	3.5	105.12	15.21	2.2	3.4
The Diamondback, 1993	J, 8 deg		155.5	10.8	3.1	
The Bunny, 1993	L, 6 deg poly	4.57	169.92	18.43	2	4.4

Plane Name	Sh (in^2)	bh (in)	ARh	We (oz)	Engine, #, position
FX/90, 1990	69.4	13.88	2.78	3.5	Astro 05 geared, 1, f
Blue Emu, 1993	221.76	24.6	2.73	4.1	Astro 15, 1, f
Gold Rush, 1993	230.4	27.6	3.3	5.968	Astro 25, 1, f
The Airplane, 1993	120	14.14	1.67	3.8	Astro 15, 1, f
The Penguin, 1990	149.76	24.96	4.16	1.5	Astro 15, 1, f
The Screem-J4D, 1990	90.72	15.65	2.72		Astro 05,1, f
The Drag-n-Fly	144	22.4	3		Astro 05, 1, f
The RTL-46, 1993	276.48	30	3.26		Astro 15, 1, f
The Diamondback, 1993	1389.6	115.8	9.65		Astro 15, 1, f
The Bunny, 1993	429.12	32.76	2.5	6.3	Astro 15, 1, f

Plane Name	Weng (oz)	Power (W)	Batteries	Wbatt (oz)
FX/90, 1990	6.5	115		5.46
Blue Emu, 1993	10.24	200	11 P90SCR 900	13.53
Gold Rush, 1993	14.176	300	13 P90SCR 900	16.9
The Airplane, 1993	10.3	200	12 P90SCR 900	14.76
The Penguin, 1990	10.3	200		5
The Screem-J4D, 1990	6.5	115	7 AA	5.46
The Drag-n-Fly		115	8 500MAH	
The RTL-46, 1993		200	12 POSC 900	
The Diamondback, 1993		200	12 P90SCR 900	
The Bunny, 1993	8.62	200	13 P90-SCR 1000	18

Plane Name	Prop type, # blades	Wprop (oz)	Prop pitch	Prop diam. (in)
FX/90, 1990	10-6, 2	2		
Blue Emu, 1993	Topflite 12-6, 2	0.5	6	12
Gold Rush, 1993	Zinger J, 2	0.98	6	13
The Airplane, 1993	Zinger	1	8	12
The Penguin, 1990	Zinger 10-4	2	4	10
The Screem-J4D, 1990	Tornado 10-6	1	6	10
The Drag-n-Fly	Zinger 10-6		6	10
The RTL-46, 1993	Zinger 12.5-6		6	12.5
The Diamondback, 1993	Zinger 11-7		7	11
The Bunny, 1993	Zinger 12-6	0.69	6	

Plane Name	Ailerons?, Size, Def	Flaps?, Size, Def	Elevators?, Size, Def
FX/90, 1990	N	N	Y, 5.97, 10
Blue Emu, 1993	N	N	Y, 9.8, 20
Gold Rush, 1993	N	N	Y, 115.2, 20
The Airplane, 1993	N	N	Y, 97.92, 16
The Penguin, 1990	Y, 80.7,	N	Y,52.5,+30/-20
The Screem-J4D, 1990	N	N	Y, 30.24, 25
The Drag-n-Fly	Y,		Y,
The RTL-46, 1993	N	Y, 350, 20	Y,33.12, 15
The Diamondback, 1993	N	N	Y, 59.04, 10/-20
The Bunny, 1993	N	Y, 100.7, 20	Y, 85.7, 18

Plane Name	Rudder?, Size, Def	CG (in): fore, aft	Vmax (ft/s)
FX/90, 1990	Y, 29.78, 20		
Blue Emu, 1993	Y, 57.5, 20	16.6,18	51.3
Gold Rush, 1993	Y, 79.2, 45	17.46,18.396	49
The Airplane, 1993	Y, 72, 30	19.36, 20.2	54.3
The Penguin, 1990	Y, 42, 20	13.1,13.9	56.1
The Screem-J4D, 1990	Y, 30.24, 25	9.71	58
The Drag-n-Fly	Y, 36, 20	9.4	
The RTL-46, 1993	Y, 56.16, 30	17.7, 19	54
The Diamondback, 1993	Y, 97.92, 20	23.3 aft	59.5
The Bunny, 1993	Y, 102.24, 30	21.23, 23.3	50

Plane Name	Vto (ft/s)	Vstall (ft/s)	Vcruise (ft/s)	Range (ft): cruise, max
FX/90, 1990	24	20.8	24	12210.,14389.
Blue Emu, 1993	25.3	22	30	23169.,23667.
Gold Rush, 1993		17.2	31	16600.,20250.
The Airplane, 1993	23	19.3	31	12100, 12500
The Penguin, 1990	20. (23.7)	22.6	25	2609,
The Screem-J4D, 1990	22.8	19	23	5500,
The Drag-n-Fly			25	4831,
The RTL-46, 1993	23.28	19.4	35	19430
The Diamondback, 1993	21.7	17.8	28	18300
The Bunny, 1993	21.7	15.95	30	14325.3, 14728.

Plane Name	Endurance(min): cruise,max	Take-off Dist. (ft)	Wg (oz)	Wav (oz)
FX/90, 1990	7.99,8.48	30		7.38
Blue Emu, 1993	12.87,14.3	30.96	3.5	5.92
Gold Rush, 1993	10.3,10.3	16.3	6	6
The Airplane, 1993	6.8, 8.7	24	5	5.95
The Penguin, 1990	1.755,	51.2	4	7.8
The Screem-J4D, 1990	3.68,	45	2.4	4.15
The Drag-n-Fly	3.22,	31		
The RTL-46, 1993	13.52	15.4		
The Diamondback, 1993	13.2	25.4		
The Bunny, 1993	8.25, 10.25	16.1	6	6

Appendix D: Performance Program

This program, written by Sean Greenwood and Jeff Scherock, calculates the performance data for a given engine and propeller.

```
      PROGRAM TS3
C
      REAL kt,kv,lf,J,Nprop,Nm,NmC,ia,NmCn
C
      OPEN(UNIT=12,FILE='end')
      OPEN(UNIT=13,FILE='rang')
      OPEN(UNIT=14,FILE='sdrain')
      OPEN(UNIT=15,FILE='stime')
      OPEN(UNIT=16,FILE='Pre')
      OPEN(UNIT=17,FILE='Pav')
      OPEN(UNIT=18,FILE='Roc')
      OPEN(UNIT=19,FILE='VH')
      OPEN(UNIT=20,FILE='para')
      OPEN(UNIT=21,FILE='ind')
      OPEN(UNIT=22,FILE='Treq')
      OPEN(UNIT=23,FILE='Ppara')
      OPEN(UNIT=24,FILE='Pind')
C
      Pi=4.*ATAN(1.0)
C
      A1=0.3361362
      A2=0.9234661
      A3=0.6159474
      A4=-1.352034
      B1=0.01321402
      B2=0.2063333
      B3=-0.3656616
      B4=0.1436228
C
      Aa1=-0.2729091
      Aa2=2.906734
      Aa3=-1.026263
      Aa4=-1.56229
      Bb1=-0.002688695
      Bb2=0.04320921
      Bb3=-0.07096458
      Bb4=0.0289369
C
      Ra=0.12
      Rb=0.08
```

```
      kv=0.000794
      kt=1.097846
      etag=.95
      Tloss=1.372935
      rho=0.002378
      AR=7.2
      b=6.75
      S=b**2/AR
      cdo=0.021
      lf=1.
      w=4.5
      e=0.82
      dprop=1.
      grat=2.21
C
      Vact=9.6
CC    V=50.
C
CC    DO 2 Range=10000.,20000.,2500.
      DO 5 V=25.,90.,5.

C
      Cl=lf*w*2*AR/(rho*V**2*b**2)
      Cd=cdo+(Cl**2/(Pi*e*AR))
      Preq=1.356*rho*V**3*b**2*Cd/(2.*AR)
C
      NmC=5000.
C
 10   CONTINUE
 20    CONTINUE
        J=V*60*grat/(NmC*dprop)
        eta=A1+A2*J+A3*J**2+A4*J**3
        Cp=(B1+B2*J+B3*J**2+B4*J**3)
        etaA=Aa1+Aa2*J+Aa3*J**2+Aa4*J**3
        CpA=2.*Pi*(Bb1+Bb2*J+Bb3*J**2+Bb4*J**3)
        Nprop=NmC/grat
        Pmob=1.356*Cp*rho*(Nprop/60.)**3*(dprop**5/etag)
        ia=(Pmob/(0.0007397*NmC*kt))+(Tloss/kt)
        Pmoa=0.0007397*NmC*(kt*ia-Tloss)
        Pavail=Pmoa*etag*eta
        ROC=0.7376*(Pavail-Preq)/w
        Nm=(Vact-ia*(Ra+Rb))/kv
       IF (ABS(Nm-NmC).GT.0.5) THEN
        NmCn=NmC+(Nm-NMc)/2.
        NmC=NmCn
        GOTO 20
```

```
        ENDIF
       IF (ABS(Pavail-Preq).GT.0.5) THEN
        Vactn=Vact-(Pavail-Preq)/Pavail
        Vact=Vactn
        GOTO 10
       ENDIF
C
CCC    WRITE(6,*)'eta,etaA',eta,etaA
CCC    WRITE(6,*)'Cp,CpA',Cp,CpA
C
       Trp=cdo*.5*rho*V**2*S
       Tri=CL**2/(Pi*AR*e)*.5*rho*S*V**2
       Prp=Trp*V*1.356
       Pri=Tri*V*1.356
       Treq=Trp+Tri
       Time=970.*3.6/ia
       Range=V*Time
       angle=ASIN(ROC/V)
       VH=V*COS(angle)
C
       WRITE(12,*)V,Time
       WRITE(13,*)V,Range
CCC    WRITE(20,*)V,Trp
CCC    WRITE(21,*)V,Tri
CCC    WRITE(22,*)V,Treq
CCC    WRITE(23,*)V,Prp
CCC    WRITE(24,*)V,Pri
CCC    WRITE(16,*)V,Preq
CCC    WRITE(17,*)V,Pavail
CCC    WRITE(18,*)V,ROC
CCC    WRITE(19,*)VH,ROC
C
CC     Time=Range/V
CC     drain=ia*Time/3.6
CC     WRITE(14,*)V,drain
CC     WRITE(15,*)V,Time
C
       WRITE(6,*)' V,Vact',V,Vact
       WRITE(6,*)' Nm,NmC,J',Nm,NmC,J
       WRITE(6,*)' ROC',ROC
       WRITE(6,*)' Range',Range
       WRITE(6,*)' Time',Time
       WRITE(6,*)' Pavail,Preq',Pavail,Preq
       WRITE(6,*)' Treqi,Treqp,Treq',Trp,Tri,Treq
       WRITE(6,*)' Pmoa,Pmob,ia',Pmoa,Pmob,ia
       WRITE(6,*)' '
```

```
C
  5    CONTINUE
CC     WRITE(14,*)' '
CC     WRITE(15,*)' '
CC  2        CONTINUE
C
       CLOSE(UNIT=12)
       CLOSE(UNIT=13)
       CLOSE(UNIT=14)
       CLOSE(UNIT=15)
       CLOSE(UNIT=16)
       CLOSE(UNIT=17)
       CLOSE(UNIT=18)
       CLOSE(UNIT=19)
       CLOSE(UNIT=20)
       CLOSE(UNIT=21)
       CLOSE(UNIT=22)
       CLOSE(UNIT=23)
       CLOSE(UNIT=24)
C
       END
```

Appendix E: Aerodynamics, Stability, and Control Program

```
      program design

      implicit real(a-z)

      open(unit=100,file='data',status='unknown')
c     input constants

      pi=4.*atan(1.)
      rhosl=0.0023769
      gamma=1.4
      p0=2116.2
      grav=32.2

c     input variables

      read(100,*) ew
      read(100,*) eac
      read(100,*) clas
      read(100,*) cmacw
      read(100,*) ast
      read(100,*) alo
      read(100,*) iw
      read(100,*) Gam
      read(100,*) ARw
      read(100,*) cf
      read(100,*) delf
      read(100,*) fpi
      read(100,*) fpo
      read(100,*) tauf
      read(100,*) delcdf
      read(100,*) kf
      read(100,*)
      read(100,*) Df
      read(100,*) Lf
      read(100,*) wf
      read(100,*) deuda
      read(100,*) k2k1
      read(100,*) Sv
      read(100,*) ARv
      read(100,*) trv
      read(100,*) clasv
      read(100,*) kn
      read(100,*) krl
      read(100,*) Sh
```

```
      read(100,*) ARh
      read(100,*) trh
      read(100,*) clash
      read(100,*) ih
      ih=ih*pi/180.
      read(100,*)
      read(100,*) nult
      read(100,*) Wtot
      read(100,*) xcg
      read(100,*) ycg
      read(100,*) xw
      read(100,*) yw
      read(100,*) xh
      read(100,*) yh
      read(100,*) xv
      read(100,*) yv
      read(100,*) xmg
      read(100,*)
      read(100,*) trad
      read(100,*) tvel
      read(100,*) talp
      read(100,*) acr
      read(100,*) vto
      read(100,*) ato
      read(100,*) vmax
      read(100,*) vvv
      read(100,*)
      read(100,*) maxde
      read(100,*) taue
      read(100,*) maxdr
      read(100,*) taur
      read(100,*) maxda
      read(100,*) taua
      read(100,*) ya2
      read(100,*) ya1
      read(100,*) prat
      read(100,*) sigma

      close(unit=100)

c     find n based upon performance requirements

      n=sqrt(1.+(tvel**2/grav/trad)**2)

c     find wing cl
```

```
clas=clas*180./pi
clash=clash*180./pi
clasv=clasv*180./pi
claw=clas/(1.+clas/(pi*ew*ARw))
clat=clash/(1.+clash/(pi*ew*ARh))
clav=clasv/(1.+clasv/(pi*ew*ARv))
claac=clas/(1.+clas/(pi*eac*ARw))
claacf=clas/(1.+clas/(pi*eac*(1.+kf)*ARw))
CLmaxw=claw*(ast-alo+iw)*pi/180.
CLmaxac=claac*(ast-alo+(fpo-fpi)*tauf*delf-2)*pi/180.

c       find wing attributes based on performance

CLper=claac*(talp-alo+iw)*pi/180.
Sw1=n*Wtot/(CLper*0.5*rhosl*tvel**2)
cw1=Sw1/(sqrt(ARw*Sw1))
bw1=sqrt(ARw*Sw1)
Gam=Gam*pi/180.
vstall1=sqrt(2.*Wtot/(rhosl*Sw1*CLmaxac))

c       find wing attributes based upon take-off

CLto=Claacf*(iw+ato-alo+(fpo-fpi)*tauf*delf)*pi/180.
Sw2=Wtot/(CLto*0.5*rhosl*(vto)**2)
cw2=Sw2/(sqrt(ARw*Sw2))
bw2=sqrt(ARw*Sw2)
vstall2=sqrt(2.*Wtot/(rhosl*Sw2*CLmaxac))

c       find wing attributes

if (Sw1.gt.Sw2) then
        Sw=Sw1
        bw=bw1
        cw=cw1
        type=1
else
        Sw=Sw2
        bw=bw2
        cw=cw2
        type=2
endif

c       find static stability coefficients

cmaw=claw*(xcg-xw)/cw
Vh=Sh*(xh-xcg)/(Sw*cw)
```

```
      deda=2*claw/(pi*ARw)
      e0=deda*(0.-alo)*pi/180.
      cmat=-Vh*clat*(1-deda)
      cmaf=1./(36.5*Sw*cw)*wf**2*deuda*Lf
      cma=cmaw+cmat+cmaf
      cm0f=k2k1/(36.5*Sw*cw)*wf**2*alo*pi/180.*Lf
      cm0w=cmacw+claw*(0.-alo)*pi/180.*(xcg-xw)/cw
      cm0t=vh*clat*(e0+iw*pi/180.-ih)
      cm0=cm0f+cm0w+cm0t
      Vv=Sv*(xv-xcg)/(Sw*bw)
      zw=Df/2.
      dsdb=0.724+3.06*(Sv/Sw)/2.+0.4*zw/Df+0.009*ARv
      cnbv=Vv*clav*(dsdb)
      sfs=wf*Lf
      cnbwf=-kn*krl*sfs/Sw*Lf/bw
      cnb=cnbv+cnbwf
      clb=-2.*Gam*cw*claw*bw**2/(Sw*bw*8)

c     find drag coefficients

      cd0=(0.007*Sw+0.11*Df**2+0.01*Sw+0.008*(Sv+Sh))/Sw
      cd0=cd0*1.15
      k=1./(pi*eac*ARw)

c     find cruise conditions

      vcr1=sqrt(wtot/(0.5*rhosl*Sw*claac*(iw-alo)*pi/180.))
      vcr2=sqrt(wtot/(0.5*rhosl*Sw*claac*(acr+iw-alo)*pi/180.))
      alpcr=2.*wtot/(rhosl*Sw*claac*pi/180.*vvv**2)-iw+alo
      CLcrac1=claac*(iw-alo)*pi/180.
      CLcrac2=claac*(acr+iw-alo)*pi/180.
      CLcrac3=claac*(alpcr+iw-alo)*pi/180.
      cdcr1=cd0+k*CLcrac1**2
      cdcr2=cd0+k*CLcrac2**2
      cdcr3=cd0+k*CLcrac3**2
      Dcr=cdcr*0.5*rhosl*vcr**2*Sw
      Treq=Dcr
      Mcr=vcr/sqrt(gamma*p0*prat/(rhosl*sigma))
      LDcr1=CLcrac1/cdcr1
      LDcr2=CLcrac2/cdcr2
      LDcr3=CLcrac3/cdcr3

      open(unit=150,file='ld.out')

      do 10 v=25.,60.,2.5
      ccll=wtot*2./(rhosl*v**2*Sw)
```

```
      ccdd=cd0+k*ccll**2
      lldd=ccll/ccdd
      write(150,*) v,lldd
10    continue

      close(unit=150)

c     find static margin to check again for pitch stability

      xnpalt=0.25-(cmaf+cmat)/claw
      xcgalt=(xcg-xw)/cw+0.25
      sm=xnpalt-xcgalt

c     find coefficients for static control and compare to requirements

      clde=Sh/Sw*clat*taue
      cmde=-(Vh*clat*taue)
      dcmmax=cmde*maxde/180.*pi
      cmmax=cm0+cma*(ast)*pi/180.
      cndr=-(Vv*clav*taur)
      dcnmax=cndr*maxdr/180.*pi
      cnmax=cnb*15.*pi/180.
      clda=2.*taua*claw/(Sw*bw)*cw*0.5*((bw*ya2)**2-(bw*ya1)**2)
      dclmax=clda*maxda/180.*pi
      cldr=Sv/Sw/bw*(0.5*sqrt(sv*arv))*taur*clav

c     takeoff performance

      liftt=clat*ih*0.5*rhosl*(0.85*vto)**2*Sh-clde*maxde/180.*pi
      liftw=claw*(0.-alo+(fpo-fpi)*tauf*delf)*pi/180.*0.5*rhosl
     &          *(0.85*vto)**2*Sw
      mtail=-liftt*(xh-xmg)
      mwing=-liftw*(xw-xmg)
      mweight=wtot*(xcg-xmg)
      mcg=mtail+mwing+mweight

c     performance characteristics

      phi=(16./pi*(yw-ymg)/bw)**2/(1+(16./pi*(yw-ymg)/bw)**2)
      cdto=cd0+k*clto**2*phi+0.02
      cdtoa=cdto-0.02
      dto=0.5*rhosl*vto**2*Sw*(cdto)
      dtoa=dto/cdto*cdtoa
      minr=vcr**2/(32.2*sqrt(nult**2-1.))
      CLm=sqrt(cd0/k)
      CDm=cd0+k*CLm**2
```

```
      LDmax=CLm/CDm
      deltcr=-(cm0*CLaac+cma*CLcrac3)/(cmde*CLaac-cma*clde)

c     output

      write(6,*)
'                                                                    '
      write(6,*) 'weight',Wtot
      write(6,*) 'Wing loading',Wtot*16./Sw
      write(6,*) 'xcg,ycg',xcg,ycg
      write(6,*) 'n during turn',n
      write(6,*) ' '
      write(6,*) 'Wing area',Sw,type
      write(6,*) 'Wing span',bw
      write(6,*) 'Wing chord',cw
      write(6,*) 'AR',ARw
      write(6,*) 'eac',eac
      write(6,*) 'iw',iw
      write(6,*) 'cf',cf
      write(6,*) 'inner and outer flap position',fpi,fpo
      write(6,*) 'Sw1,Sw2',Sw1,Sw2
      write(6,*) ' '
      write(6,*) 'max lift angle',ast
      write(6,*) 'zero lift angle',alo
      write(6,*) 'cruise angle',acr
      write(6,*) 'take-off angle',ato
      write(6,*) 'turn angle',talp
      write(6,*) 'max flap deflection',delf
      write(6,*) ' '
      write(6,*) 'CLmax aircraft',CLmaxac
      write(6,*) 'CLto',CLto
      write(6,*) 'CLper',CLper
      write(6,*) 'CLalpha aircraft',CLaac
      write(6,*) 'CLaplha wing',claw
      write(6,*) 'CLcruise aircraft',CLcrac1,CLcrac2,CLcrac3
      write(6,*) 'CDcruise aircraft',cdcr1,cdcr2,cdcr3
      write(6,*) 'cd0,k',cd0,k
      write(6,*) 'cdto,cdtoa',cdto,cdtoa
      write(6,*) 'dto,dtoa',dto,dtoa
      write(6,*) ' '
      write(6,*) 'Vto',vto,vto/vstall2
      write(6,*) 'Vstall',vstall1,vstall2
      write(6,*) 'Vcruise at 0 degrees',vcr1
      write(6,*) 'Vcruise at ',acr,' degrees',vcr2
      write(6,*) 'Alpha cruise at ',vvv,' ft/s',alpcr
      write(6,*) 'Mcr',Mcr
```

```
write(6,*) 'max vel',vmax
write(6,*) 'Minimum turn radius at cruise',minr
write(6,*) 'L/D cruise',LDcr1,LDcr2,LDcr3
write(6,*) 'L/D max,CLm',LDmax,CLm
write(6,*) ' '
write(6,*) 'Sv guess, Cnb',Sv,Cnb
write(6,*) 'Sh guess, Cma, Cm0',Sh,Cma,Cm0
write(6,*) 'dihedral guess, Clb',Gam*180./pi,Clb
write(6,*) 'Vh,Vv',Vh,Vv
write(6,*) 'sm',sm
write(6,*) 'dcmmax',dcmmax
write(6,*) 'cmmax',cmmax
write(6,*) 'clde',clde
write(6,*) 'cmde',cmde
write(6,*) 'dcnmax',dcnmax
write(6,*) 'cnmax',cnmax
write(6,*) 'cndr',cndr
write(6,*) 'dclmax',dclmax
write(6,*) 'clb',clb
write(6,*) 'cldr',cldr
write(6,*) 'delta trim cruise',deltcr*180./pi
write(6,*)
write(6,*) 'xloc',xw+0.5*cw
write(6,*) 'horiz xloc',xh+0.5*(Sh/sqrt(Sh*ARh))
write(6,*) 'vert xloc',xv+0.5*(Sv/sqrt(Sv*ARv))
write(6,*) 'xnpalt',xnpalt
write(6,*) 'xcgalt',xcgalt
write(6,*) 'Mcg',mcg
write(6,*)
```

```
open(unit=159,file='coeffs.dat')
write(159,*) cm0f,cmaf
write(159,*) cm0w,cmaw
write(159,*) cm0t,cmat
write(159,*) cnbwf,cnbv
close(unit=159)

stop
end
```

Appendix F: Manufacturing Plan

F.1 Overview

Long Shot Aeronautics is faced with the difficult task of assembling a prototype of *The Balsa Bullet*. The single largest hurdle to be overcome in this task is experience. The group members of *Long Shot Aeronautics* hold no experience in any RPV manufacturing techniques. For this reason, this manufacturing plan is set forth to be a comprehensive guide to 1) get all group members "on the same page," and 2) insure that from our first assembling steps to our "coup de grace," none of our steps are timid. This plan will first identify major components and subsystems, after which the timetable will be set forth. Following these will be a tooling schedule, critical methods, and will conclude with a cost analysis.

F.2 Major Components and Subsystems

1) Wing
    A) Main Spar
    B) Flaps
    C) Main Landing Gear
2) Fuselage
    A) Propulsion Mounts
        i) Engine Bulkhead
        ii) Battery Mount
        iii) Cowl
    B) Control Systems Mounts
        i) Servos
        ii) Avionics

C) Nosewheel Mount

3) Empennage

A) Horizontal Tail/Elevator

B) Vertical Tail/Rudder

F.3 Timetable

The timetable for manufacturing appears on the following page.

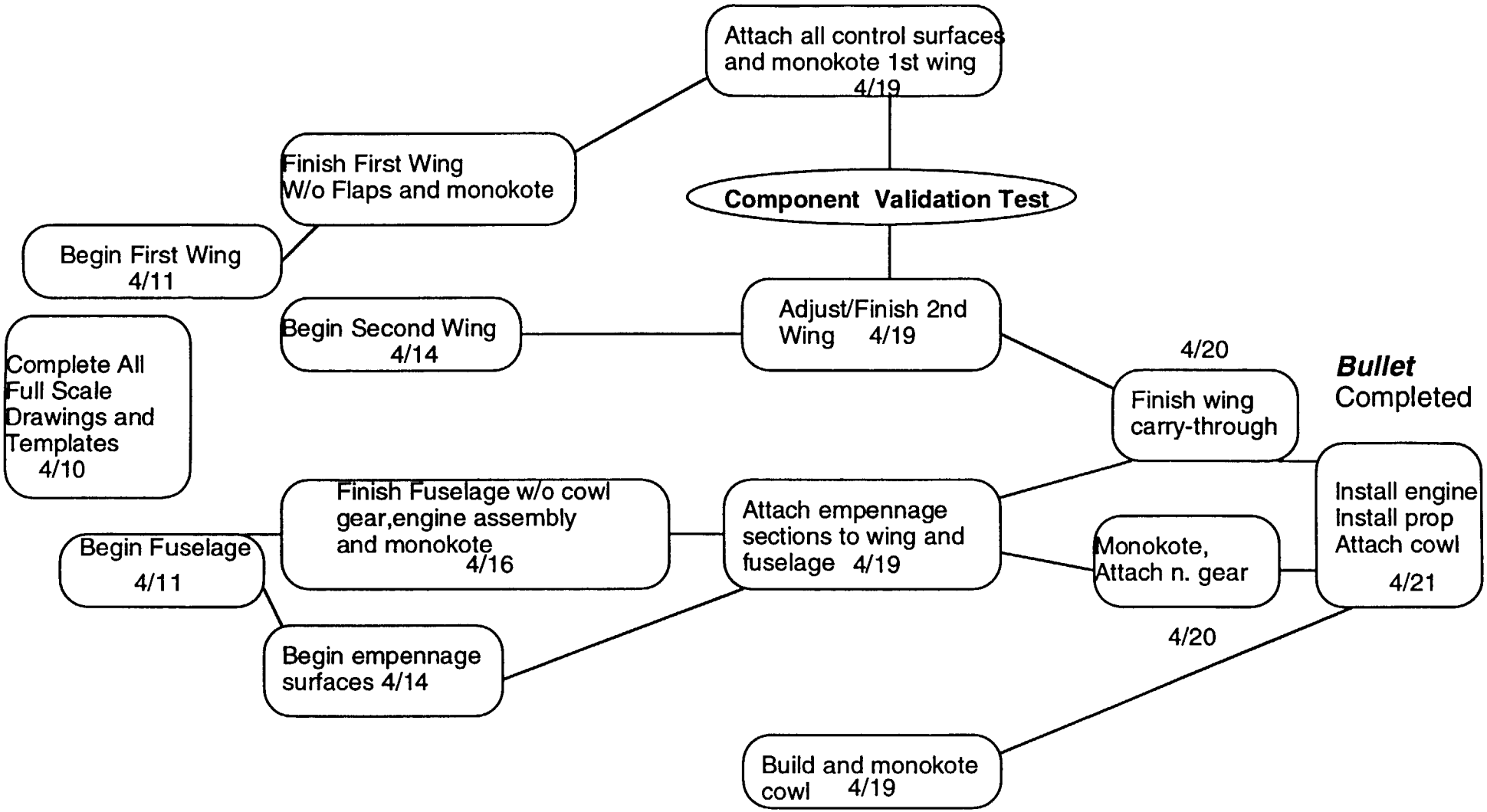

Manufacturing Schedule

F.4 Tooling Schedule

A schedule and tracking sheet for tooling requirements appears on the following page.

Tooling Cost Schedule and Tracking Sheet

Machine & Cost	Task	Estimated Time	Actual Time	Estimated Cost	Actual Cost
Large Scroll Saw		15 min		$6.75	
	Plywood cuts				
$1 Turn-on	1) engine mount	5 min			
$0.25/min	2) fuselage floor	5 min			
	3) inboard wing floor	5 min			
Small Scroll Saw		26 min		$4.60	
	All Airfoils (4 Templates)				
	1) full wing airfoil	5 min			
	2) stubbed wing airfoil for flaps	5 min			
	3) Vertical tail airfoil	3 min			
$0.5 Turn-on	4) horizontal tail airfoil	3 min			
$0.10/min					
	Rip Balsa Fuselage members	10 min			
	1/2 in x 1/4 in –1/4 in x 1/4 in				
	**Long run time				
	**Must be careful				
Drill Press		15 min		$2.50	
$1 Turn-on	**Weight savings cut-outs**				
$0.10/min	1) wing airfoil blocks				
	2) flap sections				
	3) elevator section				
Monokote Iron		120 min		$30.00	
	Cover aircraft				
$0.25/min			**Total**	**$43.85**	

F.5 Critical Methods

F.5.1 Structural Assembly Techniques

Without a doubt, the single most critical component of the aircraft assembly is the main spar joint. From consultation with Mr. Doug Staudmeister, the joint will be a butt joint reinforced with nylon mesh, carbon filament, and epoxy resin (figure F-1). The mesh and epoxy will also be used to fasten the main spar assembly to the fuselage longerons in the areas shown in figure F-1.

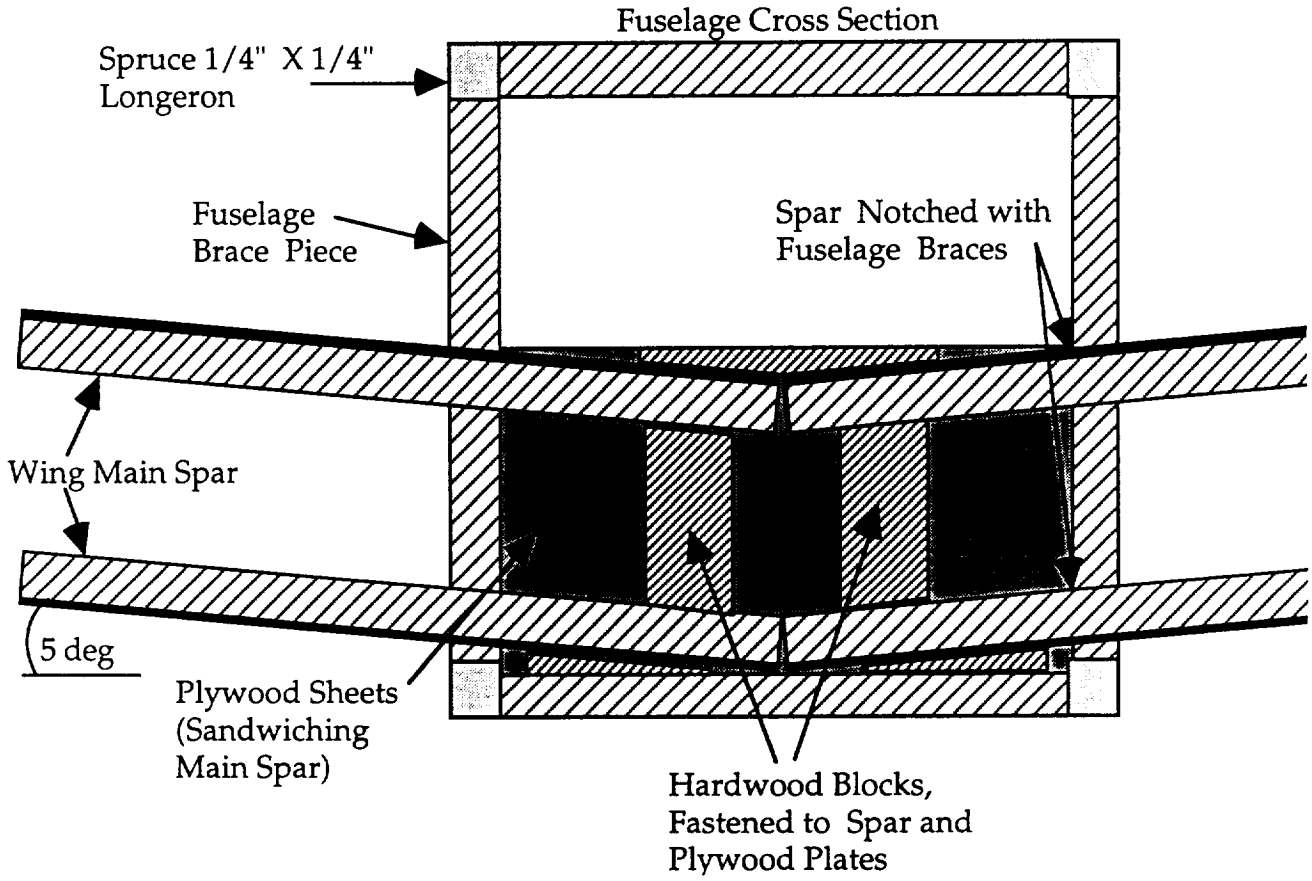

Figure F-1: Wing Carry-Through Design

Another critical component will be the main landing gear. Figure F-2 shows the configuration and attachment to the main spar. The complexity of the bends will require patience, however, a slip in this process is correctable, yet costly in time.

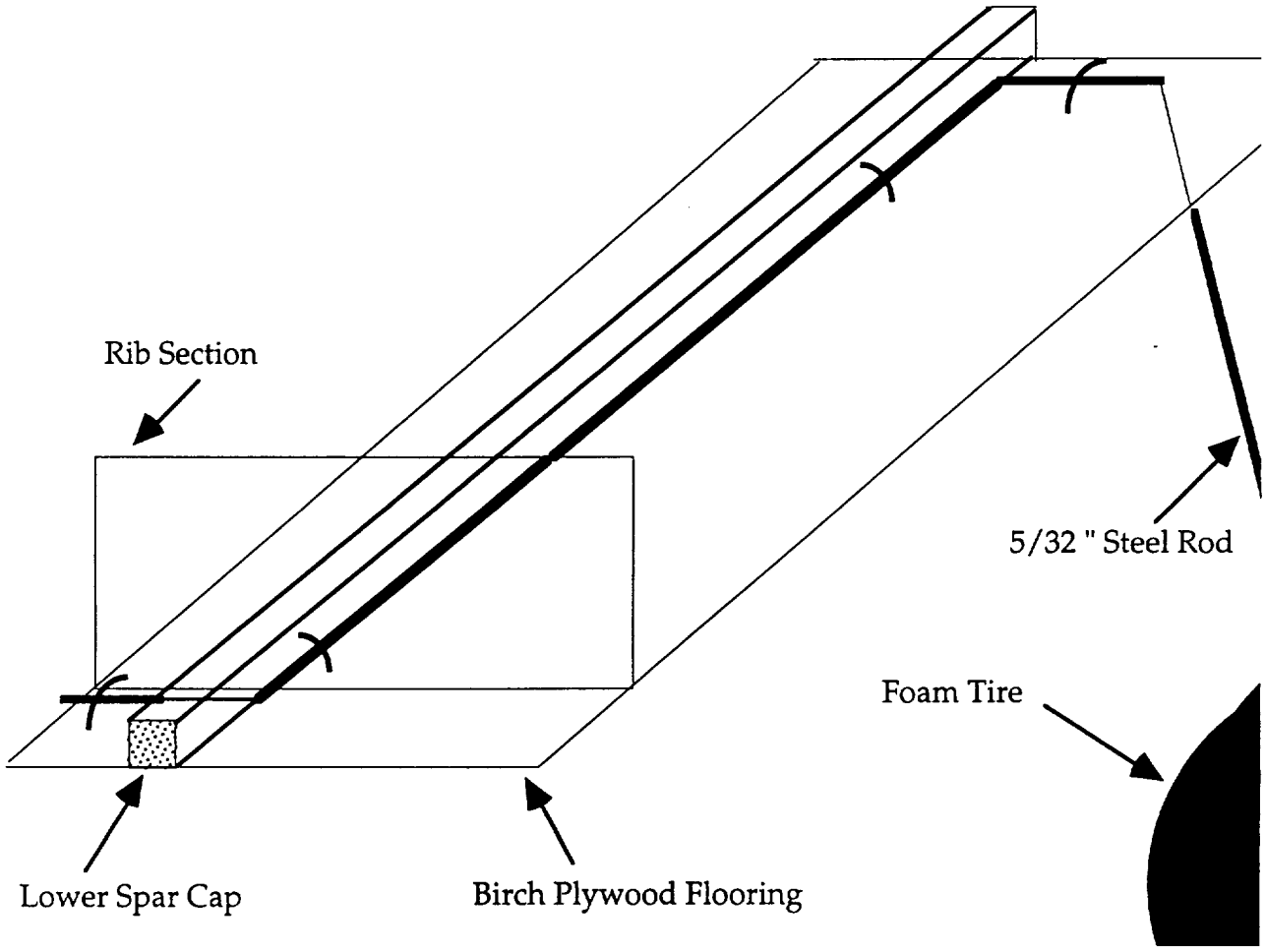

Figure F-2: Landing Gear Detail

F.5.2 Personnel Management

The philosophy behind personnel management is based on "relative expertise." Initial task assignments were distributed randomly, as no one person is qualified in any area, however, as time progresses, it is assumed that each

member will become acquainted with a certain task. For this reason, two members have been assigned construction duties for both the first and second wings, with the thought in mind that experience gained through manufacture of the first will be of use in fabricating the second. Similarly, two people will be assigned as machine operators for the first two days of construction. It is hoped that they will become proficient (in a relative way) on specific tools, saving on run time costs. The remaining two members will begin construction on the fuselage section.

As time progresses and machine time lags, the two machine operators will likely be reassigned the subsystem tasks of flaps and main landing gear. As the fuselage and empennage sections near completion, one of the responsible individuals will begin monokote testing and training, while the other, specifically the Director of Manufacturing, will provide assistance wherever it may be needed.

A rough budgeting of the ninety manufacturing hours is as follows:

Wing	30 hours
Fuselage	8 hours
Empennage	9 hours
Landing Gear (main)	7 hours
Final Assembly	10 hours
Installations	8 hours
Monokoting	8 hours
Miscellaneous	10 hours

The wing construction for component validation is budgeted an additional 35 hours, since this will be the first wing built.

F.6 Cost Evaluation

F.6.1 Raw Materials

The raw material expenditures as of the Manufacturing Plan Review was broken down as follows:

Spruce	$21.52
Balsa	$26.66
Plywood	$15.42
Monokote	$18.98
Landing Gear	$23.17
Glue	$ 7.18
Miscellaneous	$24.66
Subtotal	$137.59
Tax (5%)	$ 6.88
TOTAL	$144.47

F.6.2 Remaining Estimated Costs

The remaining costs are estimated as follows:

Fixed Subsystems	$435.00
Labor	$900.00
Tooling	$ 43.85
Waste	$ 80.00
Subtotal	$1458.85
Raw Materials	$ 144.47
New Estimate	$1603.32
Old Estimate	$1684.00
Surplus	**$ 81.68**

Although arriving at the final product under budget would be a good thing for The Balsa Bullet, a preliminary qualitative analysis would lead Long Shot Aeronautics to reallocate the surplus towards labor costs. Although a preliminary labor schedule has been laid out, totaling 90 hours, difficulties are anticipated particularly in fabricating the wing carry-through structure.

Appendix G:

Flight Validation, Component Test and Manufacturing Hours

appeared to handle much better at low speed (about 1/3 throttle setting). Turning performance was acceptable and much improved with the sealed rudder gap but there did not appear to be enough wing dihedral. A high speed leg was attempted and the speed estimated at 60 ft/sec - the turn from the high speed leg was difficult to achieve in the confines of Loftus. Take-off tests with the flaps deployed were not conducted.

Wing Component Static Load Test, April 19, 1994
Spring 1994
Balsa Bullet

Summary:
A wing component was tested to failure. The wing was completed with flaps and attached to a mockup of the center fuselage section. The center fuselage section was constructed in a manner similar to the planned fuselage construction and then mounted to the static load facility with clamps. The wing weight including the fuselage centerbody was 0.81 lb as tested.

The wing failed when a total load of 9.6 lb was applied. Failure was due to a debonding of the adhesives at the wing centerline which were used to attach fiberglass "material" which was the only connection between the spar caps at the root. The caps were simply "butt-joined" at the root and wrapped with the fiberglass cloth. There did not appear to be any structural failure in the wings themselves. Prior to failure either "cracking" or monokote debonding from the structure was "heard" at locations outboard from the root.

1-g Load Distribution:
The approximation to the 1-g load was applied starting at the root. The spanwise locations where the loads were applied started 3" from the root and were spaced at 6" intervals. The 1-g load was applied first and then the 2-g condition was applied by increasing the load starting at the root. This processes continued until the wing failed. The wing failed when the total load applied to the wing was 9.6 lb, and this occurred as the loading was being increased from 2 to 3 g's.

Spanwise location (distance from root in inches)	Load (lb)
3	.39
9	.39
15	.39
21	.35
27	.35
33	.29
39	.12

Wing Tip Deflection:

The tip deflection was measured as the load was increased. It is presented for even increments in load factor and the last data point taken before failure.

Total Load (lb) - Both wings	Tip Deflection (in)
4.6	1.0
9.2	2.5
9.6	failure

Additional Information:

Aircraft Weight = 4.6 lb (estimate at this time)
Wing Weight = 0.81 lb (as tested)

Group C
Balsa Bullet

Comparison Between Design and Actual Aircraft Data

	Design Value	Actual Value
Wing Span	84in 7ft	89.5in 7.04ft
Wing Area	945in² 6.58ft²	961.2in² 6.67ft²
Vertical Tail Area	72in² 0.5ft²	78.4in² 0.54ft²
Horizontal Tail Area	216in² 1.5ft²	229in² 1.59ft²
Wing Structural Weight (Monokote)	352g 0.777016s	370g 0.82lb
Wing Structural Weight (no Monokote)	259g 0.572016s	250g 0.55lb (est)
Fuselage Structural Weight (Monokote)	222g 0.49 lbs	400g 0.88lb (est)
Fuselage Structural Weight (no Monokote)	196g 0.432 lbs	310g 0.68 lb (est)
Vertical Tail Weight (Monokote)	21g 0.04631bs	38g 0.08378
Vertical Tail Weight (no Monokote)	14g 0.0305 lbs	24g 0.05291
Horizontal Tail Weight (Monokote)	80.5g 0.1776 lbs	77.5g 0.17086
Horizontal Tail Weight (no Monokote)	58.5g 0.1297 lbs	48.5g 0.10692
Landing Gear Weight MAIN / NOSE	151g 0.3332 lbs 32g 0.0706 lbs	160g 0.353 lb 65g 0.143 lb
Propeller Type	Zinger 12-8	Zinger 12-8
Propeller Weight	45g 0.1 lbs	22g 0.0485 lb
Total Aircraft Weight (post-construction)	2087g 4.6 lbs	2208.5g 4.871b
Total Aircraft Weight (post-flight)	2087g 4.6 lbs	
CG Location (post-construction)	13.55 in	13.5 in
CG Location (post-flight)	13.55in	
Weight of Batteries	479g 1.056 lbs	579g 1.25 lb

Please list any other deviations of the technology demonstrater from the original design.

Long Shot Aeronautics: Time Sheet 1

Name	Date	Time In	Time Out	Comments	
John Rooff	4/11	4:00	5:00		1
Kevin Eastland	4/11	4:45	5:30		0.75
John Rooff	4/11	7:30	12:00	• Finished 1 side - Balsa Sanding Fashion.	4.5
Sean Greenwood	4/11	7:45	10:30		2.75
K. Eastland	4/11	7:45	11:45	• Lots o' cuts	4.0
D. Kelly Sexy Man	4/11	8:30	10:45		2.25
C. Leonard	4/11	9:00	10:00		1.0
J. Rooff	4/12	10:15	12:00	• 2nd Side	1.75
D. Kelly IS a HOT BABE!	4/12	10:15	11:00		.75
K. Eastland	4/12	10:30	11:00	F	.5
S. Greenwood	4/12	10:30	12:00		1.5
J. Rooff	4/12	4:45	5:30	• Bottom	.75

16.25
1.75

✓ 21.5

Long Shot Aeronautics: Time Sheet 2

21.5

Name	Date	Time In	Time Out	Comments	
J. Rooff	4/12	6:00	7:00	· Bottom Finished · Start Top	1.0
D. Kelly	4/12	8:00	10:15	· Cowl	2.25
			10:15	- More Top - Start H-Tail	1.75
D. Kelly	4/13	3:30	6:00	Engine Mount Assembly Underway.	2.5
S. Greenwood	4/13	4:45	6:15	Wing	1.5
J. Scherock	4/13	4:00	6:15	↓	2.25
S. Greenwood	4/13	7:15	12:45	↓	5.5
J. Scherock	4/13	7:15	12:00		4.75
D. Kelly	4/13	10:30	12:45	· Vert Tail · Wing help.	2.25
Eastland	4/14	10:30	12:50	WING 2	45.25 2.
S. Greenwood	4/14	11:00	12:00		1
Kelly	4/14	10:30	12:00		1.5

49.75

Long Shot Aeronautics: Time Sheet 3

49.75

Name	Date	Time In	Time Out	Comments	
Roeff	4/14	10:00	12:30		2.5
Leonard	4/14	10:00	12:30		2.5
Kelly	4/14				
Eastland	4/14	7:30	10:00	HELPING W/ LOADING & AIRFOIL SHEETS	2.5
Roeff	4/14	7:30	11:00	, wing	3.5
			11:00		3
Leonard	4/14	9:30	[illegible]		1.25
	[illegible]				2.5
Roeff	4/17	12:30	1:00	wing Monokote	0.5
Leonard	4/17	[illegible]	[illegible]		2
Schenck	4/17	11:00	1:00	wing monokote	2
Schenck	4/18	11:15	11:30		0.25

Long Shot Aeronautics: Time Sheet 4

-12.25

Name	Date	Time In	Time Out	Comments	
Kelly	4/18	2:30	4:30	Carry Through (Test wing)	2
Scherock	4/18	3:30	4:45	wing	1.25
Leonard	4/18	3:30	4:45	monocoque bridal	1.25
Rooft	4/18	3:30	4:45	monocoque bridal	1.25
Kelly	4/18	8:30	10:45	Random items	2.25
Rooft	4/18	8:30	1:45	Empennage! Almost done! **	5.25
Kelly	4/19	1:15	2:00		0.75
Leonard	4/18	9:15	1:30	monocoque wing sand wing	4.25
Scherock	4/18	8:30	2:00		5.50
Kelly	4/19	4:15	5:30	wing & carry-through	1.25
Scherock	4/19	4:15	5:30	Sanding wing	1.25
Rooft	4/19	10:15	1215	Fuselage	2
					94.5

100.5

Long Shot Aeronautics: Time Sheet 5

94.5

Name	Date	Time In	Time Out	Comments	
Kelly	4/19	10 30	1200	Began Landing Gear	1.5
Greenwood	4/19	10:00	2:00	Finishing Touches on 2nd Wing	4
Kelly	4/20	2:15	3:45		1.5
"	"	545	2:00	!!! (6)	8.25
Rooff	4/20	5:30	6:45	Empennage Fuselage/Avionics	1.25
Eastland	4/20	8:00	2:30	OWES DAN $20	6.5
Rooff	4/20	10:30	3:15	A lot of shit!	4.75
Greenwood	4/20	7:30	1:00		5.5
Leonard	4/20-21	6:30	5:30		11
Rooff	4/21	5:45	8:45	Fuselage	3
Leonard	4/21	7:00	7:30		0.5
[illegible]	4/23	[illegible]	[illegible]		1

143.25

Long Shot Aeronautics: ~~Tooling~~ Time Sheet 2/6

143.25

Name	Date	Time In	Time Out	Comments	
Dan	4/24	5	9:00	Controls / Ldg Gear I	4
Dan	4/25	330	5:00		1.5
Kevin	4/24	8:00	10:00		2
[illegible]	4/25	8:00	12:00	Flaps	4
Rooff	4/25	3:30	4:30	Controls	1
Rooff	4/25	10:30	12:15	Ailerons / Flaps	1.25
Kelly	4/25	8	2:30	Ditto	6.5
Scherock	8:00	10:30		"	2.5
Leonard	8:00	10:30		Rudder	2.5
Kelly	4/27	3:30	5		1.5
Rooff	4/27	3:30	5		1.5
					175

Jeff 19.75 | Chuck 27.25 | Sean 27.25 | Kevin 22.25 | Dan 42.5 | John 59.75

1st Wing – 27.25 hrs. (est)

Long Shot Aeronautics: Tooling Sheet 1

Name	Date	Tool	Start Time	Stop Time	
K. EASTLAND	4/11	Scroll saw	4:45	4:47	2
K. EASTLAND	4/11	Scroll saw	4:49	4:50	1
S. Greenwood	4/11	Scroll Saw	8:20	8:24	2
K. Eastland	4/11	Scroll saw	9:02	9:10	8
J. Rooff	4/11	Scroll Saw	9:20	9:24	4
J. Rooff	4/11	Scroll Saw	9:40	9:44	4
K. Eastland	4/11	Drill Press	10:10	10:15	5
D. Kelly	4/11	Scroll Saw	10:28	10:32	4
D. Kelly	4/11	Scroll Saw	10:40	10:41	1
K. Eastland	4/11	Scroll saw	11:00	11:20	20
K. Eastland	4/11	Sander	11:20	11:30	6
K Eastland	4/11	Sander		- 15 seconds	

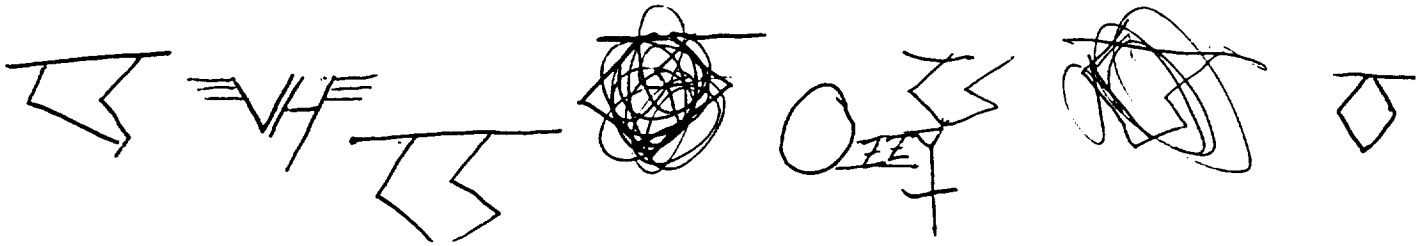

Long Shot Aeronautics: Tooling Sheet 2

Name	Date	Tool	Start Time	Stop Time
Eastland	4/13	sander	15 seconds	
Kelly	4/13	scroll	1 min	
Kelly	4/13	press	2 min	
Kelly	4/13	scroll	2 min	
EastHand	4/14	Press	3 MIN	
Eastland	4/14	scroll	2 MIN	
Kelly	4/14	Press	5 min	
Eastland	4/14	scroll	10 min	
"	4/14	sander	10 min	
Eastland	4/14	scroll		10 seconds
Roof	4/14	Press	5 min	
Roof	4/14	Sander	3 min	

Long Shot Aeronautics: Tooling Sheet 3

Name	Date	Tool	Start Time	Stop Time
Kelly	4/18	Press	7min	
Kelly	4/18	Scroll	1min	
Kelly	"	"	3min	
"	"	Sander	2min	
Greenwood	4/20	Scroll	0 min	
"	"	"	1min	
Kelly	4/20	Sander	2min	
Kelly	"	Scroll	2min	
Roark	"	"	2min	
[illegible]	4/21	Sander	2min	
[illegible]	4/21	"	2min	
Group	—	Monokote Iron	~ 8 hours	